Strategies for improving Influenza vaccines: insights from the Influenza A H1N1 and SARS-CoV-2 pandemics

Lena Hansen

Thesis for the degree of Philosophiae Doctor (PhD)
University of Bergen, Norway
2022

UNIVERSITY OF BERGEN

Strategies for improving Influenza vaccines: insights from the Influenza A H1N1 and SARS-CoV-2 pandemics

Lena Hansen

Thesis for the degree of Philosophiae Doctor (PhD)
at the University of Bergen

Date of defense: 23.09.2022

Year: 2022

Title: Strategies for improving Influenza vaccines: insights from the Influenza A H1N1 and SARS-CoV-2 pandemics

Name: Lena Hansen

Print: Skipnes Kommunikasjon / University of Bergen

"Tell me and I forget,
Teach me and I may remember,
Involve me and I learn"

- *Benjamin Franklin (1706 – 1790)*

List of abbreviations

ACE2	Angiotensin Converting Enzyme 2
ADCC	Antibody-dependent cellular cytotoxicity
AS03	Adjuvant system 03
BCR	B cell receptor
BLI	Biolayer interferometry
BSA	Bovine serum albumin
CD	Cluster of differentiation
CDC	Centers for Disease Control and Prevention
cDNA	Complementary deoxyribonucleic acid
CDR	Complementarity determining region
CHMP	Committee for Medicinal Products for Human Use
CoP	Correlate of protection
COVID-19	Corona virus disease-19
Cryo-EM	Cryo-electron microscopy
D	Diversity
DC	Dendritic cell
DEAE	Diethylaminoethyl
DMEM	Dulbecco's Modified Eagle Medium
DMSO	Dimethyl sulfoxide
dsRNA	Double stranded ribonucleic acid
EC_{50}	Effective concentration 50%
ELISA	Enzyme-linked immunosorbent assay
ELISPOT	Enzyme-linked immune absorbent spot
ELLA	Enzyme-linked lectin assay
EMA	European Medicines Agency
EMV	Escape mutant virus
Fab	Antigen-binding fragments
FC	Fragment crystallisable
FDA	Food and Drug Agency
fDC	Follicular dendritic cell
FR	Framework region
GC	Germinal centre
GISRS	Global Influenza Surveillance and Response System
GSK	GlaxoSmithKline
HA	Hemagglutinin
HAI	Hemagglutination inhibition
HCl	Hydrochloric acid
HCW	Health care worker
HEPES	4-(2-hydroxyethyl)-1-piperazineethanesulfonic acid

HIV	Human immunodeficiency virus
HRP	Horseradish peroxidase
IAV	Influenza A virus
IBV	Influenza B virus
IC_{50}	Inhibitory concentration 50%
IFN	Interferon
IFN-γ	Interferon gamma
IIV	Inactivated influenza vaccine
IL-2	Interleukin 2
ISG	Interferon-stimulating gene
J	Joining
LAIV	Live attenuated influenza virus
LIBRA-seq	Linking B cell receptor to antigen specificity through sequencing
M1	Matrix protein 1
M2	Matrix protein 2
M2e	Matrix protein 2 ectodomain
mAb	Monoclonal antibody
MBC	Memory B cell
MDCK	Madin-Darby canine kidney
MEM	Minimum essential medium
MERS-CoV	Middle Eastern Respiratory Syndrome Coronavirus
MOI	Multiplicity of infection
mRNA	Messenger ribonucleic acid
MxA	Myxovirus resistance protein A
NA	Neuraminidase
NAI	Neuraminidase inhibition
NEP	Nuclear export protein
NFAT	Nuclear Factor of Activated T cell
NIH	National Institute of Health
NK	Natural killer
NP	Nucleoprotein
NS1	Non-structural protein 1
NSP	Non-structural protein
OD	Optical density
OPD	σ-Phenylenediamine dihydrochloride
ORF	Open reading frame
PA	Polymerase acidic protein
PAMP	Pathogen-associated molecular pattern
PB1	Polymerase basic protein 1
PB2	Polymerase basic protein 2

PBMC	Peripheral blood mononuclear cell
PBS	Phosphate Buffer Saline
PBS-T	Phosphate Buffer Saline-Tween
PCR	Polymerase chain reaction
PNA	Peanut agglutinin
PRNA	Plaque reduction neutralisation assay
PRNT	Plaque reduction neutralising titer
PRR	Pattern recognition receptor
QIV	Quadrivalent influenza vaccine
RBD	Receptor binding domain
RBS	Receptor binding site
RdRp	RNA-dependent RNA polymerase
RIG-I	Retinoic acid inducible gene I
RNA	Ribonucleic acid
RPMI	Roswell Park Memorial Institute
RSV	Respiratory syncytial virus
RT	Room temperature
RT-PCR	Reverse transcription polymerase chain reaction
SARS-CoV	Severe Acute Respiratory Syndrome Coronavirus
SARS-CoV-2	Severe Acute Respiratory Syndrome Coronavirus 2
SDS/PAGE	Sodium dodecyl-sulfate polyacrylamide gel electrophoresis
SFU	Spot forming unit
ssRNA	Single stranded ribonucleic acid
TBA	Thiobarbituric acid
$TCID_{50}$	Tissue culture infectious dose 50%
TCR	T cell receptor
Tfh	T follicular helper
TIV	Trivalent influenza vaccine
TLR	Toll-like receptor
TMB	3,3',5,5'-tetramethylbenzidine
TMPRSS2	Transmembrane serine protease 2
TPCK	L-1-tosylamido-2-phenylethyl chloromethyl ketone
V	Variable
v/v	volume/volume
VE	Vaccine effectiveness
V_H	Variable domain
vRNA	Viral ribonucleic acid
vRNPs	Ribonucleoproteins
w/v	weight/volume
WHO	World Health Organisation

Scientific environment

This PhD project was carried out at the Influenza Centre at the Department of Clinical Science at the University of Bergen. Professor Rebecca Jane Cox was the main supervisor. Assistant Professor Ali Ellebedy, Dr Fan Zhou and Assistant Professor Kristin Greve-Isdahl Mohn were the co-supervisors. The work involving the monoclonal antibodies was performed in Professor Ali Ellebedy's laboratory at the Department of Pathology and Immunology, Washington University in St. Louis, USA, and in Professor Florian Krammer's laboratory at the Department of Microbiology, Icahn School of Medicine, Mount Sinai Hospital, USA, and at Influenza Centre at the University of Bergen.

The project was conducted over 4 years (2018 – 2022) and was funded by the Research Council of Norway under the FluNanoAir project. The research stay in the US was funded by the Research Council of Norway and the Norwegian Graduate School in Infection Biology and Antimicrobials (IBA).

Acknowledgements

My biggest gratitude goes of course to my main supervisor **professor Rebecca Cox**. I am incredibly grateful for all your encouragement and patience throughout this PhD, most recently while writing this thesis. One of the things I have appreciated the most during these four years, is that you have always given me the freedom to be creative and independent, but also providing guidance and the occasional push that I needed to make any impending deadlines.

Your dedication to teaching and mentoring has had a huge influence on me, and it has helped me develop as a researcher. Your devotion to science and research is truly inspiring. I now enjoy spending my time at the office writing a manuscript or analysing data just as much as being in the laboratory doing experiments. We have had a lot of fun working together and we have made many great memories, which I am very grateful for.

I also want to thank my incredible co-supervisors. To **associate professor Kristin Greve-Isdahl Mohn**, thank you for all the valuable and honest advice I have received. Knowing that I could always come to you for advice has been a source of comfort over the years and it has been reassuring to know that I always have someone in my corner. Thank you to **Dr Fan Zhou** for everything you have taught me. Your level of thoroughness and attention to detail is unmatched by any other. Thank you for all your constructive feedback and for all your encouraging words and fun conversations that have brightened up my day during these four years. A special thank you goes out to my co-supervisor **assistant professor Ali Ellebedy** for inviting me to your lab in St. Louis and realising my long-lived dream of making monoclonal antibodies. The collaboration with you, Florian and Rebecca was one of the highlights of my PhD. I am forever grateful for all the advice and the opportunities that you have given me.

I also want to thank everyone at the **influenza centre** for making this such a nice work environment and for always going out of their way to help me whenever I needed it. A special thank you goes to **Nina** and **Elisabeth**. I am so happy that we started our PhDs

at the same time, it has been so much fun having you by my side throughout this whole process. Thank you for all the fantastic memories we have made while travelling, on outings and at lunchtime. Your friendship and support in every aspect of this PhD has meant so much. I also want to thank **Linn** for your help in the lab, but most of all our friendship outside of the lab, I hope we can find a way to continue our annual hiking trips.

Thank you, **Juha**, for always taking the time to answer my endless line of questions, for indulging my ideas and for making so many of them come to life. Thank you, **Anders,** for all the advice that you have given me and especially for your excellent company and collaboration in the lab. Never in my life did I think it would be possible to run 40 plates of ELISA in one day. I am also grateful to **Stefan**, your positive energy and our conversations never fails to brighten my day. Thanks to **Sarah** and **Håkon**, I am grateful for you company and have enjoyed sharing an office with you over the last four years. I am incredibly grateful to **Sonja**, **Therese** and **Geir** for all your assistance in the lab and your help while working together on various projects. I also want to thank Chi and Amit for their support, especially all their help with the statistics for our shared papers, I have really enjoyed working together on our projects. I also want to thank **Nina Langeland,** it has been a pleasure to get to know you and collaborate with you. And to **Karl,** thank you for all your help and the valuable feedback I got while writing this thesis.

I especially want to thank everyone in the Ellebedy lab. Especially **Amena**, **Wafaa** and **Katherine** for teaching me mAb cloning, but most of all your excellent company and our fun conversations. And a special thanks to **Aaron**, **Jackson** and **Philip** for helping me while I was in St. Louis but also remotely after returning to Bergen. I am so happy I got to the opportunity to get to know and work with you all.

Thank you to **Florian Krammer** for inviting me to your lab at Mount Sinai and allowing me to work on this incredibly interesting project. I am grateful to everyone in that lab, but especially to **Meagan** and **Daniel** for all your help during my visit.

I want to thank my friend **Juli,** your friendship and moral support has helped me keep my sanity ever since we first met at Karolinska Institutet many years ago. And thank you to **Seb** for being my go-to person for nearly a decade. I am also grateful to my friends and former colleagues from the Cellnet group **Ina**, **Maria** and **Sissel**. Thank you for your fantastic company and for continuing our lunch tradition at the 5th floor at the BBB.

I especially want to thank my family that has been supporting and rooting for me all these years. Especially **Kurt** and my grandparents, **Mia** and **Kjell**, your enthusiasm for my work has always warmed my heart.

And lastly, but most importantly, I want to thank my mother, **Merethe**. Your unconditional love and support have meant everything. Thank you for teaching me that anything is possible, leading by example, and always encouraging me to follow my dreams, wherever that may take me. Without you, none of this would have been possible. I dedicate this work to you.

Summary

Current seasonal influenza vaccines provide limited protection against antigenically drifted influenza viruses. Consequently, vaccine compositions must be re-evaluated on a biannual basis and annual vaccination is recommended for high-risk groups. The objective of this thesis was to study immune responses after vaccination and infection with influenza virus and severe acute respiratory syndrome corona virus 2 (SARS-CoV-2), with the overarching aim of informing strategies for improving future influenza vaccines.

Here, we investigated the antibody response to neuraminidase (NA), the second most abundant surface glycoprotein of the influenza virus, after infection and vaccination to explore its potential as a target for broader protection against influenza. We found that AS03 adjuvanted pandemic H1N1 vaccination induced durable NA antibody responses and that NA was highly immunogenic, even with low doses in the vaccine. We also found that repeated seasonal vaccination led to maintenance of NA inhibition (NAI) titres but also to reduced seroconversion rates. Our findings support inclusion of adjuvants to increase NA immunogenicity of influenza vaccines and highlights the need for standardisation of the NA component of current vaccines.

Furthermore, we isolated and characterised human anti-NA monoclonal antibodies (mAbs) after pandemic H1N1 infection in 2009. The mAbs had potent NA inhibition activity *in vitro* and they also protected against lethal challenge with influenza A H1N1 and H5N1 viruses *in vivo.* This work led to the discovery of a highly conserved epitope on the N1 NA that can guide rational design of future NA-based vaccines.

Messenger RNA (mRNA) vaccines against SARS-CoV-2 have been highly successful during the coronavirus disease 19 (COVID-19) pandemic and are now emerging as a promising vaccine platform for next-generation influenza vaccines. We have broadly investigated the kinetics and durability of immune responses after vaccination and infection in young and elderly. Our findings indicate that different vaccination regimen may be needed for optimal protection in older adults and can inform immunisation regimens for mRNA vaccination in this high-risk group in the future.

Sammendrag

Influensa er et luftveisvirus som kan forårsake alvorlig sykdom og under stadig forandring *(drift)*. Dagens influensavaksiner gir begrenset beskyttelse mot slike *driftede* influensavirus. Dette fører til at vaksinesammensetningen må revurderes på halvårlig basis, og årlig vaksinasjon anbefales til høyrisikogrupper. Målet med denne avhandlingen var å studere immunresponser etter vaksinasjon og infeksjon med influensavirus og koronaviruset Severe Acute Respiratory Syndrome Coronavirus-2 (SARS-CoV-2), med et overordnet mål om å forbedre fremtidige influensavaksiner.

Vi studerte antistoffresponser mot overflate-proteinet neuraminidase (NA) på influensaviruset etter infeksjon og vaksinasjon. Vi ville studere dette proteinets potensiale til å aktivere bredere immunresponser og evne til å forbedre eksisterende influensavaksiner. Vi fant at den pandemiske H1N1-vaksinen med AS03-adjuvans induserte langvarige NA-antistoffresponser og at NA var svært immunogent, selv i lave mengder. Vi fant også at årlig sesongvaksinasjon bidro til å vedlikeholde antistofftiter mot NA, men resulterte i reduserte serokonversjon, målt som en stigning i NA-antistoffer. Våre funn støtter bruken av adjuvanser for å øke NA-immunogenisiteten til influensavaksiner, samtidig som de understreker behovet for en standardisering av NA-komponenten i eksisterende vaksiner.

Videre ble humane anti-NA monoklonale antistoffer isolert og karakterisert etter pandemisk H1N1-infeksjon i 2009. De monoklonale antistoffene hadde kraftig NA-hemmende aktivitet *in vitro* og beskyttet også mot infeksjon med influensa A H1N1 og H5N1 virus *in vivo*. Dette arbeidet ledet til oppdagelsen av en svært konservert epitop på N1 NA, som en kan dra nytte av i fremtidige NA-baserte vaksineformuleringer.

Messenger RNA (mRNA)-vaksiner mot SARS-CoV-2 har vært svært vellykkede under Covid-19-pandemien, og mRNA-vaksiner fremstår nå som en lovende vaksineplattform for neste generasjons influensavaksiner. Vi sammenlignet kinetikken og varigheten av immunresponser etter vaksinasjon og infeksjon hos unge og eldre voksne. Våre funn indikerer at eldre kan ha behov for et annerledes vaksinasjonsregime enn yngre for å oppnå en gunstig beskyttelse. Denne innsikten bidrar til å utvikle nye, fremtidige mRNA-vaksinasjonsanbefalinger til denne høyrisikogruppen.

List of Publications

I. **Hansen, L.**, McMahon, M., Stadlbauer, D., Vahokoski, J., Schmitz, A. J., Rizk, A. A., Turner, J. S., Alsoussi, W. B., Choreño-Parra, J. A., Jiménez-Alvarez, L., Cruz-Lagunas, A., Zúñiga, Mudd, P. A., J., Cox, R. J., Ellebedy, A. H., Krammer, F.: "Human anti-N1 neuraminidase monoclonal antibodies broadly inhibit influenza A N1 subtype viruses *in vitro* and *in vivo*", *manuscript* (2022).

II. **Hansen, L.**, Zhou, F., Amdam, H., Trieu, M.C. & Cox, R. J.: "Repeated Influenza Vaccination Boosts and Maintains H1N1pdm09 Neuraminidase Antibody Titers", *Frontiers in Immunology,* Vol. 12, (2021).

III. **Hansen, L.**, Brokstad, K.A., Bansal, A., Zhou, F., Bredholt, G., Bredholt Onyango, T., Heitmann Sandnes, H., Elyanow, R., Olofsson, J. S., Madsen, A., Trieu, M-C., Sævik, M., Søyland, H., Vahokoski, J., Ertesvåg, N. U., Fjelltveit, E. B., Shafiani, S., Tøndel, C., Chapman, H., Kaplan, I., Mohn, K. G-I., Bergen COVID-19 Research Group, Langeland, N., Cox, R. J.: "Durable immune responses after BNT162b2 vaccination in home-dwelling older adults", *submitted manuscript* (2022).

Papers not included in this thesis:

I. Turner J.S., Kim W., Kalaidina E., Goss C.W., Rauseo A.M., Schmitz A.J., **Hansen L.**, Haile A., Klebert M.K., Pusic I., O'Halloran J.A., Presti R.M., Ellebedy A.H: "SARS-CoV-2 infection induces long-lived bone marrow plasma cells in humans". *Nature* 595, 421-5, (2021).

II. Zhou F., **Hansen L.**, Pedersen G., Grodeland G., Cox R: "Matrix M Adjuvanted H5N1 Vaccine Elicits Broadly Neutralizing Antibodies and Neuraminidase Inhibiting Antibodies in Humans That Correlate With *In Vivo* Protection". *Front Immunol* 12, 747774, (2021).

III. Ertesvåg N.U., Xiao J., Zhou F., Ljostveit S., Sandnes H., Lartey S., Sævik M., **Hansen L.**, Madsen A., Mohn K.G.I., Fjelltveit E., Olofsson J.S., Tan T.K., Rijal P., Schimanski L., Øyen S., Brokstad K.A., Dunachie S., Jämsén A., James W.S., Harding A.C., Harvala H., Nguyen D., Roberts D., PHE Virology group, Zambon M., Oxford collaborative group, Townsend A., Bergen COVID-19 Research group, Langeland N., Cox R.J.: A rapid antibody screening haemagglutination test for predicting immunity to SARS-CoV-2 variants of concern. *Communications Medicine* 2, 36, (2022).

Table of contents

List of tables

List of figures

1. Introduction

Respiratory pathogens are major threats to public health that can cause significant morbidity and mortality, and vaccines are our most effective prevention against infection and severe disease. In 2009, the world experienced the first influenza pandemic of the 21st century. Although it was a novel influenza A H1N1 virus, we had pre-existing immunity that provided some protection and older adults were better protected than the younger adults (1). This was an unusual pattern because older adults are usually disproportionately affected by severe outcomes from seasonal influenza infection. Nonetheless, this pandemic emphasised the need for rapid vaccine production.

Ten years later, a novel coronavirus emerged to cause a new pandemic. The severe acute respiratory syndrome coronavirus 2 (SARS-CoV-2) spread rapidly across the globe and has had an unimaginable impact on public health, sending ripple effects through global health care systems, global politics and economy. Unlike the influenza A H1N1 pandemic in 2009, the global population had no pre-existing immunity against SARS-CoV-2 and high-risk populations, such as the elderly, have experienced high morbidity and mortality by coronavirus disease-19 (COVID-19). The rapid development and implementation of vaccines have successfully changed the trajectory of this pandemic and has demonstrated the power of vaccines to mitigate the impact of a pandemic.

No one knows which pathogen will cause the next pandemic or when it will occur, however, many lessons can be learned from the two pandemics of the 21st century that can inform the next pandemic outbreak. Here, we have used insight gained from vaccination and infection with SARS-CoV-2 and pandemic influenza A H1N1 to explore different strategies for improving future influenza vaccines.

1.1 Influenza virus

The influenza virus is a single stranded negative sense ribonucleic (RNA) virus that belongs to the *Orthomyxoviridae* family. The influenza virus causes acute respiratory infections that results in significant morbidity and mortality worldwide and is an enormous burden on health care systems. Globally, it is estimated that the 250 000 – 690 000 deaths are associated with seasonal influenza infection each year (2).

1.1.1 Influenza virus structure and genome

The genome of the influenza virus consists of eight single stranded negative sense RNA segments. The segmented genome is bound by ribonucleoproteins and encapsulated in a viral envelope derived from the host cell membrane. The genome encodes ten structural proteins and nine non-structural proteins (3-5). This includes polymerase basic protein 1 (PB1), polymerase basic protein 2 (PB2), polymerase acidic protein (PA), nucleoprotein (NP), matrix protein 1 (M1), non-structural protein 1 (NS1) and nuclear export protein (NEP), which are the internal proteins, and matrix protein 2 (M2), hemagglutinin (HA) and neuraminidase (NA), which are embedded in the envelope **(Figure 1)**. The M2 protein serves as an ion channel, while the M1 protein contributes to the structure of the virion. HA is the most abundant surface protein, followed by NA, and both proteins have essential roles during the replication cycle.

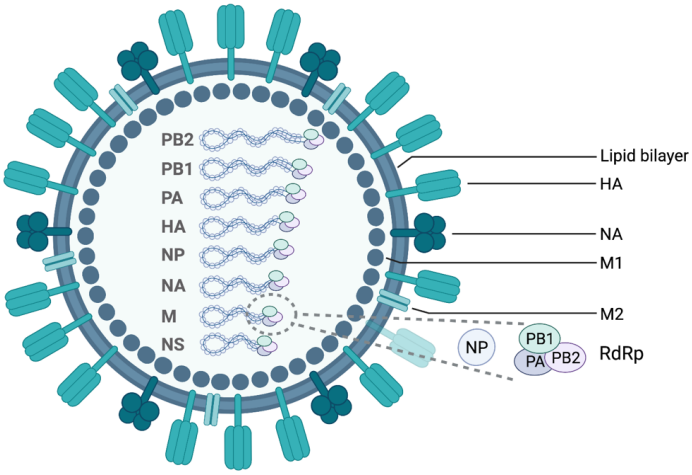

Figure 1: Structure of influenza virus
This figure shows the influenza virion. The envelope of the influenza virus is a lipid bilayer derived from the host cell membrane. It contains the two major surface glycoproteins hemagglutinin (HA) and neuraminidase (NA) and the ion channel matrix protein 2 (M2). The matrix protein 1 (M1) is located in the inside the viral envelope. The viral genome of the influenza virus consists of eight RNA segments that are located inside the virus particle and each segment is bound by the nucleoprotein (NP) and the three viral RNA-dependent RNA polymerases (RdRp). The illustration was created with Biorender.

1.1.2 Viral replication cycle

In humans, influenza virus replication primarily happens in epithelial cells in the respiratory tract. The replication cycle is initiated by HA binding to terminal sialic acids linked to glycans on glycoproteins found on the surface of host cells **(Figure 2)**. The HA-sialic acid binding initiates internalisation of the virus by endocytosis. The endosome is trafficked in the cell and the endosomal pH is reduced, which initiates conformational changes of HA. These conformational changes expose the HA fusion peptide, which is proteolytically cleaved and mediates fusion of the viral and cellular membranes. Following fusion of the viral and host cell membranes, the viral genome, that consists of eight viral ribonucleoproteins (vRNPs), is released into the cytoplasm of the host cell and imported transported to the nucleus. In the nucleus, the viral polymerase complex of the vRNP initiates transcription and replication of the viral RNA. The viral RNA is transcribed into messenger RNA (mRNA) and exported out to the cytoplasm where it is translated into viral proteins. The newly synthesised PB1,

PB2, PA and NP are imported into the nucleus to further facilitate viral RNA synthesis, while the HA, NA and M2 proteins are transported to the plasma membrane. The M1 and NEP proteins are also imported to the nucleus where they bind to newly synthesised vRNPs, which ensures their export to the plasma membrane for virion assembly. Eight vRNPs are incorporated into new virions with a membrane derived upon budding from the host cell plasma membrane that contains the viral surface proteins. During their release, NA cleaves sialic acids on the host cell to reduce binding substrates of HA, which prevents aggregation and facilitates viral spread.

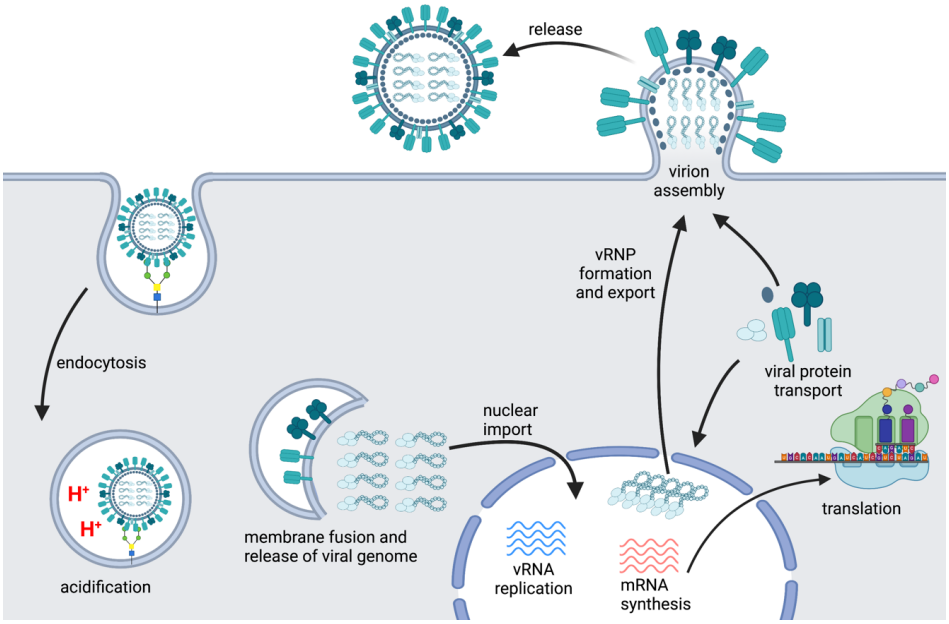

Figure 2: Viral replication cycle
The replication cycle is initiated by binding of HA to sialic acids on the host cell surface, which initiates endocytosis. The endosome is acidified and the reduced pH triggers conformational changes in the HA that initiates fusion of the viral and endosomal membranes, followed by the release of the viral genome. The viral ribonucleoproteins (vRNP) are imported into the nucleus where the viral polymerase complex transcribes and replicates the RNA. The viral RNA (vRNA) is transcribed into messenger RNA (mRNA), which is exported to cytoplasm where it translated into viral proteins. The viral proteins and the vRNPs are transported to the plasma membrane and are assembled into new virions that are released from the host cell surface. The illustration was created with Biorender.

1.1.3 Influenza virus classification

Influenza viruses can be divided into four types: A, B, C and D, where only types A and B cause seasonal epidemics in humans. Influenza A viruses are further divided into subtypes according to the two major surface glycoproteins hemagglutinin (HA) and neuraminidase (NA). HA and NA are divided into different subtypes based on their genetic and antigenic similarities. There are 18 different HA subtypes (H1-18) and 11 NA subtypes (N1-11) found in IAVs. The HA and NA subtypes are further grouped into two groups, groups 1 and 2, based on phylogeny **(Figure 3)**. Influenza B viruses are not divided into subtypes or groups; however, the viruses have diverged into two antigenically distinct lineages that circulate in humans, the Victoria and Yamagata lineages.

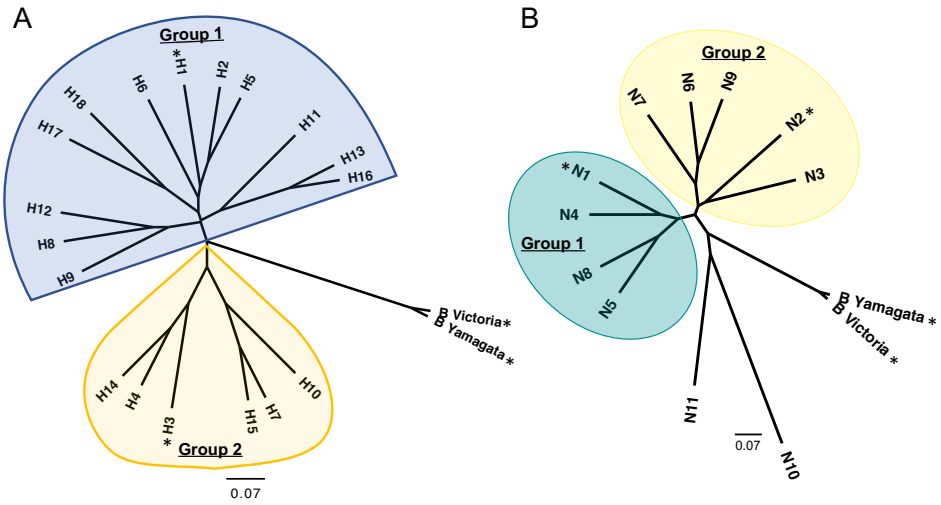

Figure 3: Phylogenetic trees HA and NA subtypes
Phylogenetic tree of HA (H1-18) (**A**) and NA (N1-11) (**B**) subtypes used by influenza A and B viruses. Amino acid sequences of representative viruses from each HA and NA subtype were downloaded from www.gisaid.org and www.fludb.org. The phylogenetic tree was generated in ClustalOmega and visualised in FigTree. The subtypes found in human seasonal influenza viruses are indicated by asterisks. The scale bar represents amino acid substitutions per site.

1.1.4 Hemagglutinin and neuraminidase functional balance

HA is the most abundant surface protein of the influenza virus. It is a trimeric protein with a globular head domain that contains the receptor binding site (RBS) that is specific for sialic acids. NA is the second most abundant surface protein of influenza virus. It is a tetrameric protein with enzymatic function that cleaves terminal sialic acids. An early study from 1942 described the ability of influenza viruses to destroyed cellular receptors that released viruses from red blood cells (6). The enzymatic function of NA was identified in 1957 and it got its name due to its ability to release *N*-acetyl neuraminic acid (7). The NA enzyme activity is essential for the release of newly formed viruses from the host cell by cleavage of the sialic acids on glycosylated host surface proteins. If the enzyme activity is inhibited, the viruses aggregate on the host cell surface through HA-sialic acid binding (8). In addition to its function at the end of the replication cycle, NA may also contribute to increased infectivity by facilitating movement through mucus in the respiratory tract (9), where sialic acids are highly abundant. The spatial distribution of HA and NA on the viral surface has been found to be clustered and asymmetrical (10, 11), which may aide the movement of viruses in the mucus of the upper respiratory tract (12).

Due to the antagonistic properties of these two proteins, a functional balance of the abundance, affinity, avidity, enzymatic activity and the spatial distribution of these proteins on the virion is essential for optimal infectivity. Although the avidity of a single HA trimer for sialic acid is low, multivalent binding of multiple HA trimers results in significant avidity. This makes attachment nearly irreversible without mitigating factors, such as NA enzyme activity or RBS-blocking antibodies. On the other hand, NA must have sufficient activity to release and disaggregate virions, but not so much that it reduces HA-mediated attachment required for initiating infection. The influenza virus utilises several mechanisms for optimising the stoichiometry of HA and NA. Influenza virus with an NA with short stalk length was found to have reduced NA activity and reduced fitness. However, mutations in the HA gene close to the RBS was identified, which compensated for the reduced NA activity, that restored viral replication (13). Furthermore, escape mutant virus (EMV) generated with anti-

HA mAbs acquired mutations in the NA gene that interfered with NA assembly or trafficking to the plasma membrane, resulting in reduced incorporation of NA on the virion (14, 15). Mutant viruses that lacked sialidase activity were capable of replication due to acquiring mutations surrounding the RBS that decrease affinity and binding to sialic acids (16).

1.1.5 Determinants of influenza A host tropism

Zoonotic influenza A viruses that cross between species, that are antigenically distinct from those circulating in human and are capable of efficient infection and sustained transmission in humans are likely to cause pandemics. The primary reservoir of influenza A viruses is wild aquatic birds; however, these viruses also circulate in a wide range of other host species including, but not limited to, humans, swine and poultry. Fortunately, there are several factors that determine host tropism and limits the likelihood of novel viruses crossing over to humans to cause pandemics. These factors influence specificity of virus attachment, genome delivery, polymerase activity and evasion of host innate responses. Some of the determinants of host tropism for influenza A viruses are described below.

The specificity of HA for various types of sialic acid linkage is a major contributor to their host and organ tropism. The linkage of terminal sialic acids to the galactose of glycoproteins dictates specificity of HA. Avian HAs favour α2,3-linked sialic acids (17), whereas human influenza B viruses have acquired mutations that generally favours binding to α2,6-linked sialic acids (18). The acquisition of mutations that allow for changes in HA specificity that do not come at a significant fitness cost is a key determining factor for the pandemic potential of many viruses. NA has also been found to contribute to host tropism. Viruses that have NA proteins with shorter stalks have lower airborne transmission between ferrets, possibly due to reduced cleavage of decoy receptors in the mucus (19). The functional balance of HA and NA is essential for efficient replication and is a determinant of host tropism (13). The HA-NA balance has implications for airborne transmission of viruses, which was found to be a contributing

factor for sustained transmission of the influenza A H1N1 pandemic virus in 2009 (20-22).

Some factors determine host tropism at the stage of viral genome delivery. Endosomal pH varies between host species and the pH that triggers HA conformational changes differ among HA proteins, thus the pH stability of HA is one of the determinants of viral tropism (23). The activity of the viral RNA polymerase protein is affected by temperature (24, 25). The temperature of the upper respiratory tract in humans is lower than that of swine and birds, which affects the activity of the RNA polymerase and the replication of viral RNA. Furthermore, the transport of vRNPs to the nucleus is inhibited by interferon-regulated GTP-binding protein myxovirus resistance protein A (MxA) (26, 27). The vRNP transportation in avian influenza viruses are inhibited by the human MxA, however, mutations in the NP protein of H7N9 have been found evade this effect (28).

1.1.6 Antigenic drift and shift

The high genetic diversity and rapid evolution of influenza viruses is a result of antigenic drift and antigenic shift. Antigenic drift is the accumulation of point mutations during replication (**Figure 4**). The virus acquires mutations due to the lack of proofreading mechanism of the viral RNA polymerase, which contributes to the high mutation rate of influenza viruses. Antigenic drift facilitates efficient immune evasion, which is often driven by selective pressure from antibodies to the surface proteins HA and NA.

Antigenic shift is the recombination of gene segments between two or more viruses during co-infection, which result in novel viruses (**Figure 4**). The segmented genome of influenza viruses permits for novel combinations of the gene segments, resulting in reassortant viruses that are antigenically distinct from those circulating and may have the potential to cause a pandemic.

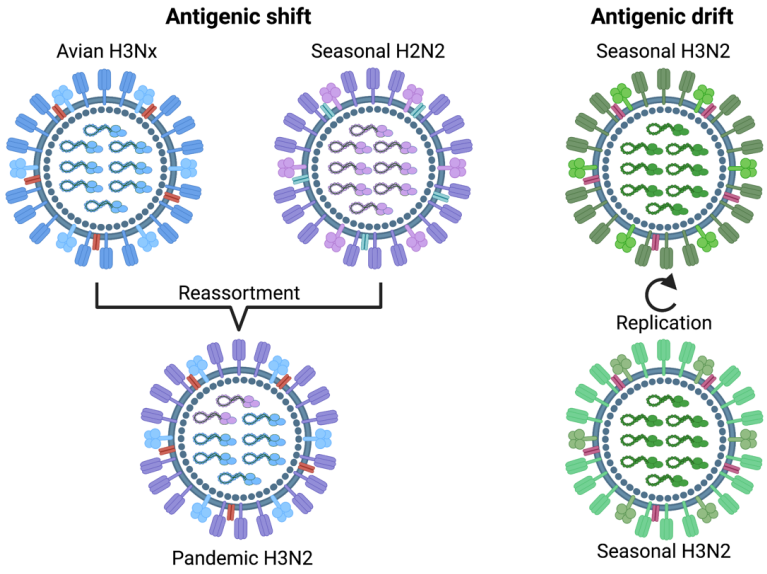

Figure 4: Antigenic shift and drift
A schematic showing the basis of antigenic drift and shift using influenza A H3N2 as an example. Antigenic shift describes the recombination of RNA segments of one or more viruses during co-infection to make a novel influenza virus. The 1968 H3N2 pandemic was caused by the reassortment of the seasonal H2N2 virus and an avian H3Nx virus, where the NA was of unknown subtype. This resulted in the novel H3N2 virus that caused a pandemic in 1968. Antigenic shift is the accumulation of mutations that arise during viral replication. The surface proteins HA and NA of the H3N2 virus mutate, resulting in the emergence of new strains of the H3N2 virus that evade our pre-existing immunity to cause seasonal epidemics. The illustration was created with biorender.

1.1.7 History of influenza pandemics

Influenza A viruses have caused several pandemics in the 20th and 21st centuries (**Figure 5**). The deadliest influenza pandemic was caused by the H1N1 virus in 1918 and is estimated to have caused 50 million deaths globally (29, 30). Descendants of the 1918 H1N1 virus have circulated in humans since its emergence, with the exception of a 20-year period between 1957 to 1977. The H1N1 virus re-emerged in 1977 and caused a pseudo-pandemic, however, it primarily infected individuals under the age of 30. This virus was similar to the H1N1 strains that had circulated from 1946 to 1957, which explained the disproportionate impact among younger individuals as they had never been exposed to any H1N1 viruses during their lifetime and had limited pre-existing immunity (31). A H2N2 virus emerged to cause a pandemic in 1957 that

resulted in 1.1 million deaths and the H2N2 continued to circulate and cause epidemics in human until 1968 (32). In 1968, another pandemic was caused by a novel H3N2 virus, which displaced the H2N2 virus and continues to circulate in humans today (**Figure 4**). The N2 NA remained unchanged (33) and pre-existing antibodies to N2 NA antibodies protected against infection, which likely decreased the impact of this pandemic (34, 35).

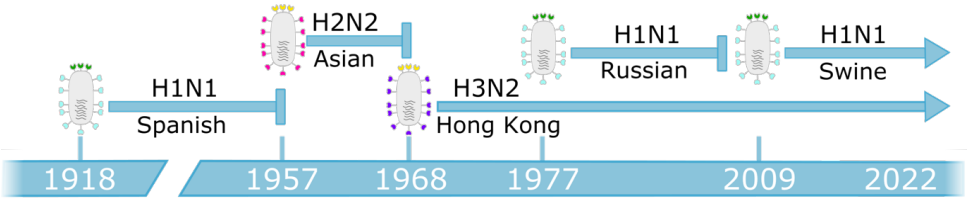

Figure 5: History of influenza pandemics
Historical overview of influenza A viruses that have caused pandemics in humans in the 20th and 21st centuries. The illustration was created with Inkscape.

The first influenza virus pandemic of the 21st century was caused by a novel H1N1 virus in 2009. The virus originated from pigs and resulted from the reassortment of North American H3N2 and H2N1 swine viruses with the Eurasian avian-like swine viruses (36) (**Figure 6**). The HA gene was of classical swine virus origin and NA was of Eurasian avian-like swine virus origin (36). The first case of pandemic H1N1 virus was reported in Mexico in February of 2009 and on June 11th 2009, the World Health Organization (WHO) declared a pandemic (37). On the 21st of April, the Centers for Disease Control and Prevention (CDC) in the US began working on developing a vaccine and the first clinical trials were started on the 22nd of July. The pandemic vaccine was approved by the Food and Drug Agency (FDA) on 15th September and the first doses were administered on the 30th September (38). In Europe, the European Medicines Agency (EMA) recommended the approval of pandemic vaccines from Novartis and GlaxoSmithKline (GSK) on the 25th September and mass vaccination in Europe started on the 25th October 2009, four months after the start of the pandemic. By 19th November, the WHO announced that around 65 million individuals had been vaccinated worldwide (39). The global mortality caused by the 2009 H1N1 pandemic

during the first year was estimated to be around 200 000 (40), although this was probably a vast underestimate.

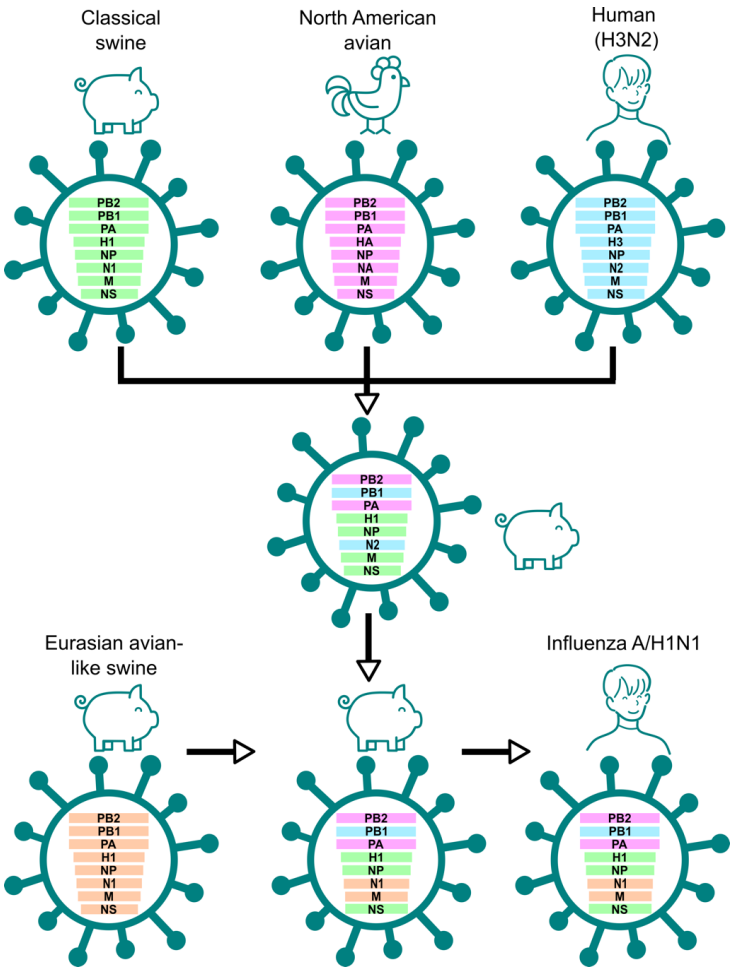

Figure 6: Origin of the 2009 pandemic H1N1 virus
A novel H1N1 virus emerged and caused a pandemic in 2009. A reassortment of a human H2N2, North American avian and a classical swine virus generated a triple reassortant virus and circulated in North American pigs. The triple reassortant virus reassorted with a Eurasian avian-like swine virus to generate the pandemic H1N1 virus that is now circulating in humans. The illustration was created in Inkscape.

1.2 Immune responses to influenza

1.2.1 Innate immune responses

The innate immune response is essential for the initial control of influenza infection. Its primary functions are to restrict viral replication in infected cells, to induce an antiviral state for alerting surrounding cells of infection and lastly, to prime the adaptive immune response.

Pattern recognition receptors (PRRs) recognise pathogen associated molecular patterns (PAMPs) and activate innate immune signalling pathways for the production of cytokines and antiviral molecules. The main PRRs that are important for the innate immune response against influenza virus are retinoic acid-inducible gene-I protein (RIG-I) and toll-like receptors (TLR) 3, 7 and 8. RIG-I recognises single stranded RNA (ssRNA) and transcriptional intermediates of the influenza virus. TLR-3 is found on the membrane of the cell surface and in the endosome. It recognises double stranded RNA; however, the RNA of the influenza virus is single stranded. The dsRNA intermediated of the influenza virus during replication is rapidly degraded (41), thus the exact interaction of the TLR3 and influenza virus is not entirely clear. Nevertheless, mice that do not express TLR3 have higher viral loads (42) and humans with mutations in the TLR3 gene is associated with encephalopathy due to influenza infection (43). TLR7 and 8 are found on the endosomal membrane and recognise ssRNA of influenza viruses at the early stages of the replication cycle during entry.

These PRRs initiate a signalling cascade that results in activation of transcription factors, such as kappa-light-chain-enhancer of activated B cells (NF-κB). This initiates production of proinflammatory cytokines and chemokines that are important for recruitment and activation of innate immune cells, such as dendritic cells, neutrophils, macrophages. Macrophages are phagocytes that are essential for eliminating influenza virus from the lower respiratory tract and macrophage ablation is known to enhance morbidity and mortality in animal models (44, 45). Type I and III IFNs induce an antiviral state by promoting expression of IFN-stimulating genes (ISGs). The proteins

encoded by ISGs have two main functions, to limit viral replication by shutting down protein synthesis (46) and to trigger apoptosis (47). They also promote antigen presentation and production of cytokines involved in T and B cell activation. The ISG encoding the MxA is important in influenza infection because it inhibits the transport of the vRNPs to the nucleus (26, 27).

In addition to initiating an antiviral state in infected cells and their surrounding environment, the innate immune response is also important for priming of the adaptive immune response. Dendritic cells (DCs) are professional antigen-presenting cells that are surveying for pathogens, which are internalised and presented to B and T cells in the draining lymph nodes.

1.2.2 Adaptive immunity

The adaptive immune response is essential for controlling most viral infections, including influenza, and the three principal cellular components of the adaptive response are B cells, $CD4^+$ T cells and $CD8^+$ T cells. B cells produce antibodies, $CD4^+$ T cells have several important helper and effector functions that modulate other immune cells, and $CD8^+$ T cells kill infected cells. The adaptive immune response is instrumental for the prevention, control and elimination of influenza virus infections. Thus, the adaptive immune response and the induction of immune memory are essential for the success of influenza vaccines.

1.2.3 Humoral immunity

B cells and antibodies are essential for protection against influenza virus infection and the main targets of the antibody response are the surface proteins HA and NA. Most naïve B cells are activated in a T cell-dependent manner, which involves help from $CD4^+$ T cells for B cell differentiation and affinity maturation (**Figure 7A**). Naive B cells are activated and become extrafollicular plasmablasts or germinal centre (GC) B cells. Activated B cells that differentiate into antibody-secreting plasmablasts are an important immediate source of antibodies. B cells that enter the GC will proliferate and

go through affinity maturation to increase the affinity of the B cell receptor (BCR). B cells in the dark zone of the GC proliferate and mutate their antibody genes to increase BCR affinity. Then, they migrate to the light zone where they compete for binding to antigen presented by folicular dendritic cells (fDC). The B cells internalise the antigens and present them as peptides to cognate $CD4^+$ T follicular helper cells (Tfh) that produce pro-survival signals, while B cells that do not engage Tfh cells wil undergo apoptosis. The Tfh cells select for high-affinity B cell clones that goes on to differentiate into long-lived plasma cells or memory B cells. Long-lived plasma cells reside in the bone marrow where they persist for many years and continue to produce antibodies that are an important source of long-term antibodies to influenza virus. Memory B cells also persist for many years but reside in tissues and the periphery where they can be rapidly reactivated upon re-exposure to the influenza virus. Seasonal influenza vaccines have been found to induced GC responses that engage both memory B and naïve B cells in humans (48).

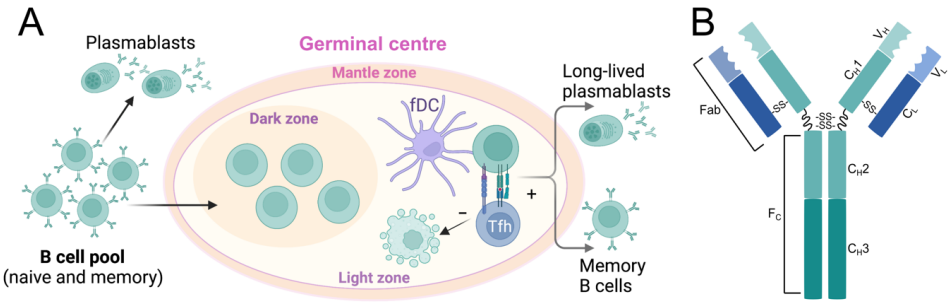

Figure 7: B cell response and antibody structure
(A) Naïve and memory B cells are activated by influenza antigens and rapidly differentiate into plasmablasts or enter the germinal centre (GC) for clonal expansion and affinity maturation. B cells in the dark zone of the GC will proliferate and mutate the antibody genes to increase affinity of the B cell receptor. The B cells migrate to the light zone where they compete for binding to antigen presented by folicular dendritic cells (fDC). The B cells internalise the antigens and present them as peptides to cognate $CD4^+$ T follicular helper cells (Tfh) that produce pro-survival signals. The B cells can differentiate into long-lived plasma cells or memory B cells. **(B)** An illustration of the structure of an antibody. The two light chains are coloured in blue and the heavy chains are coloured in green.
The illustrations were created with Biorender and Inkscape.

Antibodies are Y-shaped glycoproteins belonging to the immunoglobulin (Ig) superfamily. An antibody consists of four polypeptide chains: two identical heavy chains and two identical light chains (**Figure 7B**). The light chain consists of one variable domain (V_L) and one constant domain (C_L). Similarly, the heavy chain consists of one variable domain (V_H) but has three constant domains (C_H1, 2, 3). The antibody has a fragment crystallisable (Fc) region and two identical antigen-binding fragments (Fab). The two heavy chains are connected through two disulphide bonds, which form the flexible hinge region. The Fc region determines the isotypes of the antibody, which for human antibodies include IgG, IgM, IgA, IgE and IgD. The isotype of the antibody dictates its effector functions. The heavy and light chains of the Fabs are joined by one sulphide bond and the dimerization of paired heavy and light variable regions creates one antigen binding site. The heavy chain variable region is encoded by the three gene segments called variable (V), diversity (D) and joining (J) segments, while the light chain variable region is only encoded by the V and L segments. There are multiple copies of the V, D and J genes and it is the somatic recombination of these genes that generates the different variable regions with unique binding specificities. This process is known as V(D)J recombination. The antigen binding site consists of three hypervariable loops called complementarity-determining region (CDR) 1-3 and four framework regions (FR) on either side of the CDRs.

The high polymorphism of the heavy and light chain loci results in extensive combinatorial diversity. In addition to this, the process of joining these segments together is not perfect and nucleotides may be added or lost during this process, adding to this diversity. The diversity is further increased by the combination of different heavy and light chains. Another mechanism that contributes to the breadth of the BCR repertoire is somatic hypermutation, which is a process that takes place in the germinal centre where the variable region genes mutate to form higher affinity BCRs. In theory, an infinite number of antibodies with unique binding specificities can therefore be generated.

1.2.4 Antibody responses to neuraminidase

Early studies in the 1970s and 1990s found that NA was immunogenic in humans and mice, and that NA-specific antibodies reduced morbidity of influenza infection (49-54). The benefit of NA-specific antibodies was clearly demonstrated during the 1968 H3N2 pandemic where pre-existing antibodies to the N2 NA from H2N2 exposure protected against infection (34, 35). Since then, the correlation between NA-specific antibodies and protection has been corroborated in both human challenge and field studies (55-57). Furthermore, several animal studies have found that NA-specific antibodies protect against lethal influenza infection and are capable of preventing transmission in guinea pigs (58-61).

NA-specific antibodies can inhibit the enzyme activity of NA. Antibodies can inhibit the enzyme activity allosterically by binding directly to the active site or through steric hindrance by binding to epitopes surrounding the active site and restricting access to substrates. Inhibition of NA enzyme activity prevents the release of newly formed viruses from the host cell membrane during budding, causing them to aggregate on the surface of the dying host cell, which inhibits viral spread (**Figure 8**) (8). It is also possible that NA inhibition (NAI) antibodies may have a role in reducing infectivity by preventing penetration of the mucus layer in the airways to reach the underlying epithelial cells. Lastly, NA-specific antibodies that activate of Fc-mediated effector functions have been shown to suppress virus pathogenicity *in vivo* and antibodies lacking NAI activity may require Fc-mediated effector cell activation to achieve protection (62-64).

1.2.5 Antibody responses to hemagglutinin

HA-specific antibodies target two domains of the HA protein, the head and the stalk domain. Antibodies that target these two domains have different modes of action and inhibit the influenza virus at different stages of the replication cycle (**Figure 8**). HA head antibodies are often neutralising by blocking the binding between HA and sialic acids to prevent infection. These antibodies can be measured by the hemagglutination

inhibition (HAI) assay. The HA head has high plasticity and mutations accumulate in this domain, which limits the breadth of these antibodies.

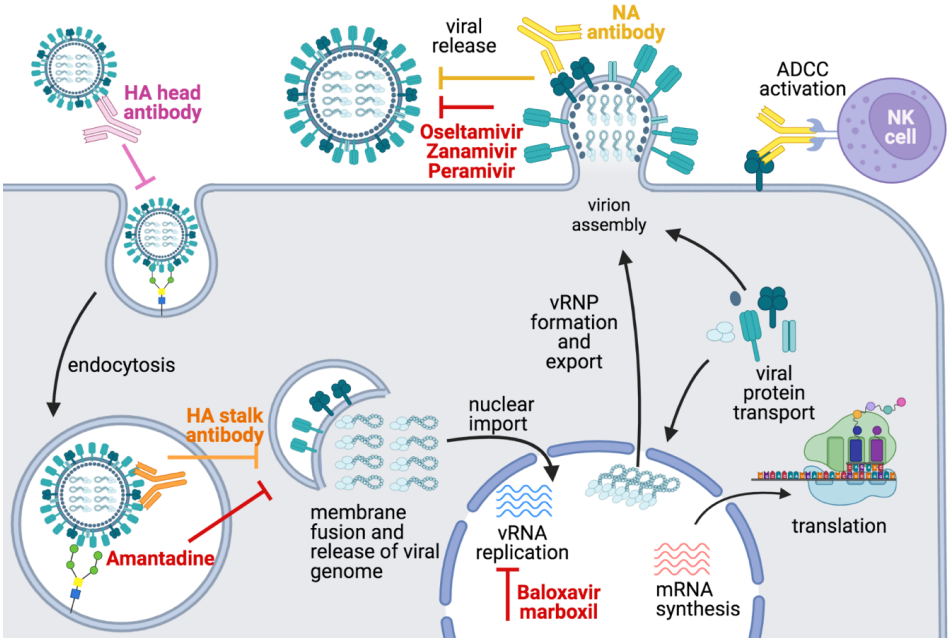

Figure 8: Mode of action for antiviral drugs and antibodies to influenza virus
Antibodies and antiviral drugs target and inhibit the viral replication cycle at various stages. Antibodies to the HA head domain can block attachment to sialic acids on the host cell surface proteins and inhibit endocytosis. HA stalk antibodies that are endocytosed together with the virus can inhibit fusion of the viral and endosomal membranes by locking the HA in the pre-fusion conformation. NA enzyme activity can be inhibited by NA antibodies and prevent release of budding viruses. HA stalk antibodies can also inhibit NA enzyme activity by steric hindrance (not shown). Both NA and HA antibodies can bind activate antibody dependent cellular cytotoxicity through effector cells such as natural killer (NK) cells.The amantadine antiviral drug inhibits M2 and prevent fusion of viral and endosomal membranes. Baloxavir marboxil inhibits the endonuclease activity of the viral polymerase complex and prevents replication of viral RNA (vRNA) in the nucleus. Oseltamivir, zanamivir and peramivir are NA inhibitors and prevent the release of budding viruses, similarly to NA antibodies. The illustration was created with Biorender.

HA stalk antibodies can also be neutralising but through different mechanisms than the HA head antibodies. Some stalk antibodies can inhibit the proteolytic cleavage of HA needed for the conformational changes that initiates fusion of the host and viral membranes (65). Consequently, they do not block attachment of the virus to the host

cell or endocytosis and cannot be measured by the HAI assay, but neutralisation can be measured by the microneutralisation assay. Some HA stalk antibodies need to interact with Fc receptor for IgG (FcγR) and to provide protection *in vivo*, possibly mediated by ADCC (62, 63).

Additionally, some HA stalk antibodies have been found to inhibit NA by steric hindrance (66, 67). The stalk is more conserved than the head domain and stalk antibodies are usually more broadly reactive. Antibodies with cross-reactivity to multiple HAs within group 1 and within group 2 (68), and even across groups and between influenza A and B viruses have been identified (69, 70). HA stalk antibodies have also been shown to reduce replication and transmission of influenza virus in ferrets (71). Therefore, the HA-stalk has been explored as a potential target for universal influenza vaccines (72).

Other influenza proteins, such as the NP, M2e are also targeted by antibodies and may contribute to protection (73), however they will not be described in further detail as it is outside the scope of this thesis.

1.2.6 Cellular immune responses

$CD4^+$ T cells have several important helper and effector functions that modulate other immune cells, including B cells and $CD8^+$ T cells, where the latter is important for killing infected cells. These functions are important for controlling infection and the contribution of influenza-specific $CD4^+$ and $CD8^+$ T cells have been reported in several human studies. $CD4^+$ Tfh cells are important for proliferation and differentiation of GC B cells and have been correlated with increased number of antibody-secreting cells and antibody titres after vaccination (74, 75). Pre-existing $CD4^+$ T cells have also been associated with reduced illness and viral shedding of influenza A H3N2 and H1N1 viruses in a human challenge study (76) and pre-existing $CD8^+$ T cells were inversely correlated with disease severity during pandemic H1N1 infection (77). In addition to surface proteins HA and NA, T cells also target the internal proteins, such as M1 and

NP (78), which are more conserved than the surface proteins HA and NA. Consequently, T cell responses can react to more influenza viruses and contribute to heterosubtypic immunity (79).

1.2.7 Correlates of protection

The primary correlate of protection (CoP) against influenza infection is the HAI titre, which is widely used by regulators for the evaluation and approval of seasonal influenza vaccines. Antibodies measured by the HAI assay block the binding between HA and sialic acids, which inhibits the attachment of the virus and are therefore considered a surrogate of neutralisation (80). Early studies conducted in the 1970s laid the foundation for the HAI titre as a CoP against influenza virus infection. A study by Hobson *et al*. in 1972 found that serum HAI titres of 40-60 were associated with 50% infection rate among individuals in a human challenge study (81). In 1977, Potter *et al.* found that only 29% of individuals with HAI titres between 40-60 were infected (82). This has since been corroborated by recent human challenge and field studies (55, 56).

Although the HI antibody titre is the only recognised CoP by regulators, there are other types of immunity and immune targets that correlate with protection against influenza infection and illness. NA-specific antibodies have also been correlated with protection, reduced viral shedding and reduce disease severity in humans (55, 57, 83, 84). Several studies have identified binding NA antibodies and NAI antibody titre as CoP, which in some studies correlated with protection independently of HAI titres (49, 55, 56, 84). HA stalk antibodies have also been correlated with protection from influenza infection (56). As mentioned in the section above, pre-existing $CD4^+$ T cells were associated with reduced illness and viral shedding of influenza A H3N2 and H1N1 virus in a human challenge study (76) and pre-existing $CD8^+$ T cells were inversely correlated with disease severity during pandemic H1N1 infection (77).

1.2.8 Repeated vaccination and pre-existing immunity

Immunity to influenza is complex as we undergo a number of influenza infections during our lifetime with most children primed against influenza virus by five years of age (85, 86). Original antigenic sin (OAS) was first described in 1960 by Francis Thomas Jr. (87). They found that the highest HAI titres were against the seasonal influenza strains that a specific age cohort had first been exposed to, thus originating "a sin" (88). The anamnestic recall of B cells to earlier influenza virus strains may preferentially boost responses to shared epitopes of the new vaccine strain. Although these B cells may recognise these shared epitopes, they may have lower affinity to the new strain, resulting in a low-affinity antibody response. Whether the OAS phenomenon can be used to explain findings of blunted immune responses after repeated vaccination remain controversial.

Annual influenza vaccination is recommended for high-risk and occupational groups, which contributes to high levels of pre-existing immunity that may impact upon vaccine-induced responses. The impact of exposure history and pre-existing immunity to influenza virus on induction of vaccine responses is a complex issue that is not fully understood. Early studies found that individuals with high pre-existing HAI titres had reduced boosting of HAI titres after re-vaccination (89, 90). Since then, other studies have elaborated on those findings. Repeated vaccination and high pre-existing titres have been associated with reduced boosting of B cell responses and antibody titres after vaccination (91-93). These studies focused on HA-specific responses, however, reduced antibody responses to NA after a second vaccination have been reported in individuals vaccinated in two consecutive years (94). Furthermore, repeated seasonal influenza vaccination has been associated with reduced immunogenicity (95-97) and VE, especially for H3N2 viruses (98-100).

Although there is evidence showing that pre-existing immunity modulates vaccine responses against influenza, the underlying mechanisms are not well understood. Three mathematical models have been proposed to explain this effect by immunological mechanisms (101, 102). The antigen clearance model propose that pre-existing

antibodies bind to and clear the antigen after vaccination. This reduces the duration and amount of available antigen, which again reduces proliferation of B cell and antibody production. The second model is the Fc receptor-mediated inhibition model, which proposes that pre-existing antibodies bind to antigens and form inhibitory immune complexes that inhibit B cell activation.

Lastly, the epitope masking model propose that pre-existing antibodies and B cells that are specific for the same epitope will compete for binding and inhibit proliferation of epitope-specific B cells. This could also happen as a result of physical inference due to the size of the antibody and would not inhibit binding of B cells that bind to spatially distant epitopes. Therefore, this model allows for boosting of antibodies to other epitopes on the antigen. This model was found to be most statistically likely to explain why antibody responses to HA after primary immunisation with novel H5N1 were skewed toward the stem, whereas the antibody response was skewed towards the HA head after secondary immunisation. They hypothesise that cross-reactive memory B cells specific for conserved stem epitopes dominate the primary response and that the high level of pre-existing antibody titres to the stem interfere with further boosting of stem antibodies in the secondary response. Epitopes on the HA head are distant to the stem, which would allow for binding and activation of head-specific B cells (102, 103).

1.3 Influenza treatment

There are several antiviral drugs used for treatment of influenza infection and they target various processes during the replication cycle (**Figure 8**). The NA inhibitors include oseltamivir, that is taken orally, zanamivir that is administered by oral inhalation, and peramivir, which is administered intravenously. Solving the three-dimensional structure of NA led to the rational design of NA inhibitors that mimic the natural substrate (104-107). A systematic review of 83 clinical trials involving oseltamivir found that it reduced the duration of symptoms, however, early administrations appear to be key for treatment efficacy (108, 109). Oseltamivir-resistance was a major issue among seasonal H1N1 viruses circulating before the 2009

pandemic (110), however, the pandemic H1N1 virus with N1 NA from Eurasian avian-like swine was sensitive to oseltamivir (111). Amantadine is an M2 inhibitor that stops the influx of protons onto the virion in the endosome, which inhibits membrane fusion and release of the viral genome. Nearly all influenza A viruses have acquired resistance to this drug now (112). The antiviral drug Baloxavir marboxil inhibits the endonuclease activity of the viral polymerase complex and prevents replication of viral RNA. This drug has been found to reduce symptoms and have similar efficacy as oseltamivir for influenza infection (113).

1.4 Seasonal influenza vaccines

Vaccination is the most effective method of preventing influenza infections during epidemics and pandemics. There are currently three different types of seasonal influenza vaccines available on the market, including inactivated split and subunit vaccines, live attenuated influenza virus (LAIV) and recombinant HA protein (**Figure 9**).

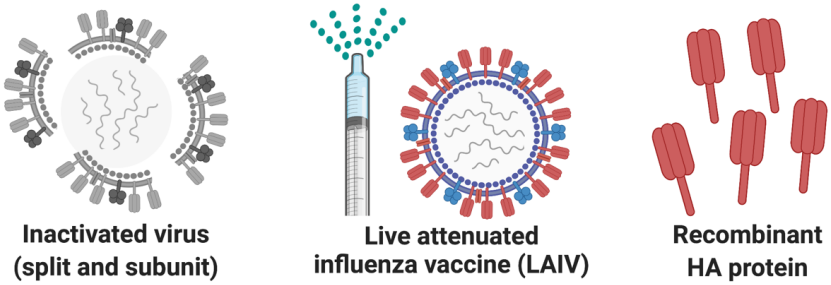

Figure 9: Types of seasonal influenza vaccines
There are currently three different types of vaccines commonly used as seasonal influenza vaccines. Inactivated virus vaccines are produced as split and subunit vaccines, which can be produced in embryonated chicken eggs or cell culture. The live attenuated influenza vaccine (LAIV) is a vaccine administered intranasally and contains temperature sensitive, cold adapted influenza virus that limits viral replication to the upper respiratory tract. These vaccines are produced in embryonated chicken eggs. Recombinant hemagglutinin (HA) protein vaccines consist of HA proteins expressed in insect cells though the baculovirus expression system. The illustration was created with Biorender.

The Global Influenza Surveillance and Response System (GISRS) is a global surveillance network for monitoring the spread of influenza viruses. The GISRS consists of more than 150 laboratories in 114 countries, which represents 91% of the global population. Over two million respiratory specimens are tested each year to monitor the spread and evolution of influenza viruses (114). The WHO reviews the data collected by the GISRS on a biannually basis and uses antigenic and genetic characterisation, antigenic cartography and predictive modelling for selecting the viruses to be included in the influenza vaccines for the upcoming Northern and Southern hemisphere season. Once the candidate viruses have been selected, seed viruses for vaccine production are generated through reassortment. The HA and NA genes of the recommended influenza A H1N1 and H3N2 viruses are reassorted with the internal protein genes of the A/Puerto Rico/8/1934 (H1N1) virus (**Figure 6A**). The A/Puerto Rico/8/1934 (H1N1) virus is adapted to growth in chicken eggs and ensures high yields and rapid production of vaccines. These reassortant viruses are then provided to vaccine manufacturers for large-scale production and global distribution of influenza vaccines.

Propagation of influenza viruses in embryonated chicken eggs is a well-established platform for influenza vaccine production that have been use since the 1940s. Today, approximately 85% of seasonal influenza vaccines are produced by this platform, while the remaining 15% are produced in cell-culture (115). The egg-based platform is used for the production of both inactivated and live attenuated influenza vaccines. Inactivated influenza vaccines (IIV) are produced as trivalent influenza vaccines (TIV), which contains one influenza A virus from each of the H1N1 and H3N2 subtypes and one influenza B virus from either the Yamagata or Victoria lineages. Quadrivalent vaccines (QIV) contain two influenza B viruses, one from each of the lineages, in addition to the influenza A H1N1 and H3N2 viruses. The TIV and QIV can be produced as inactivated whole virus, split virus or subunit virus vaccines. Inactivated whole virus vaccines have higher levels of reactogenicity, therefore split or subunit vaccines are more commonly used. Both split and subunit vaccines are produced from inactivated virus, but the downstream purification processes are different for the two vaccine types.

These vaccines involve splitting of the individual viral components by treating the inactivated virus with detergents or solvents to disrupt the viral membrane, followed by purification to enrich the viral proteins HA and NA for split vaccines, or nearly pure HA for the subunit vaccines. The LAIV is an intra-nasal vaccine. It consists of live attenuated influenza virus engineered to grow at 33°C, which limits the viral replication to the upper respiratory tract.

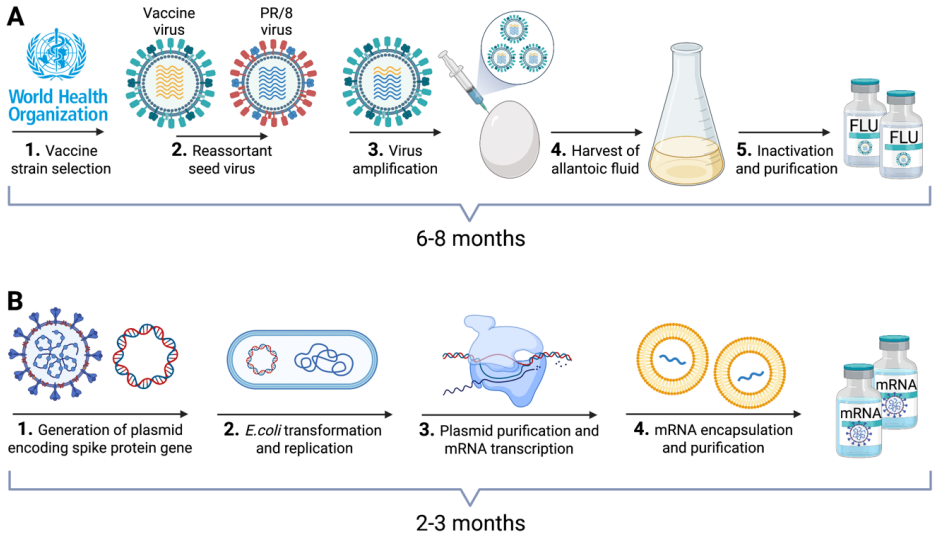

Figure 10: Production of influenza vaccines and SARS-CoV-2 mRNA vaccines
(A) Production of egg-based seasonal inactivated influenza vaccines. The WHO selects the vaccine strains in February and generates reassortant seed viruses that have the HA and NA proteins of the vaccine strains and the internal proteins of the A/Puerto Rico/8/1934 (H1N1) virus (PR/8 virus) to ensure rapid replication of vaccine viruses. The reassortant seed viruses are distributed to vaccine manufacturers that produce the vaccines by growing the viruses in embryonated chicken eggs. The allantoic fluid is harvested from the eggs and the viruses are chemically inactivated and enriched for HA and NA proteins, and purified. The vaccines are distributed and deployed 6-8 months later at the start of the influenza season. **(B)** Production of SARS-CoV-2 mRNA vaccines. A plasmid encoding the genetic sequence of the SARS-CoV-2 spike protein is generated and transformed in *E. coli* for rapid plasmid replication. The plasmids are purified, and the DNA is transcribed into mRNA, which is encapsulated in lipid nanoparticles and purified. This illustration was created with Biorender and inspired by Bartley *et al*. (116).

Although the majority of seasonal influenza vaccines are egg-based, there are several downsides associated with this production platform. The production of egg-based vaccines is time-consuming and consequently the vaccine production must start 6

months before the start of the upcoming influenza season. Therefore, the WHO has to select viruses for vaccine composition many months before the start of the influenza season to ensure adequate supply of vaccines. This increases the likelihood of mismatch of vaccine and circulating strains, as the viruses continue to mutate during this time. Mutations may arise during virus propagation due to adaptation to growth in eggs, which can also contribute to mismatching of vaccine and circulating strains (117). Furthermore, the platform is dependent on the availability of embryonated chicken eggs, which may be a limiting factor, especially in the event of a new influenza pandemic.

In addition to the egg-based vaccines, cell-based and recombinant influenza vaccines are available. The cell-based vaccine platform uses cell lines to grow up the viruses, e.g. the Madin-Darby canine kidney (MDCK) and Vero cell lines, which are more versatile than embryonated eggs. Recombinant vaccines contain recombinant influenza protein produced in insect cells that are infected by baculovirus that is engineered to express the influenza genes. Both of these vaccine platforms bypass the issue of egg-adapted mutations that may arise during virus propagation and they are safe to use for individuals with egg allergies.

Older adults are prioritised for influenza vaccination as they are considered a high-risk group with increased risk of developing severe disease, hospitalisation and death by influenza infection. The CDC estimated that 70-85% of deaths associated with seasonal influenza virus infection occur in individuals over 65 years and that 50-70% of hospitalisations occur in this age group in the United States (118). Aging is associated with reduced immune responses, a state known as immunosenescence, which leads to increased susceptibility to infections. Both humoral and cellular immune responses and the durability of the antibody response is significantly reduced in older compared to younger adults (119, 120). To overcome the effects of immunosenescence, there are several enhanced influenza vaccines available for people aged 65 years and older. These include high-dose vaccines that contain four times more antigen than standard vaccines, MF59-adjuvanted vaccines and recombinant HA protein vaccines. These

enhanced vaccines induce superior humoral and cellular immune responses compared to the standard-dose vaccines in older adults (121).

1.4.1 Production capacity of influenza vaccines

Eighty-five percent of seasonal influenza vaccines are produced in eggs, while the remaining 15% are cell culture-based vaccines. In a best-case scenario, the annual production capacity of seasonal influenza vaccine is estimated to 1.48 billion doses, with IIV making up 90%, followed by LAIV and recombinant protein vaccines at 5% each (115). These numbers demonstrate how reliant we currently are on the egg-based vaccine platform for production of seasonal influenza vaccines. Similarly, the production capacity of a pandemic vaccine is estimated to be 8.3 billion doses with egg-based vaccines making up 79% of the production capacity (115).

1.4.2 Necessity of improved influenza vaccines

Due to the rapid antigenic drift of influenza viruses, seasonal vaccines are the most effective method of preventing infections, and annual vaccination is recommended. It was estimated that seasonal vaccines saved 40 000 lives between 2005 and 2014 and that 4.4 million cases of influenza illness and 3500 deaths were prevented in the US during the 2018/2019 season (122, 123). However, vaccine effectiveness (VE) of seasonal vaccines varies greatly between different influenza seasons and has ranged from 10 – 60% in the last 15 years (124). Similar to seasonal vaccines, pandemic vaccines need to be antigenically matched, thus current seasonal vaccines provide limited or no protection against novel pandemic influenza viruses. The issue of rapid antigenic drift and the long production process of seasonal vaccines increases the likelihood of mismatch of vaccine and circulating strains, which subsequently reduces VE. Additionally, mutations may arise due to adaptation to growth in eggs that limits sequence fidelity. This has been demonstrated for influenza A H3N2 virus (125) and it has been suggested that this contributed to the low VE observed against the H3N2 virus during the 2012/2013 season (126). Consequently, there is a need for improved vaccines that provide broader and more durable immune responses, and for vaccines

that can be produced faster to limit the impact of mismatching and mutations caused by egg-adaptation.

1.4.3 Neuraminidase in seasonal influenza vaccines

Although early studies from the 1970s demonstrated that NA-specific antibodies contribute to protection against symptomatic disease (35, 49, 52), there has never been any requirements for the amount or the quality of NA in seasonal vaccines. One dose of seasonal inactivated vaccine is required to contain 15 µg HA of each virus, whereas the NA is only required to be present.

There are several reasons why there have been no specifications for the NA component of influenza vaccines, which have mainly been related to issues with measuring the NA content and immunogenicity of vaccines. Firstly, the concentration of NA in vaccines could not be easily measured. Measuring NA enzyme activity could be an appropriate method of quantification; however, this method only measures the total NA concentration and does not determine the concentration of different subtypes in seasonal vaccines. The enzymatic activity and the amount of NA on the surface varies among different viruses, making enzyme activity an inaccurate measurement for seasonal TIV and QIV that contain three and four different influenza viruses, respectively. Secondly, the current methods of inactivation might not be optimal for conserving NA in its native tetrameric form necessary for enzyme activity, which would result in misrepresentation of the NA concentration using this assay. And lastly, the method for measuring functional NAI titres have not been optimal. The thiobarbituric acid (TBA) assay was previously used for measuring NAI titres, but it is laborious, not optimal for large-scale serological measurements, and uses hazardous chemicals, thus making it unsuitable for routine use.

Historically, the lack of standardisation of NA and the issues associated with measuring NAI titres would cause the relationship between NA content and immunogenicity to be underestimated. In addition, NA-specific antibodies are not considered to be

neutralising as they do not block initial infection. This led to the belief that these antibodies could not prevent infection and only provided permissive immunity and were therefore inferior to HA-specific antibodies. Consequently, NA immunity and vaccine composition were not given the same attention as HA. However, we now have better methods of measuring NAI titres and the concentration of NA in vaccines. The enzyme linked lectin assay (ELLA) allows for high-throughput analysis of sera using non-hazardous reagents. Furthermore, capture ELISA has been used to measure the concentration of HA and NA of seasonal influenza vaccines, which was found to correspond with immunogenicity levels (127, 128). This could be a reliable method for measuring and standardising the NA concentration of future influenza vaccines.

1.4.4 NA as an antigen for improved influenza vaccines

The number of studies on NA and immune responses to NA have increased in the last decade. NA is well conserved within subtypes and has slower mutation rates compared to HA, making it an attractive target for broader protection (129). Thus, NA is now emerging as a promising vaccine target is considered a low-hanging fruit for improving influenza vaccines (130). However, induction of NA-specific antibody responses by season influenza vaccines is not optimal. NAI titre seroconversion rates following seasonal vaccination are generally poor and varies for different seasonal vaccines (131). Influenza infection has been found to induce more robust NA-specific antibody responses compared to inactivated seasonal influenza vaccines (59). Furthermore, the NA of current seasonal influenza vaccines poorly display epitopes targeted by broadly reactive human mAbs, likely limiting NA immunogenicity (59). A high-dose influenza vaccine that contained eight times more NA than standard-dose vaccines was found to induce significantly higher NA-specific antibody responses than a standard-dose vaccine in older adults (132). This suggests that increasing, or at least standardising, the amount of NA in current vaccines is important and a viable option for improving NA-specific responses and seasonal vaccines. This is particularly important for older adults as they are a high-risk group vulnerable to severe outcomes and hospitalisation from influenza infection (118, 133).

Current vaccines do not efficiently induce broadly cross-reactive antibodies to NA and optimisation of the NA antigen to direct antibody responses toward conserved epitopes is one strategy to achieve this. Several subtype-specific, multi-subtype, pan-group and universal anti-NA mAbs have been characterised, demonstrating the potential for NA as an immunogen for improved influenza vaccines (59, 134-139). However, several knowledge gaps are restricting advancements in this field, including discovery of epitopes targeted by human antibodies coupled with their functional capacities.

1.5 Rational vaccine design

Classical vaccines that are based on live attenuated or inactivated whole virus have traditionally been incredibly effective because they present the true molecular shapes found on the actual pathogen. This strategy has been highly effective against pathogens such as the measles and polio viruses, however, these viruses do not easily evolve to evade immune recognition. This is not the case for other pathogens, such as influenza virus, human immunodeficiency virus (HIV), malaria and SARS-CoV-2, which have acquired many mechanisms to aid immune evasion that complicates the design of vaccine antigens. Thus, rationally designed vaccines, rather than empirical approaches, may be needed to induce protective antibody responses against these pathogens.

To achieve rational design, we need to identify *epitopes* that are: **(I)** highly conserved, **(II)** targeted by the human BCR germline, and **(III)** targeted by *functional antibodies*.

An easier task may be to reverse this scenario and isolate these broadly reactive *functional antibodies* first, then identify the *epitope* by structural characterisation, and use this information to guide antigen design to target these epitopes. This approach is known as reverse vaccinology 2.0 and describes how human immunology, structural biology and genomics can be synergised to inform rational vaccine design (140) (**Figure 11**). Immune responses induced by natural infection or vaccination can often provide insights into how functional antibodies are elicited and which epitopes they target. Monoclonal antibodies (mAbs) can be produced by cloning and expressing

mAbs from single-sorted B cells, which will provide information on their corresponding paired heavy and light chain Ig gene sequences. The functionality of the mAbs can be determined by *in vitro* laboratory assays and promising mAbs can be used for structural characterisation by cryo-electron microscopy (cryo-EM) or x-ray crystallography to identify target epitopes. This information can be used to inform antigen design and new antigens can be produced from genomic information, either as recombinant proteins or e.g. in the form of an mRNA vaccine. Moreover, additional protein engineering can be used to further target the immune response toward specific epitopes through removal or occlusion of undesired epitopes (141).

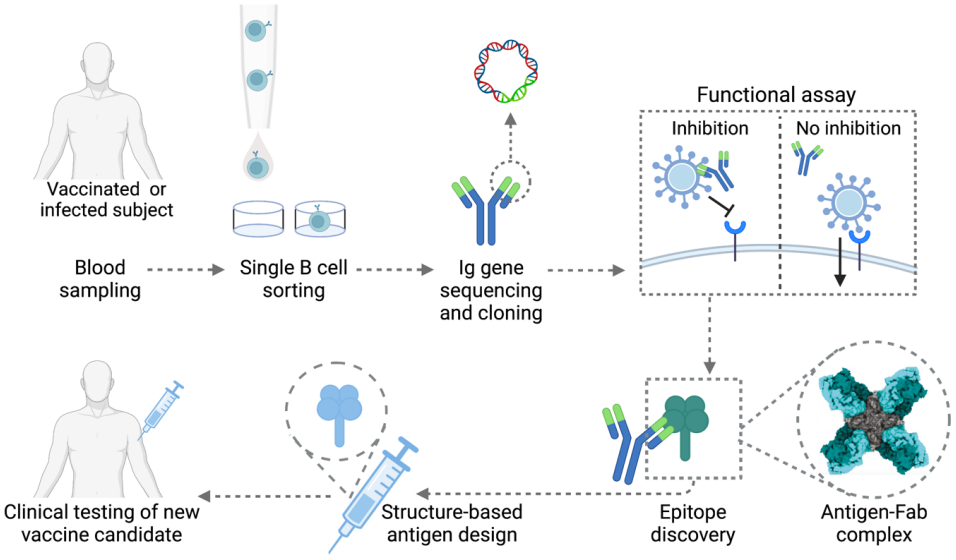

Figure 11: Reverse vaccinology 2.0
Blood samples collected from infected or vaccinated subjects can be used for isolation of B cells. B cells are single-cell sorted and used for sequencing of paired heavy and light chain immunoglobulin (Ig) genes. Ig genes amplified by PCR can be cloned into plasmid expression vectors for transfection and mAb expression in cell culture. The mAbs can be used for screening by functional assays to determine their neutralising capacity. Promising mAbs with broad binding and/or functional properties can be used to identify novel epitopes by structural methods. The information gained from structural analyses can be used to guide structure-based design of antigens for improved vaccines. Ultimately, leading to the development of new vaccine candidates that can be tested in clinical trials.
The illustration was inspired by De Gregorio and Rappuoli (142) and created with Biorender.
PDB: 64NV

1.6 SARS-CoV-2

SARS-CoV-2 is a betacoronavirus belonging to of the *Coronaviridae* family. It is a positive sense single stranded RNA virus that is the causal agent of COVID-19. SARS-CoV-2 emerged late in December of 2019 in Wuhan, China. The Chinese government reported cases of pneumonia of unknown cause (143). The patients presented with similar symptoms as those infected with SARS and Middle Eastern Respiratory Syndrome (MERS), including fever, cough, dyspnoea and lung infiltration (143, 144). On the 31st December 2019, the WHO was notified about the outbreak and on 10th January 2020 the first genomic sequence of the virus was made available online (145). The virus spread rapidly around the world and on 11th March the WHO declared it a pandemic. As of 30th May 2022, the total number of cumulative COVID-19 cases and deaths are 525 million and 6.28 million, respectively (146).

1.6.1 Viral strucure and replication

The viral envelope of SARS-CoV-2 is a lipid bilayer derived from the host cell membrane during budding and contains the surface proteins spike, membrane and envelope. The spike is a trimeric surface protein that consists of two subunits: S1 and S2. The S1 subunit contains the receptor binding domain (RBD), which binds to the host cell receptor angiotensin-converting enzyme 2 (ACE2), whereas the S2 mediates membrane fusion (**Figure 12A**). The two subunits are separated by the S1-S2 site that contains a furin cleavage motif. After binding to the ACE2 on host cells, the spike protein is cleaved by host transmembrane serine protease 2 (TMPRSS2) (147), which activates the S2 subunit trimers to fuse the viral and host cell membranes. This releases the viral RNA genome into the host cell and the positive sense RNA is immediately translated into viral proteins, which happens solely in the cytoplasm. SARS-CoV-2 has also been found to enter cells by endocytosis and the fusion between the endosomal and viral membranes releases the viral genome into the cytoplasm for translation (148). The viral RNA genome encodes at least 13 open reading frames (ORFs) that encodes four structural proteins (spike, membrane, envelope, nucleocapsid), 16 non-structural proteins (NSP1-16), and nine accessory factors.

The viral replicase proteins NSP3, NSP4 and NSP6 form vesicles by hijacking the intracellular membranes of the host cell. These vesicles are called replication organelles and is where transcription of the viral genome occurs (149-151). This compartmentalisation may shield the double stranded RNA (dsRNA) transcriptional intermediates from detection by cytoplasmic PRRs. The RNA-dependent RNA polymerase (RdRp) synthesises the viral RNA. Unlike the influenza virus, coronaviruses have a unique proofreading activity that is mediated by the RNA proofreading complex and ensures high replication fidelity (152-154). The newly synthesised viral RNA can either be translated into viral proteins, used as templates for further RNA replication or coated with nucleocapsid proteins for packaging into budding viruses.

1.6.2 COVID-19 vaccines

The whole world was racing to develop vaccine candidates for SARS-CoV-2 from the moment that the first genetic sequences were made available. Fortunately, the previous work on SARS-CoV and MERS-CoV provided useful information that could accelerate the process and showed the importance of spike-specific neutralising antibodies. The finding that two proline mutations stabilised the spike protein of MERS-CoV and seasonal coronaviruses in the prefusion state was rapidly implemented for the design of SARS-CoV-2 vaccines (155, 156). The mRNA vaccines produced by Pfizer-BioNTech and Moderna encode this mutated prefusion spike protein.

COVID-19 vaccines have been developed, tested and approved in record breaking time. Several different vaccine-platforms have been tested, including inactivated or live attenuated virus vaccines, recombinant protein, virus-like particles, nucleic acid-based vectors and replication-competent and -incompetent vectored vaccines (157). As of 30th of May 2022, 11.8 billion doses of COVID-19 vaccine have been administered globally, which is equivalent to 66% of the global population (158). Thirty-five different vaccines have been approved for use by at least one national regulatory authority, with Pfizer-BioNTech Comirnaty being the vaccine approved by the highest

number of regulatory authorities (159). Furthermore, there are currently 160 vaccine candidates in clinical development based on 11 different vaccine-platforms, protein subunit vaccines making up the largest portion (33%) followed by RNA vaccines (21%) (160).

Once the genomic sequence of SARS-CoV-2 was published, it took approximately one week for Moderna to produce the mRNA vaccine candidates and 45 days to produce enough vaccines to the start the phase I clinical trial (161). On the other hand, it took two months to produce the protein-based candidates (162). Unlike egg-based influenza vaccines that are made using a biological system, the mRNA vaccines are synthetically and chemically produced in *E. coli*, which significantly shortens the production time (**Figure 10B**). The mRNA vaccines entered clinical trials after only 66 days, whereas clinical trials involving protein-based vaccines started after six months, demonstrating how rapidly these vaccine candidates can be produced (161, 162). Although the mRNA vaccine platform has existed for many years, the COVID-19 pandemic represents the first time mRNA vaccines have been authorised and deployed at this scale.

1.6.3 Immune responses to SARS-CoV-2

Studies on immunity after COVID-19 and vaccination have demonstrated that the immune response to SARS-CoV-2 is multi-faceted and generates long-term immune memory (**Figure 12B**). Neutralising spike-specific antibodies are induced after infection, with increased levels observed with more severe disease (163), and are also the main mediator of protective immunity after vaccination. Furthermore, spike-specific antibodies that mediate antibody effector functions may also contribute to protection independently of virus neutralisation (164, 165). Persistent memory B cells have been detected six to 12 months after infection (166-168). The frequency of memory B cells have been found to increase gradually and they undergo affinity maturation to express neutralising antibodies with increased potency (169). This could potentially be linked to the presence of Tfh memory cells, as Tfh cells are important for aiding in affinity maturation of B cells in the GCs. Furthermore, mild infection

induces spike-specific long-lived bone marrow-resident plasma cells that contribute to the long-term supply of antibodies (170). $CD4^+$ and $CD8^+$ T memory cells have been detected after infection, where Th1 and Tfh $CD4^+$ T cells were most abundant (166, 171). One year after infection, polyfunctional memory T cells secreting IL-2 and IFN-γ were observed, with higher frequencies detected with increased disease severity (172).

Vaccination has also been shown to induce $CD8^+$ and $CD4^+$ T cells and persistent memory B cells (173) (174). Interestingly, these spike-specific memory B cells can be activated by natural SARS-CoV-2 infection to rapidly produce serum IgG antibodies and IgA antibodies in the saliva within 3-5 days, aiding in the control of SARS-CoV-2 infection at mucosal surfaces (175). Furthermore, mRNA vaccination has been shown to induce persistent germinal centre and Tfh responses in humans (176, 177), which are essential for induction of robust and durable humoral immunity.

There is currently no CoP recognised for SARS-CoV-2 by regulatory agencies, however, several forms of immunity and viral targets have been correlated with protection against infection and symptomatic disease. Neutralising antibodies have been found to target various sites on the spike protein and antibodies to both the RBD on S1 and the N-terminal domain on S2 have been shown to neutralise SARS-CoV-2 *in vitro* and *in vivo* (178, 179). Spike-specific antibodies have been correlated with protection against infection and reduced viral replication (180-182). $CD8^+$ T cell responses have been correlated with viral clearance and mild disease, whilst effective viral control has been associated with a type 1 $CD4^+$ T cell phenotype (183, 184).The rapid advances in understanding of immunity to SARS-CoV-2 will also benefit the influenza field.

The emergence of variants of concern (VOC) with increased transmission rates and immune escape leads to reduced vaccine effectiveness and stretches health care systems. These VOC have amino acid changes in their spike protein, particularly the RBD, and have caused waves of Alpha, Delta and then Omicron VOC across the globe.

In Norway, the Delta VOC dominated from mid-summer 2021 leading to increased infection rates, particularly in the younger unvaccinated population, with vaccination effectiveness reduced from 84% to 65% (185). Since the emergence of the Omicron VOC in late 2021, it has quickly become the dominating strain with new subvariants emerging. Significant decline in cross-reactive neutralizing antibodies is observed to Omicron (186) and significant replication advantages even compared to Delta (187, 188), highlighting the importance of a booster dose (189).

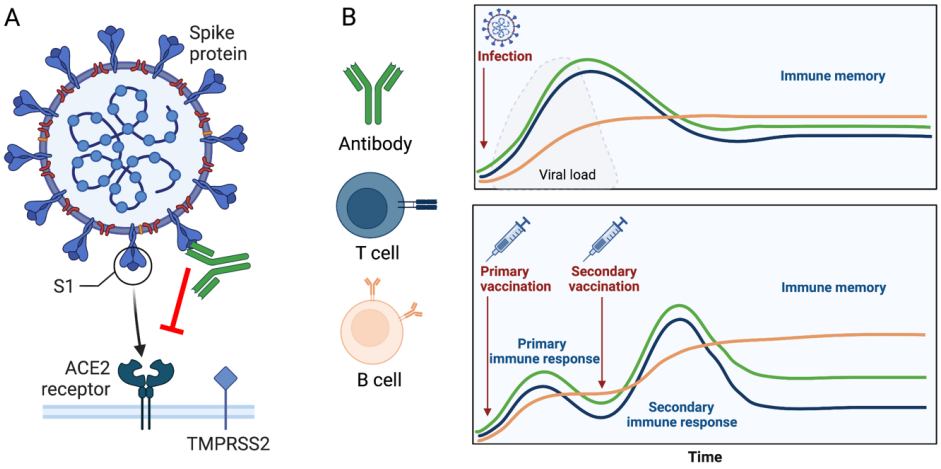

Figure 12: SARS-CoV-2 infection and vaccination
(**A**) Infection with SARS-CoV-2 is initiated by the binding of the spike protein to the host cell receptor ACE2. Cleavage of the S2 subunit of the spike protein by host transmembrane serine protease TMPRSS2 leads to fusion of the viral and host cell membranes and release of the viral genome. Antibodies that bind to the spike protein can block the interaction between spike and ACE2 to prevent infection. (**B**) Two illustrations showing the immune responses generated after SARS-CoV-2 infection (top) or after primary and secondary vaccination (bottom). The two principle cellular components of the adaptive immune response are B and T cells. Together with antibodies, these cells are essential for preventing and eliminating infection and are therefore also necessary for protection by vaccination. SARS-CoV-2 infection causes an initial increase in antibodies, B cells, and $CD4^+$ and $CD8^+$ T cell during acute infection. The magnitude of these responses decreases once the virus is cleared but immune memory is generated. Memory B cells, antibodies produced by long-lived plasma cells, and $CD4^+$ and $C8^+$ T memory cells persist long after the initial infection and contribute to immunity. Similarly, primary vaccination against SARS-CoV-2 induces a B cell response, followed by an increase in antibody levels, and $CD4^+$ and $CD8^+$ T cells. These responses are boosted upon vaccination with a second dose that results in immune memory in the form of memory B cells, T cells and increased levels of antibodies. The illustration was created with Biorender.

1.6.4 COVID-19 and SARS-CoV-2 immunity in older adults

The CDC in the US estimated that older adults between 65-84 years old had equal rates of infection as 18-29 years old but a 5-8 times higher rate of hospitalisation and strikingly 65-140 times higher rate of death (190). Although old age is a well-known risk factor for severe disease, the licensure trials for COVID-19 vaccines did not include the oldest adults aged 80 years and above (191). This meant that there was limited data to inform dose and immunisation regimens, and for assessment of adverse events for COVID-19 vaccination in this age group. We already know from influenza that immunosenescence impacts on the immune responses induced by vaccination and that enhanced influenza vaccines are necessary to overcome this effect. One could argue that inclusion of the elderly in the clinical trials should have been prioritised for COVID-19 vaccine trials to inform optimal vaccine dosing and spacing for this risk-group. Especially because there was no pre-existing immunity to SARS-CoV-2, causing the elderly being disproportionately affected by severe disease and death. This contrasted with the situation during the 2009 influenza A H1N1 pandemic where the oldest adults were less affected than the younger adults due to pre-existing immunity (1). Others have shown that immunogenicity of mRNA vaccines are reduced in elderly compared to younger adults (173, 192, 193). Therefore, it was important to study the kinetics and durability of the immune response after COVID-19 vaccination in this age group.

The last literature search was performed in May 2022.

2. Aims and objectives

The main aim of this thesis was to investigate strategies for improving influenza vaccines.

Primary objective

To investigate NA as a target for broader protection against influenza virus, by:

I. Discovery of conserved epitopes by characterisation of human mAbs induced by pandemic H1N1 infection (paper I)

II. Studying NA-specific antibody responses after adjuvanted pandemic H1N1 vaccination and repeated seasonal vaccination (paper II)

Secondary objective

To inform the use of future influenza mRNA vaccines for older adults, by:

I. Broadly investigating immune responses after SARS-CoV-2 mRNA vaccination or infection in older and younger adults (paper III)

3. Materials and methods

3.1 Study designs

3.1.1 Pandemic influenza A H1N1 infection (paper I)

The samples used for cloning and expression of mAbs were collected from a patient during acute infection with pandemic influenza A H1N1 virus in 2009. The subject was a 28-year-old female with a severe influenza virus infection. The blood samples were collected while the patient was hospitalised and admitted to the intensive care unit in 2009 at the National Institute of Respiratory Diseases in Mexico City, Mexico (IRB no. B08-09). The patient was discharged after 13 days. The number of days since symptoms onset was not known at the time of sample collection.

3.1.2 Pandemic influenza A H1N1 vaccination (paper II)

Health care workers (HCWs) (n=50) were vaccinated with pandemic influenza A H1N1 between October 2009 and March 2010 at Haukeland University Hospital, Norway (**Figure 13**). They were vaccinated with the AS03-adjuvanted low dose pandemic H1N1 split virus vaccine (3.75 μg HA A/California/7/2009) (Pandemrix, GSK). The AS03 adjuvant is composed of α-tocopherol, squalene and polysorbate 80 in an oil-in-water emulsion (194). Written informed consent was obtained from all vaccinees before inclusion in the study and additional informed consent was obtained for the 4-year extension between 2010/2011–2013/2014. The study was approved by the regional ethics committee (REKVest-2012/1772) and the Norwegian Medicines Agency (National Institute for Health database Clinical trials.gov NCT01003288) (195). In the 2010/2011–2013/2014 influenza seasons, the HCWs were vaccinated with the seasonal TIV (either subunit (Influvac, Abbott Laboratories) or split-virion (Vaxigrip, Sanofi Pasteur)) containing 15 μg HA per strain. The A/H1N1 strain was the same for all seasonal vaccines, while the A/H3N2 and B viruses changed between seasons.

Blood samples were collected pre-vaccination, 21 days, 3, 6, and 12 months after vaccination. The HCWs were divided into two groups, repeated (n=26) and single group (n=24), based on their vaccination status in influenza seasons 2010/2011 – 2013/2014. The repeated group was vaccinated with two or three TIVs in the four seasons following the 2009 pandemic. This means that HCWs in the repeated group were not vaccinated at least once during the study. The data were grouped based on number of vaccines (i.e., 1st, 2nd, 3rd seasonal TIV), rather than season, in order to study the effect each vaccination and the impact of repeated vaccination. The same sampling schedule was used for seasonal vaccination as for pandemic vaccination. The 12-month timepoint was collected from all HCW irrespective of vaccination and used as day 0 for HCWs in the repeated group for each season. HCWs in the single group were only vaccinated in 2009 but provided blood samples at the start of each influenza season, i.e. 24, 36, 48 and 60 months after pandemic H1N1 vaccination in 2009.

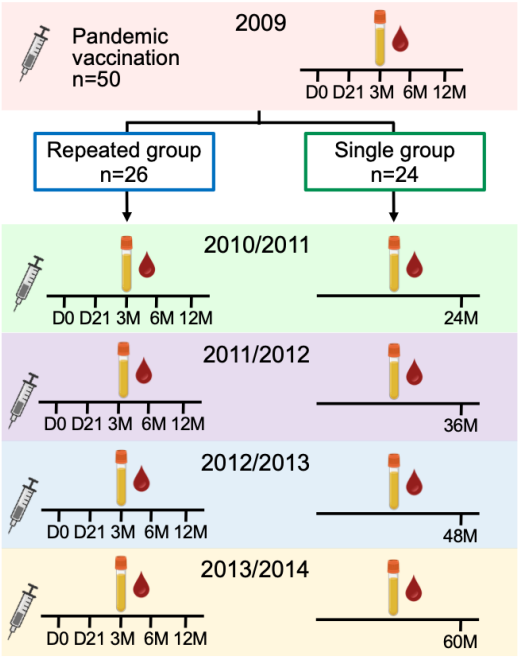

Figure 13: Study design of influenza vaccine study
An overview of the timepoints vaccination and blood sampling during the influenza A H1N1 pandemic in 2009 and subsequent influenza seasons 2010/2011 - 2013/2014.

3.1.3 COVID-19 (paper III)

A prospective cohort study of younger and older adults vaccinated with COVID-19 mRNA vaccine BNT162b2 (Pfizer-BioNTech) between January and November 2021 from Eidsvåg general practice and Haukeland University Hospital in Bergen, Norway. One hundred elderly subjects (63% female) aged 70-99 years old (median age 86 years old) were recruited and 449 healthy younger adults (69% female) aged 23-69 years (median age 38 years old) at the time of enrolment. All subjects provided written informed consent before inclusion in the study. The study was approved by the regional ethics committee (Regional Committee for Medical Research Ethics, Northern Norway (REK Nord) and is registered in the National Institute for Health database Clinical trials.gov (NCT04706390). The infected cohort was recruited during March and April 2020 from home-isolated SARS-CoV-2-infected individuals and were followed clinically and immunologically at 2 weeks, and 6 and 12 months after infection. All patients had mild to moderate infection and were not hospitalized, details are described elsewhere *(196)*.

All participants were vaccinated intramuscularly into the deltoid muscle with two doses of BNT162b2 mRNA COVID-19 vaccine at 3-week intervals. Subjects provided blood for serum samples prior to or on the day of vaccination, at 21 and 42-56 days and at 5- and 9-months post-vaccination (**Figure 14**). A subgroup of subjects in the vaccine and infection cohorts also provided PBMCs pre- and post-vaccination or post-infection, respectively, for investigation of memory B cell and T cell responses. The infected cohort provided blood samples at 8 weeks, 6- and 12-months post-infection.

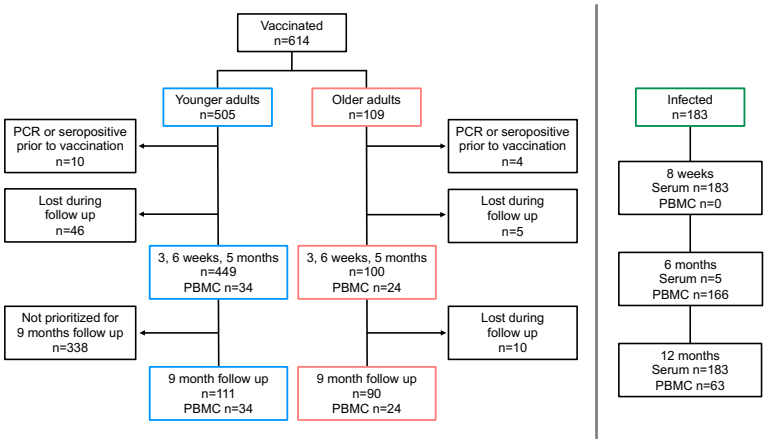

Figure 14: Study design for COVID-19 study
An overview of the number of COVID-19 infected individuals in the infected group and vaccinees eligible for inclusion at baseline.

3.2 Cloning and expression of influenza NA-specific monoclonal antibodies

Plasmablasts (live singlet $CD19^+$ $CD4^-$ IgD^{low} $CD38^+$ $CD20^-$ $CD71^+$) were single-cell sorted from cryopreserved PBMCs into 96-well plates using a FACSAria II and immediately frozen on dry ice. The mAbs were cloned as previously described (197). Briefly, reverse transcription polymerase chain reaction (RT-PCR) with single-sorted plasmablasts was performed and VH, Vκ and Vλ genes were amplified by polymerase chain reaction (PCR) using primers specific for IgM/A, IgG, Igκ and Igλ and sequenced (198). Heavy chain VDJ and light chain VJ gene fragments were amplified by PCR and cloned into IgG_1 and Igκ expression vectors by Gibson assembly (199). Heavy and light chain plasmids were co-transfected into Expi293F cells at a ratio of 1:2 for expression and the antibodies were purified from the supernatant by gravity chromatography using protein A agarose.

3.3 Influenza and SARS-CoV-2 ELISA (papers I-III)

Enzyme-linked immunosorbent assay (ELISA) was used to measure binding serum antibodies to recombinant protein or purified virus. Serum was collected from clotted

blood CAT plus blood tubes after coagulatination by centrifuging at 2000 rpm for 10 min at 4°C. Sera was aliquoted and immediately frozen at -80°C until used in the serological assays. Each individual was allocated a unique identification number. Ninety-six-well plates we coated with 100 µl/well of recombinant NA A/California/07/09 (H1N1) protein (1 µg/ml) in paper II, 50 µl/well of recombinant NA protein (2 µg/ml) or purified influenza virus (5 µg/ml) in paper I and 50 µl/well of SARS-CoV-2 spike protein (2 µg/ml) in paper III. Coating antigens were diluted in phosphate buffer saline (PBS). The plates were incubated at 4°C overnight. The following day, the plates were washed three times with PBS with Tween (PBS-T) (0.05% Tween-20) and blocked with 200 µl/well of blocking solution for 2 hours at RT. The composition of solutions used for blocking and dilution of samples and conjugated secondary antibodies can be found in **Table 1**.

Table 1. Compositions of solutions used for ELISA in papers I-III

	Blocking solution	**Sample and conjugate diluent**
Paper I	PBS with 0.05% Tween-20 (v/v), 1% milk (w/v), 3% goat serum (v/v)	PBS with 0.05% Tween-20 (v/v), 1% milk (w/v), 3% goat serum (v/v)
Paper II	PBS with 0.01% Tween-20 (v/v), 5% milk (w/v), 1% BSA (v/v)	PBS with 0.01% Tween-20 (v/v), 5% milk (w/v), 1% BSA (v/v)
Paper III	PBS with 0.01% Tween-20 (v/v), 3% milk (w/v)	PBS with 0.01% Tween-20 (v/v), 1% milk (w/v)

Volume (v), weight (w), bovine serum albumin (BSA).

MAbs were diluted in blocking solution to a concentration of 30 µg/ml and then 3-fold serially diluted with 100 µl/well in duplicates. Human sera were diluted in blocking solution and 4-fold serially diluted from a starting dilution of 1:100. The plates were incubated for 1.5 hours a RT. After incubation, the plates were washed six times with PBS-T. A secondary horseradish peroxidase (HRP)-conjugated anti-human IgG antibody was diluted in blocking solution (1:1000) and 50 µl/well was added and incubated for 2 hours at RT. The plates were washed 6 times with PBS-T and 100 µl/well of σ-Phenylenediamine dihydrochloride (OPD) substrate (paper I) or 3,3',5,5'-

tetramethylbenzidine (TMB) substrate (papers II and III) was added. The colour development was stopped after 10 min by adding 50 µl/well of HCl (3M) (paper I) or 100 µl/well of HCl (0.5M) (papers II and III). The optical density (OD) was measured immediately after stopping the reaction by a spectrophotometer at 490 nm (paper I) or 450 nm (papers II and III). The minimal binding concentration was determined as the lowest mAb concentration that was higher than the mean of blanks + 3x standard deviation (paper I). Endpoint titres were calculated in paper II and III using cut off values of 0.2 and 0.478, respectively. Analyses were performed in Graphpad Prism 9. A complete list of recombinant proteins and virus strains used in ELISA for mAb characterisation in paper I can found in **Table *2***.

3.4 ELLA (papers I and II)

ELLA was used to determine the influenza-specific NAI endpoint titre of human sera and inhibitory concentration 50 (IC_{50}) for mAbs and Fabs, as previously described (200). Ninety-six-well plates were coated with 100 µl/well of fetuin diluted in PBS (paper I: 10 µg/ml, paper II: 25 µg/ml) and incubated for minimum 18 hours at 4°C. On the day of the assay, the plates were washed six times with PBS-T. Sera, mAbs and Fabs were diluted in sample diluent (PBS with 0.9 mM $CaCl_2$, 0.5 mM $MgCl_2$, 1% BSA, 0.5% Tween-20). The mAbs were diluted to a starting concentration of 30 µg/ml (200 nM) and Fabs to 10 µg/ml (200 nM) and 3-fold serially diluted. Sera were 3-fold serially diluted in sample diluent from 1:20 in duplicates. The diluted sera, mAbs and Fabs were added to the fetuin-coated plates (50 µl/well) and mixed with diluted virus (50 µl/well). The appropriate virus concentration was determined in a separate experiment and a virus dilution equivalent to 2x 50% effective concentration (EC_{50}) (paper I) or 90% of maximum signal was used (paper II). A reassortant H7N1 virus with an irrelevant HA from A/Equine/Prague/1956 (H7N7), NA form A/California/07/2009 (H1N1) on a A/Puerto Rico/8/1934 (H1N1) backbone was used in paper II to avoid interference from HA stalk antibodies. A complete list of virus strains used in ELLA for mAb characterisation in paper I can be found in **Table *2***. The plates were incubated for 18 hours at 37°C. After incubation, the plates were washed 6 times with PBS-T and 100 µl/well of HRP-conjugated peanut agglutinin (PNA)

(1:1000) was added and incubated for 2 hours at RT in the dark. The plates were washed 6 times with PBS-T and 100 µl/well of OPD substrate was incubated for 10 min. The reaction was stopped by adding 50 µl/well of HCl (3M) (paper I) or 100 µl/well of sulfuric acid (1N) (paper II). The absorbance was read immediately after stopping the reaction at 490 nm. The percentage of NAI was calculated as reduction in signal from the control wells that only contained virus. The percentage of NAI for each dilution step was plotted in GraphPad Prism 9 and the IC_{50} (µg/ml) was calculated by non-linear regression (paper I). The 50% NAI endpoint titre of sera was calculated by non-linear regression and a cut off equivalent to 50% of the signal for the virus control wells was used (paper II).

Table 2: Influenza virus strains used for mAb characterisation (paper I)

ELLA influenza A virus strains	ELISA influenza A virus strains
A/Cambodia/0371/2007 (H1N1)	A/California/04/2009 (H1N1)
A/Denver/1/1957 (H1N1)	A/Michigan/45/2015 (H1N1)
A/Fort Monmouth/1/1947 (H1N1)	A/Nicaragua/1815/TR2/2013 (H1N1)
A/Netherlands/602/2009 (H1N1)	A/rhea/North Carolina/39482/1993 (H7N1)*
A/New Caledonia/20/1999 (H1N1)	A/swine/Jiangsu/40/2011 (H1N1)*
A/New York City/PV02669/2019 (H1N1)	A/Texas/36/1991 (H1N1)
A/Puerto Rico/8/34 (H1N1)	A/mallard/Sweden/24/2002 (H6N4)*
A/Singapore/GP1908/2015 (H1N1)	A/Vietnam/1204/2004 (H5N1)
A/Solomon Islands/03/2006 (H1N1)	A/Hong Kong/4801/2014 (H3N2)
A/Texas/36/1991 (H1N1)	
A/swine/Jiangsu/40/2011 (H1N1)	
A/mallard/Sweden/24/2002 (H6N4)$	
A/Vietnam/1204/2004 (H5N1)#	
A/rhea/North Carolina/39482/1993 (H7N1)	

* Purified virus was used as coating antigen, otherwise recombinant NA was used
$ cH6/1 chimeric HA. Head: A/mallard/Sweden/81/02. Stalk: A/Puerto Rico/8/34.
# Low pathogenic 6:2 reassortant with HA and NA from A/Vietnam/1204/04 (H5N1). Remaining genes from A/Puerto Rico/8/34 (H1N1). HA polybasic cleavage site removed.

3.5 Competition ELISA (paper I)

We used a competition ELISA to determine if the 2H08 and 3H03 had overlapping epitopes on the influenza A NA. The mAbs were biotinylated with 20x molar excess of biotin according to the manufacturer's instruction (Thermo Fisher) and buffer exchanged into PBS using Zeba spin desalting columns. Ninety-six-well plates were coated with recombinant NA A/Michigan/45/15 (H1N1) protein (2 µg/ml, 50 µl/well) and incubated overnight at 4°C. The following day, the plates were washed three times with PBS-T and blocked with blocking solution (200 µl/well) for 1.5 hours (**Table 1**). Unbiotinylated competing mAbs 2H08, 3H03, and 1G01 (positive control mAb specific for the NA active site) were added to the plate (20 µg/ml, 200 µl/well) and incubated for 2 hours at 20°C. One unbiotinylated competing mAb was added to all wells in one 96-well plate, with the exception of control wells where an anti-anthrax mAb was added (negative control) and blank wells (no mAb). After incubation, the plates were washed three times with PBS-T. Biotinylated mAbs (bio-mAbs) were 3-fold serially diluted from 30 µg/ml in blocking buffer and added in duplicates (100 µl/well). The bio-mAbs were added to the three plates containing competing mAbs to assess the competition of the 2H08, 3H03 and 1G01 mAbs against themselves and also to each other. The plates were incubated for 2 hours at 20°C and washed three times with PBS-T. HRP-conjugated streptavidin diluted in blocking solution was added (1:3000, 50 µl/well) and incubated for 1 hour at 20°C. The plates were washed four times with PBS-T and OPD substrate was added (100 µl/well) and incubated for 10 min. The development was stopped by adding 3M HCl (50 µl/well) and the absorbance was measured immediately at 490 nm using a spectrophotometer. The area under the curve (AUC) was calculated for each bio-mAb in Graphpad Prism 9. The AUC of bio-mAb incubated with the competing negative control mAb was considered maximum binding and was used to calculated percentage of reduced binding for each bio-mAb.

3.6 Neuraminidase inhibition by NA-Star (paper I)

NAI was assessed by the NA-Star assay and was performed according to the manufacturer's instructions (Applied Biosystems). The NA-star assay uses a small chemical substrate and NAI is observed when the enzyme activity of NA is inhibited allosterically. A/Singapore/GP1908/15 (H1N1) virus was diluted in assay buffer to a concentration equivalent to 40x the mean of blank wells, as determined in a separate experiment. The mAbs were 2-fold serially diluted in assay buffer from 30 µg/ml in duplicates (25 µl/well) and added to white flat-bottom 96-well plates. Diluted virus was added to each well (25 µl/well) and the mAb-virus mixture was incubated for 20 min at 37°C. Following incubation, NA-Star substrate was added per well (10 µl/well) and incubated for 30 min at RT. NA-Star Accelerator was added to the plate (60 µl/well) and the luminescence was measured immediately using a plate reader.

3.7 Influenza plaque reduction neutralisation assay (paper I)

The plaque reduction neutralisation assay (PRNA) was used to investigate if the mAbs could reduce plaque sizes. The mAbs were included before and/or after infection to assess their inhibitory capacity at different stages of the viral replication cycle. Three different conditions were tested in order to assess their function during various stages of the viral replication cycle:

I. mAbs present only in inoculum during infection (inhibition of viral entry)
II. mAbs present in inoculum during infection and in the overlay after infection (inhibition of viral entry and release)
III. mAbs <u>not</u> present in the inoculum and only in the overlay after infection (inhibition of viral release)

MDCK cells were seeded in 12-well plates (5 $x10^5$/well) in DMEM and incubated at 37°C overnight. The following day, A/Singapore/GP1908 (H1N1) virus was diluted to 1 $x10^4$ pfu/ml in 1X minimum essential medium (MEM) consisting of 10% minimum essential medium supplemented with L-glutamine (2 mM), 0.1% sodium bicarbonate (w/v), HEPES (10 mM), streptomycin (100 µg/ml), penicillin (100 U/ml), 0.2% bovine

serum albumin (BSA) and water. MAbs were 5-fold serially diluted from a starting concentration of (100 µg/ml) and 240 µl was added per well. Fifty µl of virus was diluted to a predetermined concentration equivalent to 30 pfu/50 µl/well, mixed with the diluted mAbs and incubated for 1 hour at RT with shaking (300 rpm). For condition III where mAbs were not included in the inoculum during infection, the virus was mixed with 240 µl of 1X MEM. The cells were washed once with PBS and 200 µl of the virus-mAb mixture was added per well at incubated at 37°C for 40 min with shaking every 10 min to avoid the cells drying.

The agar overlay consisted of 1X MEM, 0.67% agar (Oxoid), 0.01% diethylaminoethyl (DEAE)-dextran and 1 µg/ml L-1-tosylamido-2-phenylethyl chloromethyl ketone (TPCK)-treated trypsin. The overlay containing mAb was prepared by 5-fold serial dilution of mAbs in 1X MEM, which was added to the agar mixture. The final concentration of mAbs in the agar overlay was 100, 20, 4, 0.8 or 0.16 µg/ml. Mab 1G01 was used as positive control, anti-anthrax IgG was used as negative control and no mAb was used for the control wells. The plates were incubated at 37°C for 72 hours. Following incubation, the cells were fixed with 1 ml/well of paraformaldehyde (PBS with 3.7% formalin) at 4°C overnight. Following fixation, the agar was removed, and the plates were blocked with 3% milk in PBS for 1 hour at RT. The blocking solution was removed and 0.5 ml/well of A/Michigan/45/15 (H1N1)-reactive guinea pig sera diluted in 1% milk (1:1000) was added and incubated for 1 hour at RT with shaking. The plates were washed 3 times with PBS and HRP-conjugated donkey anti-guinea pig IgG was added (1:3000 in 1% milk) and incubated for 1 hour at RT with shaking. The plates were washed 3 times with PBS and plaques were visualized by adding 200 µl/well of KPL TrueBlue peroxidase substrate.

3.8 Microplate plaque reduction neutralisation assay (paper II)

A microplate PRNA was used to determine if sera from vaccinated individuals could reduce plaque formation by influenza NAI. The assay was performed as described by Matrosovich *et al.* (201). Briefly, MDCK cells overexpressing α-2,6-sialyltransferase (MDCK-SIAT1) (202) were seeded in 96-well plates ($2x10^4$/well) and incubated at

37°C and 5% CO_2 overnight. The following day, sera were diluted 1:20 and 1:100 in infection medium and mixed with virus and incubated for 1 hour at 37°C. A reassortant H7N1 virus with an irrelevant HA from A/Equine/Prague/1956 (H7N7), NA from A/California/07/2009 (H1N1) on an A/Puerto Rico/8/1934 (H1N1) backbone was used to avoid interference from HA stalk antibodies. The virus was diluted to a predetermined concentration equivalent to 100 pfu/well. The inoculum was added to the cell plate in quadruplets (100 µl/well) and incubated at 37°C for one hour. After incubation, a low-viscosity Avicel overlay was added to the plates together with the inoculum (100 µl/well). The plates were incubated for 24 hours at 37° and 5% CO_2. The following day, the overlay was removed and the cells were fixed with fixing solution for 30 min at 4°C. the plates were washed with PBS and the plaques were visualised by immunostaining. The cells were treated with Triton-X-100 in PBS (0.5%) for 10 min at RT and incubated with an anti-NP mAb for one hour at RT. The cells were washed again, and a peroxidase-labelled anti-mouse antibody was added and incubated for 1 hour at RT. Lastly, the cells were washed and 50 µl/well of TrueBlue peroxidase substrate was added and incubated for 40 min at RT. The development was stopped by washing the plates with distilled water and the plates were left to dry in the dark. The plaques were counted using an enzyme-linked immune absorbent spot (ELISPOT) reader. The reciprocal serum dilution resulting in 50% reduction in plaque formation was calculated using non-linear regression and defined as the plaque reduction neutralizing titer ($PRNT_{50}$).

3.9 Influenza escape mutant virus (paper I)

Generation of escape mutant virus (EMV) was used to identify the binding footprint of the mAbs. MDCK cells were plated in 12-well plates ($5x10^5$/well) and incubated overnight at 37°C. The following day, the cells were infected with $1x10^4$ pfu of A/Singapore/GP1908/15 (H1N1) virus diluted in 1X MEM (200 µl/well) with TPCK-treated trypsin (1 µg/ml). The cells were infected with 200 µl/well of virus at 37°C with shaking every 10 min to avoid drying of the cells. After infection, 800 µl/well of diluted mAb was added. The starting concentration of the mAb was 0.5x IC_{50} as determined

by ELLA. The virus-mAb mixture was incubated for 72 hours at 37°C. After incubation, the medium was collected and centrifuged for 5 min at 300 x g to remove cell debris. The harvested media were used to infect new cells (200 µl/well) and a doubling of the mAb concentration was added. This process was repeated for 7-8 passages. The medium from each passage was used to infect MDCK cells in 96-well plates for immunofluorescent staining to verify the presence of virus and for the loss of binding for the mAbs to check for viral escape. Once the mAb had reduced binding, the virus medium was used in plaque assay with the mAb present in the overlay at a concentration of 10 µg/ml for 48 hours at 37°C. Individual plaques were sampled and injected into 8-10 day old embryonated hens' eggs and incubated at 37°C. After 72 hours, the allantoic fluid was collected and the presence of virus was determined by hemagglutination assay. Viral escape was confirmed by ELLA. The viruses were sequenced to identify the escape mutations, P93L and I117M. To further verify the role of these mutations, we generated recombinant A/Singapore/GP1908/15 (H1N1) NA proteins containing both mutations and each mutation individually and were used as coating antigens in ELISA.

3.10 Influenza ADCC bioreporter assay (paper I)

The assay was performed according to the manufacturer's instructions (Promega). This assay is a bioluminescent reporter assay that quantifies activation of the nuclear factor of activated T cell (NFAT) pathway, which is needed for ADCC. The assay uses Jurkat cells that are engineered to express luciferase when the NFAT signalling pathway is activated. The assay measures the activation of gene transcription through the NFAT pathway in effector cells as a surrogate of ADCC.

Briefly, MDCK cell were seeded in 96-well white flat bottom plates (1.8 $x10^4$/well) and infected with A/Singapore/GP1908/15 (H1N1) virus (5x multiplicity of infection (MOI)) overnight at 37°C. The following day, medium was removed from the cells and fresh medium was added (25 µl/well). ADCC FcγRIIIa effector cells were diluted in RPMI-1640 medium (3 $x10^6$ cells/ml) and added to the cells (25 µl/well). MAbs were

2-fold serially diluted from 60 µg/ml and added to the cells (25 µl/well), total volume 75 µl/well. The cells were incubated for 6 hours at 37°C. Following incubation, the Bio-Glo Luciferase assay reagent was added (75 µl/well) and the luminescence was measured after 10 min using a plate reader.

3.11 Biolayer interferometry (paper I)

Biolayer interferometry (BLI) was used to measure the binding affinity of 2H08 and 3H08 to NA A/Singapore/GP1908/15 protein. Full length mAbs (2 mg/ml) were incubated with 20 µg/ml papain in PBS containing 20 mM EDTA and 20 mM cysteine for two hours at 37°C. After incubation, the enzyme was quenched with 30 mM iodoacetamide in PBS, and the Fc was removed using a protein A column. Cleavage was confirmed by sodium dodecyl-sulfate polyacrylamide gel electrophoresis (SDS-PAGE) and the Fabs were run over a size-exclusion column in PBS. The Fabs were used to measure the binding kinetics to NA A/Singapore/GP1908/15 (H1N1) by BLI using an Octet-Red96 instrument. Recombinant NA protein (0.92 mg/ml) was labelled with 3x molar excess (monomer) of NHS-biotin, and buffer was exchanged using Zeba desalting spin columns. The Octet SA sensors were soaked in BLI buffer (10 mM HEPES pH 7.6, 150 mM sodium chloride, 3 mM EDTA, 0.05% Tween-20, 1% BSA (w/v)). Biotinylated NA (3 µg/ml) were loaded onto Octet SA biosensors for 600 sec and baseline was measured in BLI buffer for 300 sec. Following baseline measurements, the sensors were loaded with Fabs (3-fold serially diluted from 50 µg/ml) and association and dissociation was measured for 600 and 1200 sec, respectively. The data was analyzed using the Octet-Red96 software and the association and dissociation rates were calculated using a 1:1 model with global curve fitting.

3.12 Murine experiments (paper I)

The capacity of mAbs 2H08 and 3H03 to protect prophylactically and therapeutically against lethal influenza infection was investigated in a murine model, as previously described (203). The challenge viruses contained the HA and NA from

A/Singapore/GP1908/2015 (H1N1) on an A/Texas/1/77 (H3N2) backbone and low pathogenic virus containing HA and NA from A/Vietnam/1204/04 (H5N1) on an A/Puerto Rico/8/34 backbone with the HA polybasic cleavage site removed. Six to eight-week-old female BALB/c mice were used for all experiments. MAbs 2H08, 3H03, anti-anthrax mAb (negative control) were administered as 100 µl and by intraperitoneal injection. The mice were anesthetized with a ketamine/xylazine mixture and challenged intranasally two hours after the passive transfer for the prophylactic experiments or 48 hours before the passive transfer for the therapeutic experiment. The mice used in the lung titre experiment were infected with 0.1 x 50% mouse lethal dose (mLD_{50}) and all other mice were infected with 5 x mLD_{50}. In the prophylactic experiments, the mice were given 5 mg/kg of each individual mAb for the A/Vietnam/1204/04 (H5N1) challenge (n=5 mice/mAb) and 5, 1 or 0.2 mg/kg mAb for the A/Singapore/GP1908/15 (H1N1) challenge (n=5 mice/concentration for each individual mAb). For the therapeutic setting, the mice were given 5 mg/kg mAb 48 hours after infection with A/Singapore/GP1908/15 (H1N1) and the A/Vietnam/1204/04 (H5N1) (n=5 mice/mAb). Weight loss was monitored daily for 14 days and mice that lost more than 25% of their initial body weight were euthanized. Lung viral titres were measured in mice treated with 5 mg/kg of mAb and challenged with A/Singapore/GP1908/15 (H1N1) virus. The lungs were harvested on day 3 (n=5 mice/mAb) and 6 post-infection (n=3 mice/mAb) and homogenized in 1 ml PBS using a BeadBlaster24 (Benchmark). The viral titers were measured in lung homogenate by plaque assay assay as described below and reported as pfu/ml.

3.13 Plaque assay (paper I)

The plaque assay was used to determine influenza viral titres using lung homogenate from the *in vivo* experiments. MDCK cells were seeded in 12-well plates (5 x10^5/well) in DMEM and incubated at 37°C overnight. On the day of infection, the cells were washed once with PBS and 200 µl/well of lung homogenate was added in triplicates. The homogenate was 10-fold serially diluted in 1x MEM. The cells were infected for 1 hour at 37°C with shaking every 15 min. After infection, the inoculum was aspirated,

and 1 ml overlay was added per well and incubated at 37°C for 72 hours. The plaques were visualised by immunostaining as described for the plaque reduction neutralisation assay in section 3.7.

3.14 SARS-CoV-2 microneutralisation assay (paper III)

The microneutralisation assay was conducted to measure SARS-CoV-2-specific neutralising antibodies in the elderly (n=100), the infected subjects (n=183) and a subgroup of younger adult vaccinees (n=41). The microneutralization assay was conducted in a certified Biosafety Level 3 Laboratory as previously described (204). Briefly, serum samples were 3-fold serially diluted from 1:20 in duplicates. Serum dilutions were mixed with 100x 50% tissue culture infectious dose ($TCID_{50}$) of ancestral D614G hCoV-19/Norway/Bergen-01/2020 virus (GISAID accession ID EPI_ISL_541970) and incubated for 1 hour at 37°C. The inoculum was transferred to 96-well plates seeded with Vero cells and incubated at 37°C for 24 hours. The following day, the cells were fixed with methanol and 0.6% H_2O_2, and incubated with anti-nucleocapsid rabbit IgG. The cells were incubated with a biotinylated secondary goat anti-rabbit IgG (H+L) antibody, followed by Extravidin-peroxidase, and developed using OPD substrate. Neutralising titres were calculated as the reciprocal of the serum dilution resulting in 50% inhibition of virus infectivity. For calculation purposes negative titres (<20) were assigned a value of 10.

3.15 SARS-CoV-2 memory B cell ELISPOT (paper III)

ELISPOT assay was used to detect SARS-CoV-2 spike-specific memory B cells after COVID-19 mRNA vaccination. The PBMCs were separated using cell preparation tube (CPT) to investigate the MBC and T cell responses, pre- and post-vaccination or post-infection (paper III). CPT tubes were mixed 3-4 times before centrifugation at 1750 x g for 20 min at RT. The plasma was removed, and the lymphocyte layer removed and washed twice with PBS by centrifuging at 350 x g for 10 min at 4°C. PBMCs were resuspended in cell culture medium alone (negative control) or in medium containing R848 (1 mg/ml) and rhIL-2 (1 µg/ml) for expansion of B cells. The cell culture medium

consisted of Roswell Park Memorial Institute (RPMI)-1640 medium supplemented with 10% heat-inactivated FBS, penicillin (100 U/ml) and streptomycin (0.1 mg/ml). Two million cells were added per well in 24-well plates and incubated for 6 days at 37°C with 5% CO_2. ELISPOT plates were coated with anti-human IgG (15 mg/ml), Spike protein (10 mg/ml), or PBS only (negative control) at 4°C overnight. Non-stimulated and stimulated PBMCs were washed twice with medium and transferred to ELISPOT plates in duplicates and incubated undisturbed for 16 hours (37°C, 5% CO_2). Plates were washed with PBS and IgG^+ memory B cells were detected with biotinylated anti-IgG mAb (1 µg/ml) for 2 hours at RT followed by HRP-conjugated streptavidin. Spots were developed with 3,3',5,5'-tetramethylbenzidine (TMB) ELISPOT substrate. The plates were dried and counted using an ELISPOT reader. SARS-CoV-2 spike-specific spots were calculated as the mean of duplicate wells after subtraction of negative control wells and presented as spot forming units per million PMBCs (SFU/10^6 PBMCs).

3.16 SARS-CoV-2 FluoroSpot assay (paper III)

FluoroSpot assay was used to measure functional T cell response after COVID-19 mRNA vaccination by an interferon-γ/interleukin-2 FluoroSpot kit (MabTech). Synthetic peptides of the full-length SARS-CoV-2 USA-WA1/2020 spike protein were solubilised in anhydrous dimethyl sulfoxide (DMSO). The PBMCs were separated by CPT tubes as described above for memory B cell ELISpot. PBMCs ($2x10^5$/well) were stimulated in duplicates with spike peptides (1 µg/ml), or medium (negative control) and anti-CD3 antibody (positive control). The plates were incubated for 16 hours (37°C, 5% CO_2) and developed according to the manufacturer's instructions. Spots were counted using a fluorescence reader (Advanced Imaging Devices, Germany) fitted with colour filters for FITC and Cy3. Spike-specific IFN-γ, IL-2, and double-positive IFN-γ^+, IL-2^+ cytokine-producing T cells were quantified. The mean of spike-specific SFU per 10^6 PBMCs of duplicate wells were calculated after subtracting the background from negative controls.

3.17 SARS-CoV-2 T cell receptor sequencing (paper III)

Blood samples were collected in Ethylene diamine tetra acetic acid (EDTA) tubes and used for sequencing of the T cell receptor (TCR). The immunoSEQ assay is a high throughput ultra-deep sequence-based method to quantify spike-specific T cell responses after natural infection or vaccination (205). It provides a quantitative view of the T cell repertoire by sequencing the CDR3 of rearranged TCRβ-chains. This method allowed us to assess the breadth and depth of the spike-specific TCR repertoire for all vaccinees at baseline and after the first (3 weeks) and second vaccination (6 weeks). Clonal breadth was defined as the relative number of distinct spike-specific T cell clonotypes of the total number of unique productive rearrangements (i.e. the total TCR repertoire) (**Figure 15**). Clonal depth accounts for the frequency of those rearrangements and was defined as the extent of expansion of spike-specific T cells. The TCR sequencing and the subsequent analysis of spike-specific breadth and depth was performed by Adaptive Biotechnologies (WA, USA).

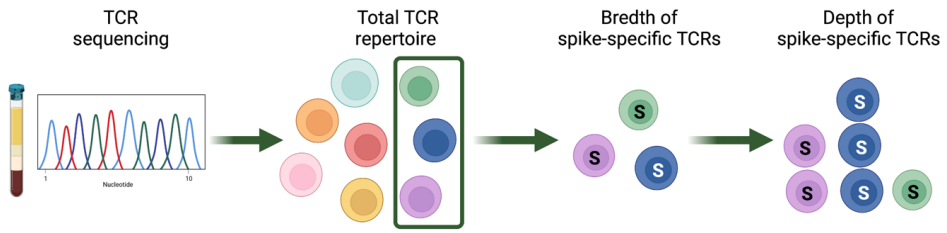

Figure 15: T cell receptor breadth and depth
The CDR3 of rearranged T cell receptor (TCR) β-chains are sequenced in bulk to examine the breadth and depth of the SARS-CoV-2 spike-specific TCR repertoire. The total repertoire represents all unique rearrangements of productive rearrangements. The breadth of the Spike-specific TCR repertoire is defined as the proportion of unique TCRs reactive to the spike protein relative to the total TCR repertoire. In the depicted example, the total TCR repertoire consists of eight unique TCR sequences, where three are spike-specific, meaning that the spike-specific TCR breadth is 3/8=0.38. The TCR breadth only measures how many unique T cell clones there are in a sample and does not take into account how many there are of each clonotype, however, some T cell clones may have undergone a larger clonal expansion than others. The depth of the spike-specific repertoire is a measurement of the frequency of the unique T cell clones that make up the total spike-specific TCR repertoire. The illustration was created with Biorender.

3.18 Statistical analysis

A non-parametric Kruskal-Wallis test was used for analysing differences in lung virus titres after lethal influenza challenge in mice treated with 2H08 and 3H03 mAbs in paper I. In paper II, non-parametric Spearman correlation was used to assess the relationship between pre-existing antibodies to NA and induction of NA-specific antibodies post-vaccination. The statistical difference between NA-specific antibody titres in the single and repeated group were determined by non-parametric Kruskal-Wallis test. The analyses were done in Graphpad Prism (version 9).

A linear mixed-effect model was used for statistical analysis of immune responses after influenza vaccination in paper II and SARS-CoV-2 vaccination and infection in paper III. The linear mixed-effects models were performed with log-transformed data with adjustments for demographic characteristics and repeated-measure subject variance. Both papers II and III were longitudinal studies and due to the long follow-up period, there were missing data for participants that did not provide samples at all timepoints during the studies (five years in paper II, one year in paper III). Any timepoints with missing data were excluded from the analyses. The linear mixed-effect model analyses were done in IBM SPSS Statistics version 26 (paper II) and in R (version 4.1.2) with libraries nlme, emmeans and ggplot (paper III). Post-hoc tests adjusted for multiple testing by Sidak (paper II) and Bonferroni correction (paper III).

4. Results

4.1 Paper I

"Human anti-N1 neuraminidase monoclonal antibodies broadly inhibit N1 subtype influenza viruses *in vitro* and *in vivo*".

In this paper, we cloned and expressed mAbs isolated from an individual infected with pandemic influenza A H1N1 virus in 2009. Thirty-three mAbs were cloned from clonally distinct plasmablasts, where five mAbs were reactive to inactivated A/California/04/09 (H1N1) virus by ELISA. The mAbs were tested against recombinant HA and NA proteins by ELISA and two of the mAbs were found to be NA-specific, while the other three had unknown specificity.

The breadth of binding and NAI activity was determined for the two NA-specific mAbs, 2H08 and 3H03. Heterosubtypic cross-reactivity was assessed against N2 of A/Hong Kong/4801/14 (H3N2) and avian N4 of A/mallard/Sweden/24/02 (H6N4) by ELISA, however, neither of the mAbs bound to these NA proteins. Among N1 NA proteins, the mAbs exhibited broad binding and NAI activity against seasonal H1N1 viruses that had circulated between 1934 and 2018. Furthermore, the mAbs bound to and had NAI activity against swine virus A/swine/Jiangsu/40/11 (H1N1) and avian origin viruses A/Vietnam/1204/04 (H5N1) and A/rhea/North Carolina/39482/93 (H7N1). 2H08 had the broadest reactivity, while 3H03 had reduced binding and NAI activity against A/New Caledonia/20/99 (H1N1), A/Solomon Islands/03/06 (H1N1) and A/Cambodia/0371/07 (H1N1). Our data indicated that the mAbs targeted highly conserved epitopes on N1 NA proteins. A competition ELISA revealed that the two mAbs inhibited each other's binding, indicating that they had overlapping binding footprints. 3H03 had higher affinity to NA A/Singapore/GP1908/15 (H1N1) than 2H08, as measured by BLI. EMV was generated using the 2H08 mAb and A/Singapore/GP1908/15 (H1N1) virus to identify the epitope. Sequencing of the NA gene segment of the 2H08 EMV revealed that Proline 93 residue was essential for the

binding and NAI activity of both mAbs. Neither of the mAbs had NAI activity by NA-Star, which indicated that the epitope was located outside of the enzymatic site.

Their functionality was further investigated *in vitro* by plaque reduction assay and ADCC bioreporter assay. Neither mAb reduced the actual formation of plaques, however, both reduced plaque sizes, most prominently when they were present in the agar overlay. This demonstrated that they functioned by reducing the release of virions from infected cells rather than inhibiting the initial infection, which is commonly considered the mode of action for anti-NA antibodies. Furthermore, the mAbs activated signalling pathways needed for ADCC in jurkat cells, indicating that the mAbs and target epitopes mediated effector functions. *In vivo* protection was assessed by lethal influenza A H1N1 and H5N1 influenza challenge in a murine model. Both mAbs provided prophylactic protection against H1N1 (100% survival) and H5N1 viruses (80% survival). The mAbs also protected therapeutically when administered 48 hours post-infection with A/Singapore/GP1908/15 (H1N1) (60-100% survival) and A/Vietnam/1204/04 (H5N1) virus (40-60% survival).

In conclusion, this study identified human mAbs that targeted a highly conserved, non-enzymatic site, epitope on the N1 NA that conferred broad NAI *in vitro* and *in vivo*. Our findings contribute to epitope-mapping of the N1 NA, combined with valuable information of the functional properties that these mAbs harbour.

4.2 Paper II

"Repeated Influenza Vaccination Boosts and Maintains H1N1pdm09 Neuraminidase Antibody Titers".

In this paper we, aimed to study the induction and durability of NA-specific antibody responses after AS03-adjuvanted monovalent pandemic influenza A H1N1 vaccination in HCWs and to investigate the impact of repeated seasonal vaccination in subsequent influenza seasons after 2009. We found that the adjuvanted pandemic vaccine induced

robust NA-specific IgG and NAI antibodies, despite the presumed low concentration of NA in the vaccine. The pandemic vaccine significantly boosted NAI titres at 21 days, with a 5-fold geometric mean fold rise from baseline. We defined the NAI seroconversion rate as ≥4-fold increase and found that 53% of the vaccinees met the criterium of seroconversion. Functional NA-specific antibodies measured by plaque reduction neutralisation assay were significantly boosted. Furthermore, NA-specific endpoint titres also increased 21 days after pandemic vaccination, although this was not significant (p=0.056).

A second aim of this paper was to investigate the induction of NA-specific antibody responses after seasonal TIVs and assess the impact of repeated annual vaccination with the same vaccine antigen. We found that the NAI titre seroconversion rate declined with each seasonal vaccine, none of the vaccinees seroconverted after the third TIV (n=16). There was a trend of increasing antibody titres after seasonal vaccination, however, the magnitude of fold increase was reduced with repeated vaccination. Pre-existing antibody titres seemed to influence the magnitude of fold-increase, which was most pronounced for functional antibodies measured by ELLA and plaque reduction neutralisation assay.

Although the magnitude of the antibody responses decreased with repeated vaccination, the repeated group had significantly higher NA-specific IgG and NAI titres five years after pandemic H1N1 vaccination compared to the single group. This indicated that seasonal vaccines contributed to the maintenance of durable NA-specific antibody responses.

In conclusion, AS03-adjuvanted pandemic influenza A H1N1 vaccine induced robust levels of NA-specific antibodies, which were maintained by repeated seasonal vaccination, although pre-existing antibodies may impact upon the induction of function NA antibody levels.

4.3 Paper III

"Durable immune responses after SARS-CoV-2 vaccination or infection in younger and older adults".

The aim of this paper was to study spike-specific immune responses after SARS-CoV-2 vaccination and infection in younger and older adults. We chose to focus on the oldest adults (aged 70-99) as they are considered a high-risk group and often have poorer immune responses due to immunosenescence. Here, we performed a comprehensive analysis of durable spike-specific humoral and cellular immune responses after BNT162b2 SARS-CoV-2 vaccination in seronegative older (n=100, median age 86, range 70-99 years) and younger adults (n=449, median age 36, range 23-69 years).

We found that the oldest adults had significantly lower spike-specific IgG and neutralising titres, which was particularly prominent after the first dose. The younger adults had significantly higher durability of antibody titres also after 9 months. The estimated antibody half-life was comparable for the two vaccine groups, however, due to the lower magnitude of antibody levels in the older adults, the estimated durability of antibodies titres was significantly shorter than for the younger adults. Neutralising titres were estimated to be detectable for 1 year in the younger adults but only 6 months for the older adults. The oldest adults had stronger boosting of the memory B cell response after the second dose, while the response was unchanged in younger adults. Both age groups maintained MBC responses 9 months after vaccination.

The vaccine primarily induced a $CD4^+$ T cell response based on TCRβ CDR3 sequencing. Lower spike-specific TCR breadth and depth was observed in the oldest adults after the first and second dose than younger vaccinees. Functional T cell responses were measured as secretion of IFN-γ and/or IL-2 by FluoroSpot. No significant differences were observed between the groups in their T cell responses, which were short-lived in both groups.

We compared immune responses to naturally infected non-hospitalised individuals that had experienced mild to moderate COVID-19 (n=183, median age 47, range 23-80). We found that immune responses were better maintained in the infected individuals, particularly the T cell and antibody responses between 6- and 12-months post-infection. Interestingly, spike-specific IgG and neutralising titres were better maintained in the oldest adults after infection. The duration of detectable neutralising antibody titres was estimated to last for one year in vaccinated younger adults, but only 6 months in older adults. In contrast, infected older adults had an estimated durability of 14 months, revealing an interesting effect of age for immune responses induced by infection and BNT162b2 vaccination.

In conclusion, we found lower magnitudes of spike-specific humoral and cellular immune responses after BNT162b2 vaccination in older compared to younger adult vaccinees, however, the estimated antibody half-life, memory B cell and T cell responses were comparable after 9 months.

5. Discussion

Continuous antigenic drift of circulating viruses and short-lived antibody responses are factors that limit the breadth and durability of immune responses against influenza viruses. Consequently, the composition of seasonal vaccines is re-evaluated biannually, and annual vaccination is recommended to maintain immunological protection. Despite this, VE of seasonal vaccines fluctuates greatly and has ranged from 10 – 60% in the last 15 years (124). Thus, influenza vaccines that induce broader and more durable immune responses are urgently needed.

A universal influenza vaccine targeting conserved epitopes on the influenza virus could potentially provide protection against both seasonal and pandemic strains. The exact definition of what constitutes a universal influenza vaccine is still under debate, however, several criteria have been proposed (**Table 3**). The criteria for breadth and durability of the immune response varies somewhat, however, the consensus is that the vaccine should provide protection against all influenza A subtypes, and possibly also influenza B viruses, for more than one year.

Table 3: Overview of the criteria for universal influenza vaccines

	WHO (206)	**BMGF (207)**	**NIAID (208)**
Breadth	All influenza A viruses	All influenza A and B viruses	All influenza A viruses, and possibly influenza B
Durability	1 year or more	3-5 years	1 year or more
Efficacy	Better than seasonal vaccines	≥70% against symptomatic infection	≥75% against symptomatic infection
Target group	All ages over >6 weeks	All ages	All ages

The table was inspired by (209). World health organization (WHO); Bill & Melinda Gates Foundation (BMGF); National Institute of Allergy and Infectious Diseases (NIAID).

Although having a universal influenza vaccine is the most advantageous, designing these vaccines have been proven to be very challenging. On the other hand, improved

seasonal vaccines may be a more rapidly achievable strategy to increase VE. Influenza vaccines can offer various levels of immunological breadth, starting with strain-specific, subtype-specific and multi subtype-specific responses, leading up to a universal influenza vaccine (**Figure 16**). Currently, seasonal vaccines primarily aim to induce strain-specific protection, yet there is room for significant improvement even at this level. Various aspects of influenza vaccine development could be modified to improve breadth and durability of immune responses. This includes optimising vaccine compositions, designing antigens to direct responses to conserved epitopes, inclusion of adjuvants, and utilising new vaccine platforms.

The aims of this thesis were to investigate immune responses to pandemic influenza A H1N1 and SARS-CoV-2 and use these insights to inform the improvement of future influenza vaccines. This included studies on NA-specific antibody responses (papers I and II) and SARS-CoV-2 mRNA vaccination in old and young adults (paper III).

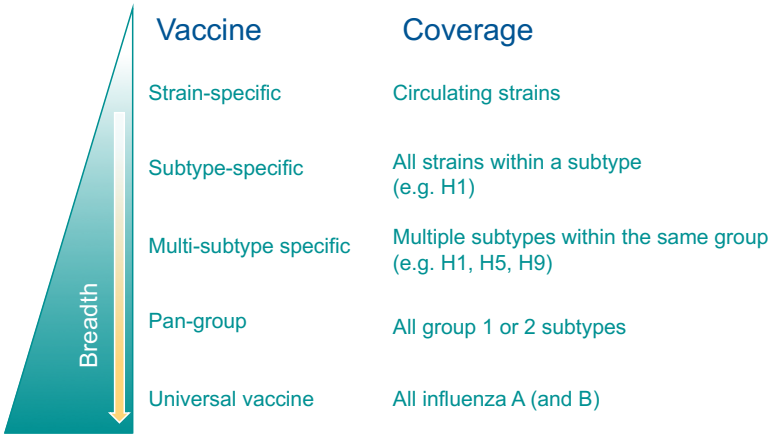

Figure 16: Improving the breadth of influenza vaccines
Immune responses to influenza virus can vary in breadth from strain-specific to universal coverage. Our current vaccines aim to achieve strain-specific immunity that covers the circulating strains. Vaccines can be improved to increase the breadth of protection to cover all influenza strains within a subtype, e.g. all viruses of the H1 subtype (subtype-specific), or to multiple strains of different subtypes within the same group, e.g. group 1 subtypes H1, H5 and H9 HA (multi-subtype). The next level of breadth would include cross-reactivity to both group 1 and group 2 subtype viruses (pan-group). The ultimate goal is to achieve breadth that provides universal protection against all influenza viruses, including type A and B influenza viruses. The figure was inspired by Erbelding *et al.* (208) and created with Inkscape.

5.1 NA as an immunogen for broader protection

NA is considered a low-hanging fruit for improving influenza vaccines (130). Anti-NA antibodies correlate with protection, reduce viral shedding and reduce disease severity in humans (55, 57, 83, 84). Several studies have identified anti-NA antibodies and NAI antibody titre as an independent correlate of protection (49, 55, 56, 84). Furthermore, NA is well conserved within subtypes and has slower mutation rates compared to HA (129). NA can evolve independently of HA, which was demonstrated during the 1968 pandemic with the emergence of the influenza A H3N2 virus, replacing the H2N2 virus. There was a shift in HA of the novel H3N2 virus but the NA of H2N2 remained the same (33). Individuals with higher NAI titres against N2 NA were less likely to be infected, demonstrating the contribution of NA immunity (34, 35). This indicates that NA-specific antibody responses can provide an additional layer of protection to HI antibodies, which could be important when there is a mismatch of HA sequences between vaccine and circulating strains. Furthermore, several subtype-specific, multi-subtype, pan-group and universal anti-NA mAbs have been characterised, demonstrating the potential for NA as an immunogen for improved influenza vaccines (59, 134, 135). Thus, optimising the design of the NA antigen and induction of NA-specific immune responses could potentially improve influenza vaccines by both increasing durability and by broadening protection.

In paper I, we identified an epitope on NA that was conserved among seasonal influenza A H1N1 viruses, swine H1N1 and avian H5N1 and H7N1 viruses. Both swine H1N1 and avian H5N1 viruses have pandemic potential (210, 211) and antibodies with cross-reactivity to the N1 subtype could potentially offer protection in the event of a pandemic. The escape mutation P93L revealed that the Pro93 residue was critical for binding of the 2H08 and 3H03 mAbs, which has not been identified as a part of a human epitope previously.

Current inactivated seasonal influenza vaccines induces a less robust anti-NA antibody response compared to infection (59). Furthermore, the NA of seasonal influenza vaccines has been found to poorly display epitopes targeted by broadly reactive human

mAbs, demonstrating the need for antigen optimisation (59). A recent study found that recombinant soluble NA proteins had an "open" conformation, which was not seen for native membrane-bound NA (212). They used structure-based design to generate recombinant NAs with a "closed" conformation, which improved stability and affinity to antibodies induced by infection. The murine mAb CD6 was found to bind better to NAs with the "closed" than the "open" conformation. The CD6 mAb binds to neighbouring monomers where the Pro93 residue is part of the epitope (213). These mutated NAs could be more native-like and may potentially improve NA-immunogenicity, particularly for mAbs targeting the Pro93 residue and area on the side of the NA. Structure-based rational design has already been described for respiratory syncytial virus (RSV) and severe acute respiratory syndrome coronavirus 2 (SARS-CoV-2). The fusion protein of RSV and spike protein of SARS-CoV-2 were mutated to produce stable pre-fusion conformations of the proteins (214, 215). The modified spike protein has subsequently been used in both Moderna's and Pfizer-BioNTech's mRNA vaccines (161, 216), demonstrating how rational design of antigens can be integrated with the mRNA vaccine platform.

As described in section 1.5 Rational vaccine design, characterisation of mAbs can be a powerful tool for epitope discovery and vaccine design. Our knowledge of NA epitopes that are targeted by human antibodies is still limited. Therefore, further characterisation of more human anti-NA mAbs is needed to guide rational design of improved NA antigens.

5.2 Increasing NA immunogenicity using an adjuvant

Current seasonal vaccines induce NA-specific IgG and NAI antibodies, however, the responses are often poor, and the immunogenicity varies greatly among different vaccines. Our study showed that the AS03-adjuvanted monovalent pandemic H1N1 vaccine induced robust and durable NA-specific antibody responses. The NAI seroconversion rate in our study, defined as ≥4-fold increase, was 53% and exceeded many of the seroconversion rates reported after unadjuvanted seasonal vaccination (84,

131, 217). These studies defined seroconversion rates as ≥2- or 4-fold, which limits direct comparability between studies. A study by Couch *et al.* investigated the induction of NAI antibody responses after vaccination with various seasonal IIVs in the 2008/2009 season. They defined seroconversion as a 2-fold increase and found that the seroconversion rates for N1 NA ranged between 23-57% for three IIVs produced by different manufacturers (131). The EMA Committee for Medicinal Products for Human Use (CHMP) had three immunological criteria for HAI titre for the pandemic vaccine: >2.5 geometric mean fold rise, and >40% seroconversion rate defined as >4 fold-increase, and >70% or higher seroprotection rate (HAI titre >40). Despite using >4-fold increase, matching the CHMP definition for HAI seroconversion, we found that NAI seroconversion rates in our study were still among the highest reported after vaccination, despite low NA concentration in the vaccine, which highlights the benefit of the AS03 adjuvant.

A study found that an AS03 adjuvanted H5N1 vaccine induced significantly higher NAI titres compared to an unadjuvanted vaccine (218). It is likely that the AS03 adjuvant was critical for the induction of robust and durable NA-specific antibody responses after pandemic H1N1 vaccination, however, a caveat of our study is the lack of control group receiving an unadjuvanted pandemic vaccine. The adjuvanted vaccine was the only vaccine offered in Norway to the general public during the 2009 pandemic, with the exception of cell culture vaccines for people with severe egg allergies. Consequently, we cannot conclude that the AS03 adjuvant was instrumental for the high NAI seroconversion rates or the long-term maintenance of NAI titres. Although an unadjuvanted monovalent pandemic H1N1 vaccine was used in Japan and a study found lower NAI seroconversion rates than in our vaccinated HCWs in paper II (219). Among the HCWs that were responders based on HAI titre, only 12% had a ≥4-fold increase in NAI titre, demonstrating that our cohort had more robust and durable NAI antibody responses, possibly due to the AS03 adjuvant.

The use of the AS03 adjuvant may be controversial due to the reported incidences of narcolepsy in children after vaccination with the Pandemrix vaccine in Nordic

countries (220). The EMA no longer recommended the use of Pandemrix in 2010 where other pandemic vaccines were available in children. Although the mechanism of narcolepsy has not been proven, there are several observations which strengthens the association with the Pandemrix vaccine. It has been linked to the HLA-DQB1*0602 haplotype and dysregulation of the hypocretin ligand-hypocretin receptor pathway. Anti-NP antibodies that cross-react with hypocretin receptor 2 and high amounts of NP in the Pandemrix vaccine have been proposed as potential explanations for the increased rates of narcolepsy after vaccination (221). Arepanrix was an AS03-adjuvanted pandemic H1N1 vaccine manufactured in Canada and was found to contain less NP than the Pandemrix vaccine produced in Germany in 2009 (221). A systemic review did not find any elevated risk of narcolepsy after vaccination with Arepanrix (222). Furthermore, an MF59-adjuvanted pandemic vaccine, which also had lower amounts of NP than Pandemrix, have not been associated with narcolepsy (221, 223). Despite these findings, it could be problematic to use this adjuvant in the future as the public may be sceptical and reluctant to get vaccinated. The COVID-19 pandemic has recently demonstrated that vaccine hesitancy is a globally important issue that can severely limit vaccine uptake. Ultimately, the most effective vaccines are the ones that make it into people's arms.

5.3 NA-specific antibody responses in the context of pre-existing immunity

In paper II, we also showed that repeated vaccination with seasonal influenza vaccines contributed to the maintenance of NAI antibodies but resulted in declining seroconversion rates and diminished magnitude of fold-induction at 21 days after vaccination. Several studies have found that repeated influenza vaccination and high pre-existing antibody levels have been associated with reduced induction of immune responses after vaccination (91-94, 224, 225). The negative effect of repeated vaccination and pre-existing immunity have primarily focused on HA-specific antibody responses. Here, we found that pre-existing immunity also impedes induction of NA-specific antibody responses, particularly for functional NAI antibodies. This

may be a consequence of functional NAI antibodies being restricted to certain epitopes/areas surrounding the enzyme active site. Masking of epitopes by pre-existing antibodies that block binding and proliferation of B cells specific for the same epitope may be a possible explanation for this observation. A mathematical model of epitope masking predicts that pre-existing antibodies and B cells that compete for binding to the same epitope, will inhibit proliferation of other B cells specific for the same epitope (101, 102). This model allows for B cells specific for other epitopes to proliferate, which is consistent with functional antibodies being more influenced by pre-existing antibody levels than the total binding antibody levels. A potential strategy to overcome this issue could be to increase the antigen dose (102), possibly by supplementing the vaccine with recombinant NA protein. This could be particularly beneficial when the same antigen is used over several consecutive seasons and pre-existing antibody levels are high. Overall, our findings highlight the need for standardisation and potentially supplementing of the NA component of seasonal vaccines.

SARS-CoV-2 has clearly demonstrated its capacity for immune evasion with the emergence of several successful variants of concern that have influenced VE (226, 227). If SARS-CoV-2 becomes endemic and causes seasonal outbreaks in the future, updating vaccine composition and periodic boosters may be needed to maintain protection, similarly to the updating of influenza vaccines. Repeated influenza vaccination has been associated with reduced induction of immune responses, especially when the vaccine antigen is unchanged from previous seasons (224). A third homologous booster shot of the COVID-19 mRNA vaccine has been found to induce similar levels of VE as the second dose (228) and to induce potent neutralising antibody responses to the Omicron variant (229). A fourth dose has been used in Israel which further reduced infection, although short lived, and severe disease (230). However, we do not know how further booster vaccinations and emergence of other variants of concern may impact effectiveness in the future. Thus, the issue of repeated vaccination may be taken into consideration for choosing vaccine composition and vaccination schedules for COVID-19 vaccines in the future (231).

5.4 Lessons from SARS-CoV-2 mRNA vaccines

COVID-19 mRNA vaccines were the first mRNA vaccines approved for use in humans and will likely represent a paradigm shift in vaccine development going forwards. There are many lessons to be learned from the development and deployment of these vaccines that can inform the design, production and use of mRNA vaccines for other pathogens, including influenza virus.

The COVID-19 pandemic has become the deadliest since the influenza A H1N1 pandemic in 1918. An estimate of years of life lost due to COVID-19 deaths during the first year of the pandemic in the United States alone was found to be 3.9 million years (232). Today, nearly 2.5 years after the start of the pandemic, there have been 525 million COVID-19 cases and 6.28 million deaths registered (146). This pandemic has been unique in numerous ways, but one aspect is the modern tools for efficient real-time surveillance of transmission and evolution of the virus combined with rapid data sharing. This allowed scientific knowledge and vaccine development to be conducted at an unprecedented pace. The first official cases of COVID-19 was reported in December of 2019 in Wuhan, China (233), and the genetic sequence of SARS-CoV-2 was made available online in January 10th 2020 (145). Once the sequence was published, it only took approximately one week for Moderna and the National Institute of Health (NIH) Vaccine Research Center to produce the mRNA vaccine candidates and 45 days to produce enough vaccines to the start the phase I clinical trial (234, 235).

A major advantage of the mRNA vaccine platform is that it is faster to produce than the classical inactivated whole virus vaccines. This aspect is especially relevant for future influenza vaccines and for future outbreaks. Today, approximately 85% of seasonal influenza vaccines are produced in embryonated chicken eggs, which is a well-established manufacturing platform for influenza vaccines with current production estimated at 1.5 billion doses annually (115). However, there are several downsides to the egg-based platform. The production is time-consuming (approximately 6 months) and consequently the recommendation for vaccine strains is made several months before the start of the influenza season, increasing the likelihood

of mismatching of vaccine and circulating strains. The platform is dependent on the availability of embryonated chicken eggs, which may be a limiting factor in the event of a new influenza pandemic. The production timeline for mRNA vaccines is estimated to be 2-3 months and can start once the sequence is available, which is substantially shorter than for egg-based seasonal influenza vaccines. The reduced production time would allow for strain recommendations to be made closer to the start of the influenza season, resulting in more accurate strain selection. This would reduce the risk of mismatch of vaccine and circulating strains and could significantly increase vaccine effectiveness. Furthermore, viral mutations may arise due to adaptation to growth in eggs, which limits sequence fidelity and contributes to mismatch of vaccine and circulating strains. This has been demonstrated for influenza A H3N2 virus (125) and it has been suggested that this contributed to the low VE observed against the H3N2 virus during the 2012/2013 season (126). This issue is bypassed by mRNA vaccines because they are manufactured synthetically by inserting the gene of interest into a plasmid, which is replicated with high sequence fidelity in *E. coli*.

Vaccines are essential for mitigating the impact of a pandemic. The current production timeline and capacity of influenza vaccines are not sufficient to meet the global demand during a pandemic. The production capacity of a pandemic vaccine is estimated to be 8.3 billion doses in a best-case scenario with 80% of the vaccines being produced in eggs. Furthermore, it is estimated that it would take 23-34 weeks from the time of the vaccine strain recommendation is made and the genetic sequence is available until first doses are ready for deployment (115). The egg-based platform and IIVs are dominating the production capacity of pandemic influenza vaccines, however, the use of other platforms may be considered to increase production capacity. The successful production and deployment of COVID-19 mRNA vaccines demonstrates the feasibility of this platform in a pandemic setting. Increasing production capacity of pandemic influenza vaccines by also using the mRNA platform in addition to egg-based vaccines may help to meet the global demand for pandemic vaccines more rapidly. Furthermore, this platform is faster to produce and could potentially mitigate the impact of the pandemic at the early stages, while IIVs are under production. This may be appropriate

for high-risk groups, such as elderly and HCWs, where we and others have shown that COVID-19 mRNA vaccines are immunogenic and protective.

As highlighted by the criteria for universal influenza vaccines, they should be suitable for all ages, including elderly that are at higher risk of developing severe disease and dying. In paper III, we investigated the kinetics and durability of humoral and cellular immune responses to SARS-CoV-2 spike after BNT162b2 mRNA vaccination in a high-risk elderly group and younger adult HCWs. Seasonal influenza vaccines for individuals aged 65 years and over have been developed to address the issue of reduced vaccine responses in older adults. This includes the inclusion of adjuvants, such as MF59, and high-dose vaccines that contain four times more antigen than the standard-dose vaccines. Based on our findings of older adults having immune responses with lower magnitude after COVID-19 mRNA vaccination, future mRNA vaccines against influenza may also require certain adjustments to accommodate the reduced immunogenicity in this age group. Using a high-dose mRNA vaccine for the oldest adults could be a potential solution, as the mRNA vaccines were well-tolerated and resulted in low frequencies of side reactions in this age group (236). Despite the lower magnitude of antibody responses in older adults, this group had comparable rates of antibody waning to the younger adults. This suggests that the durability of protection can be similar for younger and older adults if the magnitude of antibody response induced by initial vaccinations is significantly increased in the elderly. Overall, we found that the BNT162b2 mRNA vaccine was suitable for older adults, although some adjustments of the immunisation schedule may be necessary optimise immunogenicity compared to younger adults. These findings can guide the use of mRNA vaccines in the future against other pathogens during both endemic and pandemic outbreaks.

The initial FDA guidance for emergency use authorisation of COVID-19 vaccine stated that the primary efficacy endpoint should be at least 50% (237, 238). However, the mRNA vaccines proved to be far better and provided up to 96% protection against severe disease during the first two months after the second dose of BNT162b2 and 84% protection up to 7 months after the second dose (239). With the success and licensure

of COVID-19 mRNA vaccines, it is less risky for pharmaceutical companies to use the mRNA platform to make vaccines against other pathogens in the future. The platform is easily adaptable to other pathogens with a known antigenic target and its corresponding genetic sequence. Additionally, the COVID-19 pandemic has demonstrated the feasibility of this platform for emerging novel pathogens and in the event of another pandemic. More manufacturing sites are available, increasing the manufacturing capacity to meet the global demand of vaccines during a pandemic. Importantly, the global deployment of COVID-19 mRNA vaccines have proven to the general public that these vaccines are safe and effective, increasing their trust in this "new" technology.

Influenza mRNA vaccines have already shown promise in preclinical trials in mice, rabbits and ferrets (240, 241). These studies showed induction of protective antibody responses after vaccination with mRNA vaccines encoding full length HA or a combination of HA stalk, NA, NP and M2e. However, influenza mRNA vaccine candidates in human clinical trials have been less successful. The phase I clinical trial of Moderna's mRNA vaccine encoding the HA of avian H10N8 and H7N9 viruses was found to be well tolerated and induced HAI antibodies (242). However, the antibody responses were short-lived, and the vaccine did not induce T cell responses.

Since the start of the COVID-19 pandemic, four leading vaccine manufacturers (Sanofi, GSK, Moderna, Pfizer) have started clinical testing of seasonal influenza mRNA vaccine candidates. The vaccine manufacturers are taking different approaches for the selection of antigens to include in their vaccines. Sanofi started a phase 1 clinical trial in July 2021 testing a monovalent influenza A H3N2 HA mRNA vaccine (243). Moderna is currently conducting a phase 1/2 clinal trial testing vaccine candidates that contain eight mRNAs each. The mRNA encodes HA and NA of the influenza A H1N1, H3N2 and influenza B Yamagata and Victoria lineages based on sequences recommended by the WHO (244). Pfizer is testing monovalent, bivalent and quadrivalent mRNA vaccines encoding the HA of the vaccine strains recommended by the WHO (245).

COVID-19 mRNA vaccines undeniably changed the trajectory of the current pandemic and proved that it is a viable and effective vaccine platform that can be produced rapidly and in large scale to keep up with global demand. Messenger RNA vaccines will undoubtedly influence future vaccine design, however, factors such as pre-existing immunity, repeated vaccination and age may impact the efficacy of this vaccine platform against influenza. Only time will tell if they will be as successful for influenza as they have been for COVID-19.

5.5 Limitations and methodological considerations

5.5.1 Paper I

As with all scientific work, there are also some limitations to our studies. We did not use any antigen-probes for single-cell sorting of plasmablasts in paper I. This likely minimised the proportion of NA-specific plasmablasts that were used for mAb cloning. However, we lacked antigens with high structural integrity that we were confident displayed all the native epitopes of the NA protein. This was the basis of our decision to not include antigen-probes for the plasmablasts sorting in our experiment.

We generated escape mutant viruses to identify the epitope of the anti-NA mAbs. A limitation with this method is that mutations may arise at residues that are not part of the binding interface of the mAb but still reduce or inhibit mAb-binding. Mutations that disrupt and alter the structure of a conformation epitope or that add or remove glycosylation sites can significantly interfere with antibody binding. Although only one mutation was needed to abolish binding of the mAbs, an epitope will typically comprise more than one amino acid and there are likely other residues that make up the epitopes of 2H08 and 3H03. Structural methods, such as cryo-EM or x-ray crystallography would be needed to determine the total antibody-antigen binding interface for each mAb.

5.5.2 Paper II

In paper II, the HCWs received two or three seasonal vaccinations in the four subsequent influenza seasons following 2009. This meant that the vaccinees were not vaccinated in at least one season, however, which year this occurred varied among the HCWs. Although this is not optimal for the design of our study, these vaccination habits reflect that of HCWs in a busy clinical environment. Due to the small group sizes, we were not able to stratify the vaccine responses based on the vaccine intervals and consequently we were not able to determine the effect that the various vaccination intervals had on vaccine immunogenicity. This may have influenced our results seeing as repeated vaccination impacted on induction of NA-specific antibody responses and the group sizes were not large enough to determine if the vaccinees that had skipped seasonal vaccination the previous year had a superior antibody response than those that had been vaccinated in consecutive years. However, it would have been interesting to investigate this for our vaccination cohort.

In paper II, we only measured serum antibody levels to NA. It is possible that other NA-specific immune responses were boosted, such as memory B and T cell responses. Thus, it may be misleading to say that repeated vaccination resulted in limited boosting of NA-specific immune responses. Furthermore, the durability of the immune responses was measured as serum antibody levels; however, memory B cells are an important part of the durable immune response, which is not measured by serological assays. A study recent demonstrated the benefit of vaccine-induced memory B cells during infection with SARS-CoV-2. They found that spike-specific memory B cells induced by mRNA vaccination were activated by SARS-CoV-2 infection and rapidly produced antibodies found in both serum and saliva after 3-5 days (175).

5.5.3 Paper III

Our study had few infected individuals over 80 years old, as we focused on home-dwelling isolated cases, whilst the majority of the elderly vaccinees were over 80 years old. This limited the comparability of age-related variation of the immune response

after vaccination and infection in the oldest adults. Although all infected individuals experienced mild-to-moderate disease, we do not know how disease severity and the duration of illness and viral shedding impacted on the magnitude and durability of the immune responses.

The timing of sample collection for the infection (8 weeks, 6 and 12 months) and vaccination (6 weeks, 5 and 9 months) groups could have been more similar to improve comparability of the two groups. Furthermore, the sample sizes of adults (n=41) that were tested by microneutralisation assay and vaccinees that provided PBMC samples were small as they were limited by laboratory capacity (adults n=34, elderly n=24). This limited the power of our statistical analyses for neutralising antibodies, functional T and memory B cell responses in relation to age.

6. Conclusions

The objective of this thesis was to study immune responses after vaccination and infection with SARS-CoV-2 or influenza virus, with the overarching aim of informing strategies for improving future influenza vaccines. Here, we have broadly investigated immune responses after vaccination and infection in different populations groups and gained valuable knowledge of how factors such as age, pre-existing immunity, adjuvants and type of vaccine influence immunity.

NA has emerged as a potential target for broader protection against influenza virus infection. We investigated immune responses to NA after repeated vaccination and found that the AS03 adjuvant improved NA-specific immune responses and that after repeated vaccination pre-existing immunity negatively influenced induction of antibody responses to NA after vaccination. Although we found that seasonal vaccines induced NA-specific antibody responses, our findings highlight the need for standardisation of the NA component of current vaccines and an official requirement for the amount and quality of antigen per dose. A possible solution to increase the NA concentration of vaccines is by supplementing current vaccines with recombinant NA. This would be particularly important for overcoming pre-existing immunity when the NA vaccine component is unchanged in consecutive seasons and levels of pre-existing antibodies are high.

Epitope-mapping of NA, particularly epitopes targeted by antibodies that confer NAI activity, can inform the design of improved NA antigens. We found that pandemic H1N1 infection induced broadly cross-reactive antibodies that inhibited N1 NA *in vitro* and *in vivo*. Characterisation of anti-NA mAbs revealed a novel epitope involving the Pro93 residue on the underside of the NA head that is targeted by human antibodies. This can guide the design of future NA-based vaccines for broader protection against influenza A viruses expressing N1 NA.

Conclusions

As influenza mRNA vaccines move ahead in clinical trials, we need to take advantage of and apply the knowledge we have gained from current influenza vaccines and the deployment of COVID-19 vaccines to maximise their immunogenicity and efficacy. The main findings from our study on SARS-CoV-2 mRNA vaccination in older and younger adults are that the vaccination schedule in older adults should be optimised for this age group to increase immunogenicity of mRNA vaccines. Furthermore, SARS-CoV-2 infection induces more robust and durable immune responses in the elderly, suggesting that vaccine immunogenicity can be further improved for this age group.

7. Future perspectives

NA is emerging as a potential target for improved influenza vaccines and consequently there is a need for characterisation of epitopes to guide the design of NA antigens for targeting of broadly reactive B cells. Several knowledge gaps are restricting advancements in this field, including characterisation of epitopes targeted by human antibodies coupled with their functional capacities. Therefore, characterisation of both strain- and subtype-specific human mAbs is necessary for epitope-mapping of the NA. LIBRA-seq (linking B cell receptor to antigen specificity through sequencing) is a high-throughput method for single-cell sequencing that allows for coupling of paired heavy and light chain B cell receptor sequences with antigen-specificity. This method may be more efficient for identifying broadly reactive B cells compared to the method that were used in paper I where antigen-specificity and breadth was determined after cloning and expression of the mAbs. The LIBRA-seq method can easily feed into the reverse vaccinology 2.0 pipeline and be combined with the mRNA vaccine platform. Furthermore, as we identify more epitopes on NA, we can utilise protein engineering to selectively focus antibody responses toward these epitope (141).

In paper I, we generated escape mutant viruses with a mutation on Pro93, which was highly conserved in viruses expressing N1 NA. Substitution of highly conserved residues to enable immune evasion may result in viruses with reduce fitness. Understanding how certain mutations impacts viral fitness can provide insights on possible antibody-related antigenic drift. It would be interesting to investigate if and how the mutation of residue Pro93 affected viral fitness in future *in vitro* and *in vivo* experiments.

Currently, the NAI antibody titre is not a correlate of protection recognised by regulators, however, a correlate of protection for NAI antibodies is needed for evaluating immunogenicity and efficacy for NA-based vaccine in the future. Therefore, studies to establish a recognised correlate of protection for NAI antibody titres are warranted, including infection cohort studies and human challenge studies.

Our finding of superior magnitude and durability of antibody responses in the elderly after SARS-CoV-2 infection compared to vaccination in paper III demonstrates that there is room for improving vaccine responses in this age group. By dissecting and comparing immune responses after vaccination and infection, we may identify strategies for improving immunogenicity of mRNA vaccines in older adults. Future studies comparing vaccine- and infection-induced immune responses in the elderly are therefore warranted.

8. References

1. Chowell G, Bertozzi SM, Colchero MA, Lopez-Gatell H, Alpuche-Aranda C, Hernandez M, et al. Severe respiratory disease concurrent with the circulation of H1N1 influenza. N Engl J Med. 2009;361(7):674-9.
2. Iuliano AD, Roguski KM, Chang HH, Muscatello DJ, Palekar R, Tempia S, et al. Estimates of global seasonal influenza-associated respiratory mortality: a modelling study. Lancet. 2018;391(10127):1285-300.
3. Hutchinson EC, Charles PD, Hester SS, Thomas B, Trudgian D, Martinez-Alonso M, et al. Conserved and host-specific features of influenza virion architecture. Nat Commun. 2014;5:4816.
4. McCrone JT, Woods RJ, Martin ET, Malosh RE, Monto AS, Lauring AS. Stochastic processes constrain the within and between host evolution of influenza virus. Elife. 2018;7.
5. Muramoto Y, Noda T, Kawakami E, Akkina R, Kawaoka Y. Identification of novel influenza A virus proteins translated from PA mRNA. J Virol. 2013;87(5):2455-62.
6. Hirst GK. Adsorption of Influenza Hemagglutinins and virus by red blood cells. J Exp Med. 1942;76(2):195-209.
7. Gottschalk A. Neuraminidase: the specific enzyme of influenza virus and Vibrio cholerae. Biochim Biophys Acta. 1957;23(3):645-6.
8. Palese P, Tobita K, Ueda M, Compans RW. Characterization of temperature sensitive influenza virus mutants defective in neuraminidase. Virology. 1974;61(2):397-410.
9. Matrosovich MN, Matrosovich TY, Gray T, Roberts NA, Klenk HD. Neuraminidase is important for the initiation of influenza virus infection in human airway epithelium. J Virol. 2004;78(22):12665-7.
10. Calder LJ, Wasilewski S, Berriman JA, Rosenthal PB. Structural organization of a filamentous influenza A virus. Proc Natl Acad Sci U S A. 2010;107(23):10685-90.
11. Leser GP, Lamb RA. Lateral Organization of Influenza Virus Proteins in the Budozone Region of the Plasma Membrane. J Virol. 2017;91(9).
12. Vahey MD, Fletcher DA. Influenza A virus surface proteins are organized to help penetrate host mucus. Elife. 2019;8.
13. Mitnaul LJ, Matrosovich MN, Castrucci MR, Tuzikov AB, Bovin NV, Kobasa D, et al. Balanced hemagglutinin and neuraminidase activities are critical for efficient replication of influenza A virus. J Virol. 2000;74(13):6015-20.
14. Hensley SE, Das SR, Gibbs JS, Bailey AL, Schmidt LM, Bennink JR, et al. Influenza A virus hemagglutinin antibody escape promotes neuraminidase antigenic variation and drug resistance. PLoS One. 2011;6(2):e15190.
15. Das SR, Hensley SE, Ince WL, Brooke CB, Subba A, Delboy MG, et al. Defining influenza A virus hemagglutinin antigenic drift by sequential monoclonal antibody selection. Cell Host Microbe. 2013;13(3):314-23.
16. Hughes MT, Matrosovich M, Rodgers ME, McGregor M, Kawaoka Y. Influenza A viruses lacking sialidase activity can undergo multiple cycles of replication in cell culture, eggs, or mice. J Virol. 2000;74(11):5206-12.

17. Rogers GN, Paulson JC. Receptor determinants of human and animal influenza virus isolates: differences in receptor specificity of the H3 hemagglutinin based on species of origin. Virology. 1983;127(2):361-73.
18. Rogers GN, Paulson JC, Daniels RS, Skehel JJ, Wilson IA, Wiley DC. Single amino acid substitutions in influenza haemagglutinin change receptor binding specificity. Nature. 1983;304(5921):76-8.
19. Blumenkrantz D, Roberts KL, Shelton H, Lycett S, Barclay WS. The short stalk length of highly pathogenic avian influenza H5N1 virus neuraminidase limits transmission of pandemic H1N1 virus in ferrets. J Virol. 2013;87(19):10539-51.
20. Xu R, Zhu X, McBride R, Nycholat CM, Yu W, Paulson JC, et al. Functional balance of the hemagglutinin and neuraminidase activities accompanies the emergence of the 2009 H1N1 influenza pandemic. J Virol. 2012;86(17):9221-32.
21. Yen HL, Liang CH, Wu CY, Forrest HL, Ferguson A, Choy KT, et al. Hemagglutinin-neuraminidase balance confers respiratory-droplet transmissibility of the pandemic H1N1 influenza virus in ferrets. Proc Natl Acad Sci U S A. 2011;108(34):14264-9.
22. Lakdawala SS, Lamirande EW, Suguitan AL, Jr., Wang W, Santos CP, Vogel L, et al. Eurasian-origin gene segments contribute to the transmissibility, aerosol release, and morphology of the 2009 pandemic H1N1 influenza virus. PLoS Pathog. 2011;7(12):e1002443.
23. Reed ML, Bridges OA, Seiler P, Kim JK, Yen HL, Salomon R, et al. The pH of activation of the hemagglutinin protein regulates H5N1 influenza virus pathogenicity and transmissibility in ducks. J Virol. 2010;84(3):1527-35.
24. Hatta M, Gao P, Halfmann P, Kawaoka Y. Molecular basis for high virulence of Hong Kong H5N1 influenza A viruses. Science. 2001;293(5536):1840-2.
25. Mehle A, Doudna JA. Adaptive strategies of the influenza virus polymerase for replication in humans. Proc Natl Acad Sci U S A. 2009;106(50):21312-6.
26. Haller O, Staeheli P, Schwemmle M, Kochs G. Mx GTPases: dynamin-like antiviral machines of innate immunity. Trends Microbiol. 2015;23(3):154-63.
27. Xiao H, Killip MJ, Staeheli P, Randall RE, Jackson D. The human interferon-induced MxA protein inhibits early stages of influenza A virus infection by retaining the incoming viral genome in the cytoplasm. J Virol. 2013;87(23):13053-8.
28. Riegger D, Hai R, Dornfeld D, Manz B, Leyva-Grado V, Sanchez-Aparicio MT, et al. The nucleoprotein of newly emerged H7N9 influenza A virus harbors a unique motif conferring resistance to antiviral human MxA. J Virol. 2015;89(4):2241-52.
29. Taubenberger JK, Morens DM. 1918 Influenza: the mother of all pandemics. Emerg Infect Dis. 2006;12(1):15-22.
30. Johnson NP, Mueller J. Updating the accounts: global mortality of the 1918-1920 "Spanish" influenza pandemic. Bull Hist Med. 2002;76(1):105-15.
31. Kendal AP, Joseph JM, Kobayashi G, Nelson D, Reyes CR, Ross MR, et al. Laboratory-based surveillance of influenza virus in the United States during the winter of 1977-1978. I. Periods of prevalence of H1N1 and H3N2 influenza A strains, their relative rates of isolation in different age groups, and detection of antigenic variants. Am J Epidemiol. 1979;110(4):449-61.

32. Viboud C, Simonsen L, Fuentes R, Flores J, Miller MA, Chowell G. Global Mortality Impact of the 1957-1959 Influenza Pandemic. J Infect Dis. 2016;213(5):738-45.
33. Schulman JL, Kilbourne ED. Independent variation in nature of hemagglutinin and neuraminidase antigens of influenza virus: distinctiveness of hemagglutinin antigen of Hong Kong-68 virus. Proc Natl Acad Sci U S A. 1969;63(2):326-33.
34. Monto AS, Kendal AP. Effect of neuraminidase antibody on Hong Kong influenza. Lancet. 1973;1(7804):623-5.
35. Murphy BR, Kasel JA, Chanock RM. Association of serum anti-neuraminidase antibody with resistance to influenza in man. N Engl J Med. 1972;286(25):1329-32.
36. Novel Swine-Origin Influenza AVIT, Dawood FS, Jain S, Finelli L, Shaw MW, Lindstrom S, et al. Emergence of a novel swine-origin influenza A (H1N1) virus in humans. N Engl J Med. 2009;360(25):2605-15.
37. Hsieh YH, Ma S, Velasco Hernandez JX, Lee VJ, Lim WY. Early outbreak of 2009 influenza A (H1N1) in Mexico prior to identification of pH1N1 virus. PLoS One. 2011;6(8):e23853.
38. CDC. 2009 H1N1 Pandemic Timeline [Available from: https://www.cdc.gov/flu/pandemic-resources/2009-pandemic-timeline.html.
39. Timeline: Swine flu. Nature. 2009.
40. Dawood FS, Iuliano AD, Reed C, Meltzer MI, Shay DK, Cheng PY, et al. Estimated global mortality associated with the first 12 months of 2009 pandemic influenza A H1N1 virus circulation: a modelling study. Lancet Infect Dis. 2012;12(9):687-95.
41. Wisskirchen C, Ludersdorfer TH, Muller DA, Moritz E, Pavlovic J. The cellular RNA helicase UAP56 is required for prevention of double-stranded RNA formation during influenza A virus infection. J Virol. 2011;85(17):8646-55.
42. Le Goffic R, Balloy V, Lagranderie M, Alexopoulou L, Escriou N, Flavell R, et al. Detrimental contribution of the Toll-like receptor (TLR)3 to influenza A virus-induced acute pneumonia. PLoS Pathog. 2006;2(6):e53.
43. Hidaka F, Matsuo S, Muta T, Takeshige K, Mizukami T, Nunoi H. A missense mutation of the Toll-like receptor 3 gene in a patient with influenza-associated encephalopathy. Clin Immunol. 2006;119(2):188-94.
44. Schneider C, Nobs SP, Heer AK, Kurrer M, Klinke G, van Rooijen N, et al. Alveolar macrophages are essential for protection from respiratory failure and associated morbidity following influenza virus infection. PLoS Pathog. 2014;10(4):e1004053.
45. Tumpey TM, Garcia-Sastre A, Taubenberger JK, Palese P, Swayne DE, Pantin-Jackwood MJ, et al. Pathogenicity of influenza viruses with genes from the 1918 pandemic virus: functional roles of alveolar macrophages and neutrophils in limiting virus replication and mortality in mice. J Virol. 2005;79(23):14933-44.
46. Iwasaki A, Pillai PS. Innate immunity to influenza virus infection. Nat Rev Immunol. 2014;14(5):315-28.
47. Platanias LC. Mechanisms of type-I- and type-II-interferon-mediated signalling. Nat Rev Immunol. 2005;5(5):375-86.

48. Turner JS, Zhou JQ, Han J, Schmitz AJ, Rizk AA, Alsoussi WB, et al. Human germinal centres engage memory and naive B cells after influenza vaccination. Nature. 2020;586(7827):127-32.
49. Couch RB, Kasel JA, Gerin JL, Schulman JL, Kilbourne ED. Induction of partial immunity to influenza by a neuraminidase-specific vaccine. J Infect Dis. 1974;129(4):411-20.
50. Johansson BE, Grajower B, Kilbourne ED. Infection-permissive immunization with influenza virus neuraminidase prevents weight loss in infected mice. Vaccine. 1993;11(10):1037-9.
51. Johansson BE, Matthews JT, Kilbourne ED. Supplementation of conventional influenza A vaccine with purified viral neuraminidase results in a balanced and broadened immune response. Vaccine. 1998;16(9-10):1009-15.
52. Kilbourne ED. Comparative efficacy of neuraminidase-specific and conventional influenza virus vaccines in induction of antibody to neuraminidase in humans. J Infect Dis. 1976;134(4):384-94.
53. Kilbourne ED, Couch RB, Kasel JA, Keitel WA, Cate TR, Quarles JH, et al. Purified influenza A virus N2 neuraminidase vaccine is immunogenic and non-toxic in humans. Vaccine. 1995;13(18):1799-803.
54. Schulman JL, Khakpour M, Kilbourne ED. Protective effects of specific immunity to viral neuraminidase on influenza virus infection of mice. J Virol. 1968;2(8):778-86.
55. Memoli MJ, Shaw PA, Han A, Czajkowski L, Reed S, Athota R, et al. Evaluation of Antihemagglutinin and Antineuraminidase Antibodies as Correlates of Protection in an Influenza A/H1N1 Virus Healthy Human Challenge Model. mBio. 2016;7(2):e00417-16.
56. Ng S, Nachbagauer R, Balmaseda A, Stadlbauer D, Ojeda S, Patel M, et al. Novel correlates of protection against pandemic H1N1 influenza A virus infection. Nat Med. 2019;25(6):962-7.
57. Couch RB, Atmar RL, Franco LM, Quarles JM, Wells J, Arden N, et al. Antibody correlates and predictors of immunity to naturally occurring influenza in humans and the importance of antibody to the neuraminidase. J Infect Dis. 2013;207(6):974-81.
58. Wohlbold TJ, Podolsky KA, Chromikova V, Kirkpatrick E, Falconieri V, Meade P, et al. Broadly protective murine monoclonal antibodies against influenza B virus target highly conserved neuraminidase epitopes. Nat Microbiol. 2017;2(10):1415-24.
59. Chen YQ, Wohlbold TJ, Zheng NY, Huang M, Huang Y, Neu KE, et al. Influenza Infection in Humans Induces Broadly Cross-Reactive and Protective Neuraminidase-Reactive Antibodies. Cell. 2018;173(2):417-29.e10.
60. Wan H, Gao J, Xu K, Chen H, Couzens LK, Rivers KH, et al. Molecular basis for broad neuraminidase immunity: conserved epitopes in seasonal and pandemic H1N1 as well as H5N1 influenza viruses. J Virol. 2013;87(16):9290-300.
61. McMahon M, Kirkpatrick E, Stadlbauer D, Strohmeier S, Bouvier NM, Krammer F. Mucosal Immunity against Neuraminidase Prevents Influenza B Virus Transmission in Guinea Pigs. mBio. 2019;10(3).

62. DiLillo DJ, Palese P, Wilson PC, Ravetch JV. Broadly neutralizing anti-influenza antibodies require Fc receptor engagement for in vivo protection. J Clin Invest. 2016;126(2):605-10.
63. DiLillo DJ, Tan GS, Palese P, Ravetch JV. Broadly neutralizing hemagglutinin stalk-specific antibodies require FcgammaR interactions for protection against influenza virus in vivo. Nat Med. 2014;20(2):143-51.
64. Yasuhara A, Yamayoshi S, Kiso M, Sakai-Tagawa Y, Koga M, Adachi E, et al. Antigenic drift originating from changes to the lateral surface of the neuraminidase head of influenza A virus. Nat Microbiol. 2019;4(6):1024-34.
65. Brandenburg B, Koudstaal W, Goudsmit J, Klaren V, Tang C, Bujny MV, et al. Mechanisms of hemagglutinin targeted influenza virus neutralization. PLoS One. 2013;8(12):e80034.
66. Kosik I, Yewdell JW. Influenza A virus hemagglutinin specific antibodies interfere with virion neuraminidase activity via two distinct mechanisms. Virology. 2017;500:178-83.
67. Chen YQ, Lan LY, Huang M, Henry C, Wilson PC. Hemagglutinin Stalk-Reactive Antibodies Interfere with Influenza Virus Neuraminidase Activity by Steric Hindrance. J Virol. 2019;93(4).
68. Throsby M, van den Brink E, Jongeneelen M, Poon LL, Alard P, Cornelissen L, et al. Heterosubtypic neutralizing monoclonal antibodies cross-protective against H5N1 and H1N1 recovered from human IgM+ memory B cells. PLoS One. 2008;3(12):e3942.
69. Corti D, Voss J, Gamblin SJ, Codoni G, Macagno A, Jarrossay D, et al. A neutralizing antibody selected from plasma cells that binds to group 1 and group 2 influenza A hemagglutinins. Science. 2011;333(6044):850-6.
70. Dreyfus C, Laursen NS, Kwaks T, Zuijdgeest D, Khayat R, Ekiert DC, et al. Highly conserved protective epitopes on influenza B viruses. Science. 2012;337(6100):1343-8.
71. Nachbagauer R, Miller MS, Hai R, Ryder AB, Rose JK, Palese P, et al. Hemagglutinin Stalk Immunity Reduces Influenza Virus Replication and Transmission in Ferrets. J Virol. 2015;90(6):3268-73.
72. Nachbagauer R, Feser J, Naficy A, Bernstein DI, Guptill J, Walter EB, et al. A chimeric hemagglutinin-based universal influenza virus vaccine approach induces broad and long-lasting immunity in a randomized, placebo-controlled phase I trial. Nat Med. 2021;27(1):106-14.
73. Guthmiller JJ, Utset HA, Wilson PC. B Cell Responses against Influenza Viruses: Short-Lived Humoral Immunity against a Life-Long Threat. Viruses. 2021;13(6).
74. Herati RS, Muselman A, Vella L, Bengsch B, Parkhouse K, Del Alcazar D, et al. Successive annual influenza vaccination induces a recurrent oligoclonotypic memory response in circulating T follicular helper cells. Sci Immunol. 2017;2(8).
75. Bentebibel SE, Lopez S, Obermoser G, Schmitt N, Mueller C, Harrod C, et al. Induction of ICOS+CXCR3+CXCR5+ TH cells correlates with antibody responses to influenza vaccination. Sci Transl Med. 2013;5(176):176ra32.

76. Wilkinson TM, Li CK, Chui CS, Huang AK, Perkins M, Liebner JC, et al. Preexisting influenza-specific CD4+ T cells correlate with disease protection against influenza challenge in humans. Nat Med. 2012;18(2):274-80.
77. Sridhar S, Begom S, Bermingham A, Hoschler K, Adamson W, Carman W, et al. Cellular immune correlates of protection against symptomatic pandemic influenza. Nat Med. 2013;19(10):1305-12.
78. Babon JA, Cruz J, Orphin L, Pazoles P, Co MD, Ennis FA, et al. Genome-wide screening of human T-cell epitopes in influenza A virus reveals a broad spectrum of CD4(+) T-cell responses to internal proteins, hemagglutinins, and neuraminidases. Hum Immunol. 2009;70(9):711-21.
79. Koutsakos M, Illing PT, Nguyen THO, Mifsud NA, Crawford JC, Rizzetto S, et al. Human CD8(+) T cell cross-reactivity across influenza A, B and C viruses. Nat Immunol. 2019;20(5):613-25.
80. Kaufmann L, Syedbasha M, Vogt D, Hollenstein Y, Hartmann J, Linnik JE, et al. An Optimized Hemagglutination Inhibition (HI) Assay to Quantify Influenza-specific Antibody Titers. J Vis Exp. 2017(130).
81. Hobson D, Curry RL, Beare AS, Ward-Gardner A. The role of serum haemagglutination-inhibiting antibody in protection against challenge infection with influenza A2 and B viruses. J Hyg (Lond). 1972;70(4):767-77.
82. Potter CW, Jennings R, Nicholson K, Tyrrell DAJ, Dickinson KG. Immunity to Attenuated Influenza-Virus Wrl-105 Infection Induced by Heterologous, Inactivated Influenza-a Virus-Vaccines. J Hyg-Cambridge. 1977;79(3):321-32.
83. Maier HE, Nachbagauer R, Kuan G, Ng S, Lopez R, Sanchez N, et al. Pre-existing Antineuraminidase Antibodies Are Associated With Shortened Duration of Influenza A(H1N1)pdm Virus Shedding and Illness in Naturally Infected Adults. Clin Infect Dis. 2020;70(11):2290-7.
84. Monto AS, Petrie JG, Cross RT, Johnson E, Liu M, Zhong W, et al. Antibody to Influenza Virus Neuraminidase: An Independent Correlate of Protection. J Infect Dis. 2015;212(8):1191-9.
85. Nachbagauer R, Choi A, Izikson R, Cox MM, Palese P, Krammer F. Age Dependence and Isotype Specificity of Influenza Virus Hemagglutinin Stalk-Reactive Antibodies in Humans. mBio. 2016;7(1):e01996-15.
86. Bodewes R, de Mutsert G, van der Klis FR, Ventresca M, Wilks S, Smith DJ, et al. Prevalence of antibodies against seasonal influenza A and B viruses in children in Netherlands. Clin Vaccine Immunol. 2011;18(3):469-76.
87. Francis T. On the Doctrine of Original Antigenic Sin. Proceedings of the American Philosophical Society. 1960;104(6):572-8.
88. Davenport FM, Hennessy AV, Francis T, Jr. Epidemiologic and immunologic significance of age distribution of antibody to antigenic variants of influenza virus. J Exp Med. 1953;98(6):641-56.
89. Hobson D, Baker FA, Curry RL. Effect of influenza vaccines in stimulating antibody in volunteers with prior immunity. Lancet. 1973;2(7821):155-6.
90. Pyhala R, Kumpulainen V, Alanko S, Forsten T. HI antibody kinetics in adult volunteers immunized repeatedly with inactivated trivalent influenza vaccine in 1990-1992. Vaccine. 1994;12(10):947-52.

91. Andrews SF, Kaur K, Pauli NT, Huang M, Huang Y, Wilson PC. High preexisting serological antibody levels correlate with diversification of the influenza vaccine response. J Virol. 2015;89(6):3308-17.
92. Ellebedy AH, Krammer F, Li GM, Miller MS, Chiu C, Wrammert J, et al. Induction of broadly cross-reactive antibody responses to the influenza HA stem region following H5N1 vaccination in humans. Proc Natl Acad Sci U S A. 2014;111(36):13133-8.
93. Sanyal M, Holmes TH, Maecker HT, Albrecht RA, Dekker CL, He XS, et al. Diminished B-Cell Response After Repeat Influenza Vaccination. J Infect Dis. 2019;219(10):1586-95.
94. Petrie JG, Ohmit SE, Johnson E, Truscon R, Monto AS. Persistence of Antibodies to Influenza Hemagglutinin and Neuraminidase Following One or Two Years of Influenza Vaccination. J Infect Dis. 2015;212(12):1914-22.
95. Huang KA, Chang SC, Huang YC, Chiu CH, Lin TY. Antibody Responses to Trivalent Inactivated Influenza Vaccine in Health Care Personnel Previously Vaccinated and Vaccinated for The First Time. Sci Rep. 2017;7:40027.
96. Leung VKY, Fox A, Carolan LA, Aban M, Laurie KL, Druce J, et al. Impact of prior vaccination on antibody response and influenza-like illness among Australian healthcare workers after influenza vaccination in 2016. Vaccine. 2021;39(24):3270-8.
97. Thompson MG, Naleway A, Fry AM, Ball S, Spencer SM, Reynolds S, et al. Effects of Repeated Annual Inactivated Influenza Vaccination among Healthcare Personnel on Serum Hemagglutinin Inhibition Antibody Response to A/Perth/16/2009 (H3N2)-like virus during 2010-11. Vaccine. 2016;34(7):981-8.
98. Morimoto N, Takeishi K. Change in the efficacy of influenza vaccination after repeated inoculation under antigenic mismatch: A systematic review and meta-analysis. Vaccine. 2018;36(7):949-57.
99. Saito N, Komori K, Suzuki M, Morimoto K, Kishikawa T, Yasaka T, et al. Negative impact of prior influenza vaccination on current influenza vaccination among people infected and not infected in prior season: A test-negative case-control study in Japan. Vaccine. 2017;35(4):687-93.
100. Belongia EA, Skowronski DM, McLean HQ, Chambers C, Sundaram ME, De Serres G. Repeated annual influenza vaccination and vaccine effectiveness: review of evidence. Expert Rev Vaccines. 2017;16(7):1-14.
101. Linderman SL, Ellebedy AH, Davis C, Eberhardt CS, Antia R, Ahmed R, et al. Influenza Immunization in the Context of Preexisting Immunity. Cold Spring Harb Perspect Med. 2020.
102. Zarnitsyna VI, Lavine J, Ellebedy A, Ahmed R, Antia R. Multi-epitope Models Explain How Pre-existing Antibodies Affect the Generation of Broadly Protective Responses to Influenza. PLoS Pathog. 2016;12(6):e1005692.
103. Zarnitsyna VI, Ellebedy AH, Davis C, Jacob J, Ahmed R, Antia R. Masking of antigenic epitopes by antibodies shapes the humoral immune response to influenza. Philos Trans R Soc Lond B Biol Sci. 2015;370(1676).
104. Varghese JN, McKimm-Breschkin JL, Caldwell JB, Kortt AA, Colman PM. The structure of the complex between influenza virus neuraminidase and sialic acid, the viral receptor. Proteins. 1992;14(3):327-32.

105. von Itzstein M, Wu WY, Kok GB, Pegg MS, Dyason JC, Jin B, et al. Rational design of potent sialidase-based inhibitors of influenza virus replication. Nature. 1993;363(6428):418-23.
106. Varghese JN, Epa VC, Colman PM. Three-dimensional structure of the complex of 4-guanidino-Neu5Ac2en and influenza virus neuraminidase. Protein Sci. 1995;4(6):1081-7.
107. Colman PM, Varghese JN, Laver WG. Structure of the catalytic and antigenic sites in influenza virus neuraminidase. Nature. 1983;303(5912):41-4.
108. Aoki FY, Macleod MD, Paggiaro P, Carewicz O, El Sawy A, Wat C, et al. Early administration of oral oseltamivir increases the benefits of influenza treatment. J Antimicrob Chemother. 2003;51(1):123-9.
109. Jefferson T, Jones M, Doshi P, Spencer EA, Onakpoya I, Heneghan CJ. Oseltamivir for influenza in adults and children: systematic review of clinical study reports and summary of regulatory comments. BMJ. 2014;348:g2545.
110. Dharan NJ, Gubareva LV, Meyer JJ, Okomo-Adhiambo M, McClinton RC, Marshall SA, et al. Infections with oseltamivir-resistant influenza A(H1N1) virus in the United States. JAMA. 2009;301(10):1034-41.
111. Gubareva LV, Trujillo AA, Okomo-Adhiambo M, Mishin VP, Deyde VM, Sleeman K, et al. Comprehensive assessment of 2009 pandemic influenza A (H1N1) virus drug susceptibility in vitro. Antivir Ther. 2010;15(8):1151-9.
112. Hussain M, Galvin HD, Haw TY, Nutsford AN, Husain M. Drug resistance in influenza A virus: the epidemiology and management. Infect Drug Resist. 2017;10:121-34.
113. Ison MG, Portsmouth S, Yoshida Y, Shishido T, Mitchener M, Tsuchiya K, et al. Early treatment with baloxavir marboxil in high-risk adolescent and adult outpatients with uncomplicated influenza (CAPSTONE-2): a randomised, placebo-controlled, phase 3 trial. Lancet Infect Dis. 2020;20(10):1204-14.
114. Broor S, Campbell H, Hirve S, Hague S, Jackson S, Moen A, et al. Leveraging the Global Influenza Surveillance and Response System for global respiratory syncytial virus surveillance-opportunities and challenges. Influenza Other Respir Viruses. 2020;14(6):622-9.
115. Sparrow E, Wood JG, Chadwick C, Newall AT, Torvaldsen S, Moen A, et al. Global production capacity of seasonal and pandemic influenza vaccines in 2019. Vaccine. 2021;39(3):512-20.
116. Bartley JM, Cadar AN, Martin DE. Better, Faster, Stronger: mRNA Vaccines Show Promise for Influenza Vaccination in Older Adults. Immunol Invest. 2021;50(7):810-20.
117. Ping J, Lopes TJS, Nidom CA, Ghedin E, Macken CA, Fitch A, et al. Development of high-yield influenza A virus vaccine viruses. Nat Commun. 2015;6:8148.
118. Prevention CfDCa. Influenza disease burden Centers for Disease Control and Prevention2022 [Available from: https://www.cdc.gov/flu/about/burden/past-seasons.html.
119. Wagner A, Garner-Spitzer E, Jasinska J, Kollaritsch H, Stiasny K, Kundi M, et al. Age-related differences in humoral and cellular immune responses after primary

immunisation: indications for stratified vaccination schedules. Sci Rep. 2018;8(1):9825.
120. Osterholm MT, Kelley NS, Sommer A, Belongia EA. Efficacy and effectiveness of influenza vaccines: a systematic review and meta-analysis. Lancet Infect Dis. 2012;12(1):36-44.
121. Cowling BJ, Perera RAPM, Valkenburg SA, Leung NHL, Iuliano AD, Tam YH, et al. Comparative Immunogenicity of Several Enhanced Influenza Vaccine Options for Older Adults: A Randomized, Controlled Trial. Clinical Infectious Diseases. 2019;71(7):1704-14.
122. Chung JR, Rolfes MA, Flannery B, Prasad P, O'Halloran A, Garg S, et al. Effects of Influenza Vaccination in the United States During the 2018-2019 Influenza Season. Clin Infect Dis. 2020;71(8):e368-e76.
123. Foppa IM, Cheng PY, Reynolds SB, Shay DK, Carias C, Bresee JS, et al. Deaths averted by influenza vaccination in the U.S. during the seasons 2005/06 through 2013/14. Vaccine. 2015;33(26):3003-9.
124. CDC. Past Seasons Vaccine Effectiveness Estimates 2022 [Available from: https://www.cdc.gov/flu/vaccines-work/past-seasons-estimates.html.
125. Zost SJ, Parkhouse K, Gumina ME, Kim K, Diaz Perez S, Wilson PC, et al. Contemporary H3N2 influenza viruses have a glycosylation site that alters binding of antibodies elicited by egg-adapted vaccine strains. Proc Natl Acad Sci U S A. 2017;114(47):12578-83.
126. Skowronski DM, Janjua NZ, De Serres G, Sabaiduc S, Eshaghi A, Dickinson JA, et al. Low 2012-13 influenza vaccine effectiveness associated with mutation in the egg-adapted H3N2 vaccine strain not antigenic drift in circulating viruses. PLoS One. 2014;9(3):e92153.
127. Wan H, Sultana I, Couzens LK, Mindaye S, Eichelberger MC. Assessment of influenza A neuraminidase (subtype N1) potency by ELISA. J Virol Methods. 2017;244:23-8.
128. Kuck LR, Byrne-Nash R, Gillis J, Bueter K, Couzens LK, Eichelberger MC, et al. VaxArray for hemagglutinin and neuraminidase potency testing of influenza vaccines. Vaccine. 2018;36(21):2937-45.
129. Westgeest KB, de Graaf M, Fourment M, Bestebroer TM, van Beek R, Spronken MIJ, et al. Genetic evolution of the neuraminidase of influenza A (H3N2) viruses from 1968 to 2009 and its correspondence to haemagglutinin evolution. J Gen Virol. 2012;93(Pt 9):1996-2007.
130. Eichelberger MC, Morens DM, Taubenberger JK. Neuraminidase as an influenza vaccine antigen: a low hanging fruit, ready for picking to improve vaccine effectiveness. Curr Opin Immunol. 2018;53:38-44.
131. Couch RB, Atmar RL, Keitel WA, Quarles JM, Wells J, Arden N, et al. Randomized comparative study of the serum antihemagglutinin and antineuraminidase antibody responses to six licensed trivalent influenza vaccines. Vaccine. 2012;31(1):190-5.
132. Cate TR, Rayford Y, Nino D, Winokur P, Brady R, Belshe R, et al. A high dosage influenza vaccine induced significantly more neuraminidase antibody than standard vaccine among elderly subjects. Vaccine. 2010;28(9):2076-9.

133. Czaja CA, Miller L, Alden N, Wald HL, Cummings CN, Rolfes MA, et al. Age-Related Differences in Hospitalization Rates, Clinical Presentation, and Outcomes Among Older Adults Hospitalized With Influenza-U.S. Influenza Hospitalization Surveillance Network (FluSurv-NET). Open Forum Infect Dis. 2019;6(7).
134. Rijal P, Wang BB, Tan TK, Schimanski L, Janesch P, Dong T, et al. Broadly Inhibiting Antineuraminidase Monoclonal Antibodies Induced by Trivalent Influenza Vaccine and H7N9 Infection in Humans. J Virol. 2020;94(4).
135. Stadlbauer D, Zhu X, McMahon M, Turner JS, Wohlbold TJ, Schmitz AJ, et al. Broadly protective human antibodies that target the active site of influenza virus neuraminidase. Science. 2019;366(6464):499-504.
136. Madsen A, Dai YN, McMahon M, Schmitz AJ, Turner JS, Tan J, et al. Human Antibodies Targeting Influenza B Virus Neuraminidase Active Site Are Broadly Protective. Immunity. 2020;53(4):852-63 e7.
137. Kirkpatrick E, Henry C, McMahon M, Jiang K, Strohmeier S, van Bakel H, et al. Characterization of Novel Cross-Reactive Influenza B Virus Hemagglutinin Head Specific Antibodies That Lack Hemagglutination Inhibition Activity. J Virol. 2020;94(23).
138. Kirkpatrick Roubidoux E, McMahon M, Carreno JM, Capuano C, Jiang K, Simon V, et al. Identification and Characterization of Novel Antibody Epitopes on the N2 Neuraminidase. mSphere. 2021;6(1).
139. Kirkpatrick Roubidoux E, Sano K, McMahon M, Carreno JM, Capuano C, Jiang K, et al. Novel Epitopes of the Influenza Virus N1 Neuraminidase Targeted by Human Monoclonal Antibodies. J Virol. 2022:e0033222.
140. Rappuoli R, Bottomley MJ, D'Oro U, Finco O, De Gregorio E. Reverse vaccinology 2.0: Human immunology instructs vaccine antigen design. J Exp Med. 2016;213(4):469-81.
141. Caradonna TM, Schmidt AG. Protein engineering strategies for rational immunogen design. NPJ Vaccines. 2021;6(1):154.
142. De Gregorio E, Rappuoli R. From empiricism to rational design: a personal perspective of the evolution of vaccine development. Nat Rev Immunol. 2014;14(7):505-14.
143. Zhu N, Zhang D, Wang W, Li X, Yang B, Song J, et al. A Novel Coronavirus from Patients with Pneumonia in China, 2019. New England Journal of Medicine. 2020;382(8):727-33.
144. Wu Z, McGoogan JM. Characteristics of and Important Lessons From the Coronavirus Disease 2019 (COVID-19) Outbreak in China: Summary of a Report of 72314 Cases From the Chinese Center for Disease Control and Prevention. JAMA. 2020;323(13):1239-42.
145. Paden CR, Tao Y, Queen K, Zhang J, Li Y, Uehara A, et al. Rapid, Sensitive, Full-Genome Sequencing of Severe Acute Respiratory Syndrome Coronavirus 2. Emerg Infect Dis. 2020;26(10):2401-5.
146. WHO. WHO Coronavirus (COVID-19) Dashboard 2022 [Available from: https://covid19.who.int/.
147. Hoffmann M, Kleine-Weber H, Schroeder S, Kruger N, Herrler T, Erichsen S, et al. SARS-CoV-2 Cell Entry Depends on ACE2 and TMPRSS2 and Is Blocked by a Clinically Proven Protease Inhibitor. Cell. 2020;181(2):271-80 e8.

148. Bayati A, Kumar R, Francis V, McPherson PS. SARS-CoV-2 infects cells after viral entry via clathrin-mediated endocytosis. J Biol Chem. 2021;296:100306.
149. Oudshoorn D, Rijs K, Limpens R, Groen K, Koster AJ, Snijder EJ, et al. Expression and Cleavage of Middle East Respiratory Syndrome Coronavirus nsp3-4 Polyprotein Induce the Formation of Double-Membrane Vesicles That Mimic Those Associated with Coronaviral RNA Replication. mBio. 2017;8(6).
150. Angelini MM, Akhlaghpour M, Neuman BW, Buchmeier MJ. Severe acute respiratory syndrome coronavirus nonstructural proteins 3, 4, and 6 induce double-membrane vesicles. mBio. 2013;4(4).
151. Cortese M, Lee JY, Cerikan B, Neufeldt CJ, Oorschot VMJ, Kohrer S, et al. Integrative Imaging Reveals SARS-CoV-2-Induced Reshaping of Subcellular Morphologies. Cell Host Microbe. 2020;28(6):853-66 e5.
152. Bouvet M, Imbert I, Subissi L, Gluais L, Canard B, Decroly E. RNA 3'-end mismatch excision by the severe acute respiratory syndrome coronavirus nonstructural protein nsp10/nsp14 exoribonuclease complex. Proc Natl Acad Sci U S A. 2012;109(24):9372-7.
153. Denison MR, Graham RL, Donaldson EF, Eckerle LD, Baric RS. Coronaviruses: an RNA proofreading machine regulates replication fidelity and diversity. RNA Biol. 2011;8(2):270-9.
154. Smith EC, Sexton NR, Denison MR. Thinking Outside the Triangle: Replication Fidelity of the Largest RNA Viruses. Annu Rev Virol. 2014;1(1):111-32.
155. Duan L, Zheng Q, Zhang H, Niu Y, Lou Y, Wang H. The SARS-CoV-2 Spike Glycoprotein Biosynthesis, Structure, Function, and Antigenicity: Implications for the Design of Spike-Based Vaccine Immunogens. Front Immunol. 2020;11:576622.
156. Pallesen J, Wang N, Corbett KS, Wrapp D, Kirchdoerfer RN, Turner HL, et al. Immunogenicity and structures of a rationally designed prefusion MERS-CoV spike antigen. Proc Natl Acad Sci U S A. 2017;114(35):E7348-E57.
157. Krammer F. SARS-CoV-2 vaccines in development. Nature. 2020;586(7830):516-27.
158. Hannah Ritchie EM, Lucas Rodés-Guirao, Cameron Appel, Charlie Giattino, Esteban Ortiz-Ospina, Joe Hasell, Bobbie Macdonald, Diana Beltekian, Max Roser. Coronavirus Pandemic (COVID-19) OurWorldInData.org2022 [Available from: https://ourworldindata.org/coronavirus.
159. Organization WH. COVID-19 Vaccine Market Dashboard 2022 [Available from: https://www.unicef.org/supply/covid-19-vaccine-market-dashboard.
160. Organization WH. The COVID-19 vaccine tracker [Available from: https://www.who.int/publications/m/item/draft-landscape-of-covid-19-candidate-vaccines.
161. Corbett KS, Edwards DK, Leist SR, Abiona OM, Boyoglu-Barnum S, Gillespie RA, et al. SARS-CoV-2 mRNA vaccine design enabled by prototype pathogen preparedness. Nature. 2020;586(7830):567-71.
162. Rappuoli R, De Gregorio E, Del Giudice G, Phogat S, Pecetta S, Pizza M, et al. Vaccinology in the post-COVID-19 era. Proc Natl Acad Sci U S A. 2021;118(3).
163. Blomberg B, Mohn KG, Brokstad KA, Zhou F, Linchausen DW, Hansen BA, et al. Long COVID in a prospective cohort of home-isolated patients. Nat Med. 2021;27(9):1607-13.

164. Gorman MJ, Patel N, Guebre-Xabier M, Zhu AL, Atyeo C, Pullen KM, et al. Fab and Fc contribute to maximal protection against SARS-CoV-2 following NVX-CoV2373 subunit vaccine with Matrix-M vaccination. Cell Rep Med. 2021;2(9):100405.
165. Mercado NB, Zahn R, Wegmann F, Loos C, Chandrashekar A, Yu J, et al. Single-shot Ad26 vaccine protects against SARS-CoV-2 in rhesus macaques. Nature. 2020;586(7830):583-8.
166. Dan JM, Mateus J, Kato Y, Hastie KM, Yu ED, Faliti CE, et al. Immunological memory to SARS-CoV-2 assessed for up to 8 months after infection. Science. 2021;371(6529).
167. Robbiani DF, Gaebler C, Muecksch F, Lorenzi JCC, Wang Z, Cho A, et al. Convergent antibody responses to SARS-CoV-2 in convalescent individuals. Nature. 2020;584(7821):437-42.
168. Kang CK, Kim M, Hong J, Kim G, Lee S, Chang E, et al. Distinct Immune Response at 1 Year Post-COVID-19 According to Disease Severity. Frontiers in Immunology. 2022;13.
169. Muecksch F, Weisblum Y, Barnes CO, Schmidt F, Schaefer-Babajew D, Wang Z, et al. Affinity maturation of SARS-CoV-2 neutralizing antibodies confers potency, breadth, and resilience to viral escape mutations. Immunity. 2021;54(8):1853-68 e7.
170. Turner JS, Kim W, Kalaidina E, Goss CW, Rauseo AM, Schmitz AJ, et al. SARS-CoV-2 infection induces long-lived bone marrow plasma cells in humans. Nature. 2021;595(7867):421-5.
171. Zuo J, Dowell AC, Pearce H, Verma K, Long HM, Begum J, et al. Robust SARS-CoV-2-specific T cell immunity is maintained at 6 months following primary infection. Nat Immunol. 2021;22(5):620-6.
172. Lu Z, Laing ED, Pena DaMata J, Pohida K, Tso MS, Samuels EC, et al. Durability of SARS-CoV-2-Specific T-Cell Responses at 12 Months Postinfection. J Infect Dis. 2021;224(12):2010-9.
173. Goel RR, Apostolidis SA, Painter MM, Mathew D, Pattekar A, Kuthuru O, et al. Distinct antibody and memory B cell responses in SARS-CoV-2 naive and recovered individuals following mRNA vaccination. Sci Immunol. 2021;6(58).
174. Sahin U, Muik A, Vogler I, Derhovanessian E, Kranz LM, Vormehr M, et al. BNT162b2 vaccine induces neutralizing antibodies and poly-specific T cells in humans. Nature. 2021;595(7868):572-7.
175. Terreri S, Piano Mortari E, Vinci MR, Russo C, Alteri C, Albano C, et al. Persistent B cell memory after SARS-CoV-2 vaccination is functional during breakthrough infections. Cell Host Microbe. 2022.
176. Turner JS, O'Halloran JA, Kalaidina E, Kim W, Schmitz AJ, Zhou JQ, et al. SARS-CoV-2 mRNA vaccines induce persistent human germinal centre responses. Nature. 2021;596(7870):109-13.
177. Mudd PA, Minervina AA, Pogorelyy MV, Turner JS, Kim W, Kalaidina E, et al. SARS-CoV-2 mRNA vaccination elicits a robust and persistent T follicular helper cell response in humans. Cell. 2022;185(4):603-13 e15.
178. Altomare CG, Adelsberg DC, Carreno JM, Sapse IA, Amanat F, Ellebedy AH, et al. Structure of a Vaccine-Induced, Germline-Encoded Human Antibody Defines a

Neutralizing Epitope on the SARS-CoV-2 Spike N-Terminal Domain. mBio. 2022:e0358021.
179. Alsoussi WB, Turner JS, Case JB, Zhao H, Schmitz AJ, Zhou JQ, et al. A Potently Neutralizing Antibody Protects Mice against SARS-CoV-2 Infection. J Immunol. 2020;205(4):915-22.
180. Feng S, Phillips DJ, White T, Sayal H, Aley PK, Bibi S, et al. Correlates of protection against symptomatic and asymptomatic SARS-CoV-2 infection. Nat Med. 2021;27(11):2032-40.
181. Corbett KS, Nason MC, Flach B, Gagne M, O'Connell S, Johnston TS, et al. Immune correlates of protection by mRNA-1273 vaccine against SARS-CoV-2 in nonhuman primates. Science. 2021;373(6561):eabj0299.
182. Khoury DS, Cromer D, Reynaldi A, Schlub TE, Wheatley AK, Juno JA, et al. Neutralizing antibody levels are highly predictive of immune protection from symptomatic SARS-CoV-2 infection. Nat Med. 2021;27(7):1205-11.
183. Notarbartolo S, Ranzani V, Bandera A, Gruarin P, Bevilacqua V, Putignano AR, et al. Integrated longitudinal immunophenotypic, transcriptional and repertoire analyses delineate immune responses in COVID-19 patients. Sci Immunol. 2021;6(62).
184. Bergamaschi L, Mescia F, Turner L, Hanson AL, Kotagiri P, Dunmore BJ, et al. Longitudinal analysis reveals that delayed bystander CD8+ T cell activation and early immune pathology distinguish severe COVID-19 from mild disease. Immunity. 2021;54(6):1257-75 e8.
185. Seppala E, Veneti L, Starrfelt J, Danielsen AS, Bragstad K, Hungnes O, et al. Vaccine effectiveness against infection with the Delta (B.1.617.2) variant, Norway, April to August 2021. Euro Surveill. 2021;26(35).
186. Dejnirattisai W, Huo J, Zhou D, Zahradnik J, Supasa P, Liu C, et al. SARS-CoV-2 Omicron-B.1.1.529 leads to widespread escape from neutralizing antibody responses. Cell. 2022;185(3):467-84 e15.
187. (UKHSA) UHSA. SARS-CoV-2 variants of concern and
variants under investigation in
England, Technical briefing 31: UK Health Security Agency (UKHSA); 2021 [Available from: https://assets.publishing.service.gov.uk/government/uploads/system/uploads/attachment_data/file/1042367/technical_briefing-31-10-december-2021.pdf.
188. Gu H, Krishnan P, Ng DYM, Chang LDJ, Liu GYZ, Cheng SSM, et al. Probable Transmission of SARS-CoV-2 Omicron Variant in Quarantine Hotel, Hong Kong, China, November 2021. Emerg Infect Dis. 2022;28(2):460-2.
189. Garcia-Beltran WF, St Denis KJ, Hoelzemer A, Lam EC, Nitido AD, Sheehan ML, et al. mRNA-based COVID-19 vaccine boosters induce neutralizing immunity against SARS-CoV-2 Omicron variant. Cell. 2022;185(3):457-66 e4.
190. CDC. Risk for COVID-19 Infection, Hospitalization, and Death By Age Group 2022 [Available from: https://www.cdc.gov/coronavirus/2019-ncov/covid-data/investigations-discovery/hospitalization-death-by-age.html.
191. Helfand BKI, Webb M, Gartaganis SL, Fuller L, Kwon C-S, Inouye SK. The Exclusion of Older Persons From Vaccine and Treatment Trials for Coronavirus Disease 2019—Missing the Target. JAMA Internal Medicine. 2020;180(11):1546-9.

192. Collier DA, Ferreira I, Kotagiri P, Datir RP, Lim EY, Touizer E, et al. Age-related immune response heterogeneity to SARS-CoV-2 vaccine BNT162b2. Nature. 2021;596(7872):417-22.
193. Tober-Lau P, Schwarz T, Vanshylla K, Hillus D, Gruell H, Group ECS, et al. Long-term immunogenicity of BNT162b2 vaccination in older people and younger health-care workers. Lancet Respir Med. 2021;9(11):e104-e5.
194. Garcon N, Vaughn DW, Didierlaurent AM. Development and evaluation of AS03, an Adjuvant System containing alpha-tocopherol and squalene in an oil-in-water emulsion. Expert Rev Vaccines. 2012;11(3):349-66.
195. Madhun AS, Akselsen PE, Sjursen H, Pedersen G, Svindland S, Nostbakken JK, et al. An adjuvanted pandemic influenza H1N1 vaccine provides early and long term protection in health care workers. Vaccine. 2010;29(2):266-73.
196. Kuwelker K, Zhou F, Blomberg B, Lartey S, Brokstad KA, Trieu MC, et al. Attack rates amongst household members of outpatients with confirmed COVID-19 in Bergen, Norway: A case-ascertained study. Lancet Reg Health Eur. 2021;3:100014.
197. Wrammert J, Koutsonanos D, Li GM, Edupuganti S, Sui J, Morrissey M, et al. Broadly cross-reactive antibodies dominate the human B cell response against 2009 pandemic H1N1 influenza virus infection. J Exp Med. 2011;208(1):181-93.
198. Smith K, Garman L, Wrammert J, Zheng NY, Capra JD, Ahmed R, et al. Rapid generation of fully human monoclonal antibodies specific to a vaccinating antigen. Nat Protoc. 2009;4(3):372-84.
199. Ho IY, Bunker JJ, Erickson SA, Neu KE, Huang M, Cortese M, et al. Refined protocol for generating monoclonal antibodies from single human and murine B cells. J Immunol Methods. 2016;438:67-70.
200. Couzens L, Gao J, Westgeest K, Sandbulte M, Lugovtsev V, Fouchier R, et al. An optimized enzyme-linked lectin assay to measure influenza A virus neuraminidase inhibition antibody titers in human sera. J Virol Methods. 2014;210:7-14.
201. Matrosovich M, Matrosovich T, Garten W, Klenk HD. New low-viscosity overlay medium for viral plaque assays. Virol J. 2006;3:63.
202. Matrosovich M, Matrosovich T, Carr J, Roberts NA, Klenk HD. Overexpression of the alpha-2,6-sialyltransferase in MDCK cells increases influenza virus sensitivity to neuraminidase inhibitors. J Virol. 2003;77(15):8418-25.
203. Stadlbauer D, Amanat F, Strohmeier S, Nachbagauer R, Krammer F. Cross-reactive mouse monoclonal antibodies raised against the hemagglutinin of A/Shanghai/1/2013 (H7N9) protect against novel H7 virus isolates in the mouse model. Emerg Microbes Infect. 2018;7(1):110.
204. Trieu M-C, Bansal A, Madsen A, Zhou F, Sævik M, Vahokoski J, et al. SARS-CoV-2–Specific Neutralizing Antibody Responses in Norwegian Health Care Workers After the First Wave of COVID-19 Pandemic: A Prospective Cohort Study. The Journal of Infectious Diseases. 2020;223(4):589-99.
205. Snyder TM, Gittelman RM, Klinger M, May DH, Osborne EJ, Taniguchi R, et al. Magnitude and Dynamics of the T-Cell Response to SARS-CoV-2 Infection at Both Individual and Population Levels. medRxiv. 2020.
206. Organization WH. WHO preferred product characteristics for next generation influenza vaccines 2017 [Available from: https://apps.who.int/iris/bitstream/handle/10665/258767/9789241512466-eng.pdf.

207. Foundation BaMG. Ending the Pandemic Threat: A Grand Challenge for Universal Influenza Vaccine Development 2018 [Available from: https://gcgh.grandchallenges.org/challenge/ending-pandemic-threat-grand-challenge-universal-influenza-vaccine-development.
208. Erbelding EJ, Post DJ, Stemmy EJ, Roberts PC, Augustine AD, Ferguson S, et al. A Universal Influenza Vaccine: The Strategic Plan for the National Institute of Allergy and Infectious Diseases. J Infect Dis. 2018;218(3):347-54.
209. Jang YH, Seong BL. The Quest for a Truly Universal Influenza Vaccine. Front Cell Infect Microbiol. 2019;9:344.
210. Sun H, Xiao Y, Liu J, Wang D, Li F, Wang C, et al. Prevalent Eurasian avian-like H1N1 swine influenza virus with 2009 pandemic viral genes facilitating human infection. Proc Natl Acad Sci U S A. 2020;117(29):17204-10.
211. Peiris JS, de Jong MD, Guan Y. Avian influenza virus (H5N1): a threat to human health. Clin Microbiol Rev. 2007;20(2):243-67.
212. Ellis D, Lederhofer J, Acton OJ, Tsybovsky Y, Kephart S, Yap C, et al. Structure-based design of stabilized recombinant influenza neuraminidase tetramers. Nat Commun. 2022;13(1):1825.
213. Wan H, Yang H, Shore DA, Garten RJ, Couzens L, Gao J, et al. Structural characterization of a protective epitope spanning A(H1N1)pdm09 influenza virus neuraminidase monomers. Nat Commun. 2015;6:6114.
214. Hsieh CL, Goldsmith JA, Schaub JM, DiVenere AM, Kuo HC, Javanmardi K, et al. Structure-based design of prefusion-stabilized SARS-CoV-2 spikes. Science. 2020;369(6510):1501-5.
215. McLellan JS, Chen M, Joyce MG, Sastry M, Stewart-Jones GB, Yang Y, et al. Structure-based design of a fusion glycoprotein vaccine for respiratory syncytial virus. Science. 2013;342(6158):592-8.
216. Polack FP, Thomas SJ, Kitchin N, Absalon J, Gurtman A, Lockhart S, et al. Safety and Efficacy of the BNT162b2 mRNA Covid-19 Vaccine. N Engl J Med. 2020;383(27):2603-15.
217. Laguio-Vila MR, Thompson MG, Reynolds S, Spencer SM, Gaglani M, Naleway A, et al. Comparison of serum hemagglutinin and neuraminidase inhibition antibodies after 2010-2011 trivalent inactivated influenza vaccination in healthcare personnel. Open Forum Infect Dis. 2015;2(1):ofu115.
218. Khurana S, Coyle EM, Manischewitz J, King LR, Gao J, Germain RN, et al. AS03-adjuvanted H5N1 vaccine promotes antibody diversity and affinity maturation, NAI titers, cross-clade H5N1 neutralization, but not H1N1 cross-subtype neutralization. NPJ Vaccines. 2018;3:40.
219. Ito H, Nishimura H, Kisu T, Hagiwara H, Watanabe O, Kadji FMN, et al. Low response in eliciting neuraminidase inhibition activity of sera among recipients of a split, monovalent pandemic influenza vaccine during the 2009 pandemic. PLoS One. 2020;15(5):e0233001.
220. Sarkanen T, Alakuijala A, Julkunen I, Partinen M. Narcolepsy Associated with Pandemrix Vaccine. Curr Neurol Neurosci Rep. 2018;18(7):43.
221. Ahmed SS, Volkmuth W, Duca J, Corti L, Pallaoro M, Pezzicoli A, et al. Antibodies to influenza nucleoprotein cross-react with human hypocretin receptor 2. Sci Transl Med. 2015;7(294):294ra105.

222. Sarkanen TO, Alakuijala APE, Dauvilliers YA, Partinen MM. Incidence of narcolepsy after H1N1 influenza and vaccinations: Systematic review and meta-analysis. Sleep Med Rev. 2018;38:177-86.
223. Tsai TF. MF59 adjuvanted seasonal and pandemic influenza vaccines. Yakugaku Zasshi. 2011;131(12):1733-41.
224. Skowronski DM, Chambers C, De Serres G, Sabaiduc S, Winter AL, Dickinson JA, et al. Serial Vaccination and the Antigenic Distance Hypothesis: Effects on Influenza Vaccine Effectiveness During A(H3N2) Epidemics in Canada, 2010-2011 to 2014-2015. J Infect Dis. 2017;215(7):1059-99.
225. Ellebedy AH, Nachbagauer R, Jackson KJL, Dai YN, Han J, Alsoussi WB, et al. Adjuvanted H5N1 influenza vaccine enhances both cross-reactive memory B cell and strain-specific naive B cell responses in humans. Proc Natl Acad Sci U S A. 2020;117(30):17957-64.
226. Andrews N, Stowe J, Kirsebom F, Toffa S, Rickeard T, Gallagher E, et al. Covid-19 Vaccine Effectiveness against the Omicron (B.1.1.529) Variant. New England Journal of Medicine. 2022;386(16):1532-46.
227. Dagan N, Barda N, Kepten E, Miron O, Perchik S, Katz MA, et al. BNT162b2 mRNA Covid-19 Vaccine in a Nationwide Mass Vaccination Setting. New England Journal of Medicine. 2021;384(15):1412-23.
228. Ferdinands JM, Rao S, Dixon BE, Mitchell PK, DeSilva MB, Irving SA, et al. Waning 2-Dose and 3-Dose Effectiveness of mRNA Vaccines Against COVID-19-Associated Emergency Department and Urgent Care Encounters and Hospitalizations Among Adults During Periods of Delta and Omicron Variant Predominance - VISION Network, 10 States, August 2021-January 2022. MMWR Morb Mortal Wkly Rep. 2022;71(7):255-63.
229. Gruell H, Vanshylla K, Tober-Lau P, Hillus D, Schommers P, Lehmann C, et al. mRNA booster immunization elicits potent neutralizing serum activity against the SARS-CoV-2 Omicron variant. Nat Med. 2022;28(3):477-80.
230. Bar-On YM, Goldberg Y, Mandel M, Bodenheimer O, Amir O, Freedman L, et al. Protection by a Fourth Dose of BNT162b2 against Omicron in Israel. N Engl J Med. 2022;386(18):1712-20.
231. Thompson MG, Cowling BJ. How repeated influenza vaccination effects might apply to COVID-19 vaccines. Lancet Respir Med. 2022.
232. Quast T, Andel R, Gregory S, Storch EA. Years of life lost associated with COVID-19 deaths in the USA during the first year of the pandemic. J Public Health (Oxf). 2022;44(1):e20-e5.
233. Huang C, Wang Y, Li X, Ren L, Zhao J, Hu Y, et al. Clinical features of patients infected with 2019 novel coronavirus in Wuhan, China. Lancet. 2020;395(10223):497-506.
234. Corbett KS, Edwards D, Leist SR, Abiona OM, Boyoglu-Barnum S, Gillespie RA, et al. SARS-CoV-2 mRNA Vaccine Development Enabled by Prototype Pathogen Preparedness. bioRxiv. 2020.
235. Jackson LA, Anderson EJ, Rouphael NG, Roberts PC, Makhene M, Coler RN, et al. An mRNA Vaccine against SARS-CoV-2 - Preliminary Report. N Engl J Med. 2020;383(20):1920-31.

236. Naaber P, Tserel L, Kangro K, Sepp E, Jurjenson V, Adamson A, et al. Dynamics of antibody response to BNT162b2 vaccine after six months: a longitudinal prospective study. Lancet Reg Health Eur. 2021;10:100208.
237. Addministration FaD. Development and Licensure of Vaccines to Prevent COVID-19; Guidance for Industry 2020 [Available from: https://www.fda.gov/media/139638/download.
238. Organization WH. WHO Target Product Profiles for COVID-19 Vaccines. Revised version April 2022 2022 [Available from: https://www.who.int/publications/m/item/who-target-product-profiles-for-covid-19-vaccines.
239. Thomas SJ, Moreira ED, Jr., Kitchin N, Absalon J, Gurtman A, Lockhart S, et al. Safety and Efficacy of the BNT162b2 mRNA Covid-19 Vaccine through 6 Months. N Engl J Med. 2021;385(19):1761-73.
240. Freyn AW, Ramos da Silva J, Rosado VC, Bliss CM, Pine M, Mui BL, et al. A Multi-Targeting, Nucleoside-Modified mRNA Influenza Virus Vaccine Provides Broad Protection in Mice. Mol Ther. 2020;28(7):1569-84.
241. Pardi N, Parkhouse K, Kirkpatrick E, McMahon M, Zost SJ, Mui BL, et al. Nucleoside-modified mRNA immunization elicits influenza virus hemagglutinin stalk-specific antibodies. Nat Commun. 2018;9(1):3361.
242. Feldman RA, Fuhr R, Smolenov I, Mick Ribeiro A, Panther L, Watson M, et al. mRNA vaccines against H10N8 and H7N9 influenza viruses of pandemic potential are immunogenic and well tolerated in healthy adults in phase 1 randomized clinical trials. Vaccine. 2019;37(25):3326-34.
243. Sanofi. Sanofi and Translate Bio initiate Phase 1 clincal trial of mRNA influenza vaccine 2021 [Available from: https://ml-eu.globenewswire.com/Resource/Download/0238ed99-8f1e-47d5-84c1-be68393029b3.
244. moderna. MODERNA ANNOUNCES FIRST PARTICIPANTS DOSED IN PHASE 1/2 STUDY WITH MRNA-1020 AND MRNA-1030 SEASONAL INFLUENZA VACCINE CANDIDATES 2022 [Available from: https://investors.modernatx.com/news/news-details/2022/Moderna-Announces-First-Participants-Dosed-in-Phase-12-Study-with-mRNA-1020-and-mRNA-1030-Seasonal-Influenza-Vaccine-Candidates/default.aspx.
245. Pfizer. A Study to Evaluate the Safety, Tolerability, and Immunogenicity of a Modified RNA Vaccine Against Influenza: clinicaltrial.gov; [Available from: https://www.clinicaltrials.gov/ct2/show/NCT05052697?cond=NCT05052697&draw=2&rank=1.

Papers I-III

I

Papers I-III

II

frontiers in Immunology

ORIGINAL RESEARCH
published: 14 October 2021
doi: 10.3389/fimmu.2021.748264

Repeated Influenza Vaccination Boosts and Maintains H1N1pdm09 Neuraminidase Antibody Titers

Lena Hansen[1]*, *Fan Zhou*[1], *Håkon Amdam*[1], *Mai-Chi Trieu*[1] and *Rebecca Jane Cox*[1,2]*

[1] Influenza Centre, Department of Clinical Science, University of Bergen, Bergen, Norway, [2] Department of Microbiology, Haukeland University Hospital, Bergen, Norway

Antibodies to influenza surface protein neuraminidase (NA) have been found to reduce disease severity and may be an independent correlate of protection. Despite this, current influenza vaccines have no regulatory requirements for the quality or quantity of the NA antigen and are not optimized for induction of NA-specific antibodies. Here we investigate the induction and durability of NA-specific antibody titers after pandemic AS03-adjuvanted monovalent H1N1 vaccination and subsequent annual vaccination in health care workers in a five-year longitudinal study. NA-specific antibodies were measured by endpoint ELISA and functional antibodies measured by enzyme-linked lectin assay (ELLA) and plaque reduction naturalisation assay. We found robust induction of NA inhibition (NAI) titers with a 53% seroconversion rate (>4-fold) after pandemic vaccination in 2009. Furthermore, the endpoint and NAI geometric mean titers persisted above pre-vaccination levels up to five years after vaccination in HCWs that only received the pandemic vaccine, which demonstrates considerable durability. Vaccination with non-adjuvanted trivalent influenza vaccines (TIV) in subsequent influenza seasons 2010/2011 – 2013/2014 further boosted NA-specific antibody responses. We found that each subsequent vaccination increased durable endpoint titers and contributed to maintaining the durability of functional antibody titers. Although the trivalent influenza vaccines boosted NA-specific antibodies, the magnitude of fold-increase at day 21 declined with repeated vaccination, particularly for functional antibody titers. High levels of pre-existing antibodies were associated with lower fold-induction in repeatedly vaccinated HCWs. In summary, our results show that durable NA-specific antibody responses can be induced by an adjuvanted influenza vaccine, which can be maintained and further boosted by TIVs. Although NA-specific antibody responses are boosted by annual influenza vaccines, high pre-existing titers may negatively affect the magnitude of fold-increase in repeatedly vaccinated individuals. Our results support continued development and standardization of the NA antigen to supplement current influenza vaccines and reduce the burden of morbidity and mortality.

Keywords: influenza, neuraminidase, neuraminidase inhibition, neuraminidase inhibition (NAI) titer, repeated vaccination, pre-existing immunity, pandemic vaccination

OPEN ACCESS

Edited by:
Cornelis Joseph Melief, Leiden University, Netherlands

Reviewed by:
Carolyn M. Nielsen, University of Oxford, United Kingdom
Osaretin Emmanuel Asowata, Population Council, United States

***Correspondence:**
Rebecca Jane Cox
Rebecca.Cox@uib.no
Lena Hansen
Lena.Hansen@uib.no

Specialty section:
This article was submitted to Vaccines and Molecular Therapeutics, a section of the journal Frontiers in Immunology

Received: *27 July 2021*
Accepted: *28 September 2021*
Published: *14 October 2021*

Citation:
Hansen L, Zhou F, Amdam H, Trieu M-C and Cox RJ (2021) Repeated Influenza Vaccination Boosts and Maintains H1N1pdm09 Neuraminidase Antibody Titers. Front. Immunol. 12:748264. doi: 10.3389/fimmu.2021.748264

INTRODUCTION

Influenza is an acute respiratory disease that is annually estimated to cause 3 – 5 million cases of severe illness and 290 000 – 650 000 deaths worldwide (1, 2). Influenza vaccines are currently the most effective method of prevention of influenza infection. Hemagglutinin (HA) is the major surface glycoprotein on the virus that mediates viral entry by binding to sialic acid receptors on the surface of host cells. Antibodies that target the HA globular head and block binding to sialic acids are considered the classical mediators of protection against influenza infection. These antibodies are measured by hemagglutination inhibition (HI) assay and the HI titer has been the gold standard for measuring vaccine immunogenicity for many years. Thus, current seasonal influenza vaccines are optimized for induction of HA-specific antibodies. Each vaccine dose is standardized by the HA content, however, there are no concentration requirements for the other vaccine components, such as neuraminidase. Neuraminidase (NA) is the second major surface glycoprotein. It is a sialidase that cleaves terminal sialic acids and facilitates the release and spread of newly formed viruses from host cells (3). HI antibodies tend to be strain-specific and have reduced cross-reactivity with new and drifted influenza strains due to the high mutation rate of the HA head region. Antigenic drift and shift may occur independently for HA and NA proteins and NA is a potential target for more broadly protective vaccines. Early studies established that NA is immunogenic and that NA-specific antibodies reduce disease in humans (4, 5). More recent studies have found that antibodies with NA inhibition (NAI) activity correlate with reduced viral shedding and clinical disease, and may be a possible correlate of protection (6, 7). Despite NA being an antigenic target for induction of protective antibody responses, the quantity and quality of NA is not regulated in current influenza vaccines. Consequently, the amount and stability of the NA antigen has been found to vary between influenza vaccines and key epitopes targeted by human monoclonal antibodies are poorly displayed (8, 9). Studies have reported variable seroconversion rates for NA-specific antibody responses after vaccination with inactivated influenza vaccines, ranging between 23 – 64% (7, 10, 11).

Annual vaccination is recommended due to antigenic drift of influenza viruses and waning of antibody titers. However, there is growing evidence showing that repeated influenza vaccination can lead to a diminished B cell response (12) and that high pre-existing antibody titers can reduce boosting of antibody titers after vaccination (13). The impact of repeated vaccination has mainly been studied in the context of HA-specific antibody responses (12, 13). Thus, there is limited data on whether repeated vaccination and pre-existing titers impact the induction of NA-specific antibody responses after vaccination.

This study aimed to investigate the induction and durability of NA-specific antibodies with AS03-adjuvanted pandemic H1N1pdm09 vaccination and determine the impact of subsequent annual vaccination with trivalent inactivated vaccines (TIV) in health care workers (HCWs). We found that AS03-adjuvanted monovalent H1N1pdm09 vaccination induced robust and durable NA-specific antibody responses. The antibody titers were further boosted after immunization with TIVs, however, we found that the magnitude of the functional NA antibody fold-increase declined with repeated vaccination.

MATERIALS AND METHODS

Study Design and Blood Sampling

Healthy HCWs (n=50) were vaccinated between October 2009 and March 2010 at Haukeland University Hospital, Norway with the AS03-adjuvanted pandemic H1N1pdm09 split virus vaccine (3.75 µg hemagglutinin A/California/7/2009 (H1N1) (Pandemrix, GlaxoSmithKline-GSK, Belgium). Written informed consent was obtained before inclusion in the study. Further informed consent was obtained for the 4-year extension between 2010/2011–2013/2014 where vaccination was with the trivalent seasonal inactivated influenza vaccine [TIV; either subunit (Influvac, Abbott Laboratories) or split-virion (Vaxigrip, Sanofi Pasteur)] containing 15 µg hemagglutinin per strain. Throughout the study, the A/H1N1 strain remained the same [A/California/07/2009 (H1N1)], however the A/H3N2 and B viruses changed between seasons. Demographic and clinical information including working department were collected. The study was approved by the regional ethics committee (REKVest-2012/1772) and the Norwegian Medicines Agency (Clinical trials.gov NCT01003288) (14).

Blood samples were collected pre-vaccination (D0), 21 days (D21), 3, 6, and 12 months (3M, 6M, 12M, respectively) after vaccination. Annual influenza vaccination is recommended, but not mandatory for HCWs in Norway. The HCWs were divided into two groups, repeated and single group, based on their vaccination status in influenza seasons 2010/2011 – 2013/2014. The single group did not receive any TIVs during the study. The repeated group was vaccinated with two or three TIVs in the four seasons following the 2009 pandemic. An overview of the number of vaccinations and the intervals that these were given for the repeated group can be found in **Supplemental Table 2**. The same sampling schedule was followed after all vaccinations. The 12M timepoint was collected from all HCW irrespective of vaccination and used as D0 for HCWs in the repeated group for each season. Blood samples collected before vaccination were considered as day 0 whenever HCWs had not been vaccinated during the previous season, which more accurately reflected the true baseline titers. HCWs in the single group (n=24) were only vaccinated in 2009 but provided yearly blood samples at the start of each influenza season, i.e. 24, 36, 48 and 60 months after H1N1pdm09 vaccination. The samples collected from the single group after the 2009 season were labelled as 12M for each subsequent season as seen in **Figure 2**. All serum samples were heat inactivated at 56°C for one hour before use in serological assays.

ELISA

Flat bottom 96-well plates (Invitrogen) were coated with recombinant N1 NA A/California/07/2009 (H1N1) (Cal09) produced in a baculovirus expression system as previously

described (15). N1 NA Cal09 (100 µl/well) diluted in PBS (1 µg/ml) was added and incubated overnight at 4°C. The plates were washed six times with PBS-T (PBS with 0.05% Tween 20) and blocked with 200 µl of blocking solution [PBS with 0.1% Tween-20 (Sigma), 1% BSA (Sigma), 5% milk (Marvel)] and incubated for 1 hour at 37°C. Sera were 4-fold serially diluted from 1:100 in blocking solution and 100 µl of diluted serum was added per well in duplicates and incubated at 37°C for 1 hour. Following incubation, the plates were washed six times with PBS-T and 100 µl horseradish peroxidase (HRP)-conjugated mouse anti-human IgG (BD Biosciences) diluted in blocking buffer (1:4000) was added per well and incubated at 37°C for 1 hour. The plates were washed six times with PBS-T and the secondary antibody signal was developed by adding 100 µl per well of 3,3′,5,5′-Tetramethylbenzidine (TMB) substrate (BD Biosciences). The reaction was stopped after 10 min by adding 100 µl of 1M HCl (Sigma). Absorbance was measured at 450 and 620 nm with a microplate reader (Bio-Tek). Background measured at 620 nm was subtracted from the absorbance measured at 450 nm. The endpoint titer was determined using a sigmoidal dose response curve in GraphPad Prism 9.

ELLA

Inhibition of NA enzyme activity was determined using enzyme-linked lectin assay (ELLA) using an influenza reassortant H7N1 virus (NIBSC, UK) with an irrelevant HA from A/Equine/Prague/56 (H7N7) and NA from A/California/07/09 (H1N1), matching the vaccine strain. ELLA was performed according to Couzens et al. (16). Briefly, 96-well plates were coated with 100 µl/well of fetuin (25 µg/ml) (Sigma) diluted in PBS and incubated at 4°C for a minimum of 18 hours. The plates were washed three times with PBS-T. Sera were 5-fold serially diluted from 1:50 in sample diluent (PBS with 0.9 mM $CaCl_2$ and 0.5 mM $MgCl_2$ (Life Technologies), 1% BSA (Sigma), 0.5% Tween-20) and 50 µl was added per well in duplicates. The virus was diluted in sample buffer at a concentration equivalent to 90% of the maximum signal and 50 µl was added per well. The plates were incubated at 37°C for 18 hours. After incubation, the plates were washed six times with PBS-T and 100 µl of HRP-conjugated peanut agglutinin (1 mg/ml) (Sigma) diluted in conjugate diluent (PBS with 0.9 mM $CaCl_2$ and 0.5 mM $MgCl_2$, 1% BSA) was added to per well and incubated in the dark at room temperature for 2 hours. The plates were washed three times with PBS-T. 100 µl of o-Phenylenediamine dihydrochloride (OPD) substrate (Sigma) in phosphate-citrate buffer (50 mM) (Sigma) was added to each well and incubated in the dark for 10 min. The reaction was stopped by adding 100 µl 1N sulfuric acid (Sigma). The absorbance was measured at 490 nm. 50% inhibitory concentration was calculated for each serum sample using a sigmoidal dose response curve in GraphPad Prism 9 and considered as the neuraminidase inhibition (NAI) titer.

Plaque Reduction Neutralization Assay

A 96-well microplate plaque reduction neutralization assay was used to measure the capacity of sera to inhibit viral replication *in vitro*. The reassortant H7N1 virus used in ELLA was used for this assay. The plaque reduction neutralization assay was performed according to Matrosovich et al. (17, 18). MDCK SIAT1 cells were seeded ($2x10^4$ per well) and incubated overnight at 37°C. The virus was diluted to a concentration that would generate 100 plaques per well. Sera were diluted 1:20 and 1:100 and mixed with the virus, and incubated at 37°C for one hour. This inoculum was added in quadruplets and incubated at 37°C for 40 min. A low-viscosity Avicel overlay (FMC BioPolymer) was added to each well and the plates were incubated with the inoculum-overlay mixture for 24 hours. The plaques were visualized by immunostaining of nucleoprotein and the plaques were counted using ELISpot counter (AID). The number of plaques in the control wells was used to determine 50% inhibition and the highest reciprocal dilution giving 50% reduction in plaque formation was defined as plaque reduction neutralizing titer ($PRNT_{50}$ titer). The NA inhibitor oseltamivir (Roche) was used as a positive control to confirm that the assay could detect reduction in plaque forming units (PFU) as a result of NA inhibition in a dose-dependent manner (**Supplementary Figure 1**). Human serum depleted for IgA, IgM, and IgG (Sigma) was used as negative control.

Statistical Analysis

Endpoint, NAI and $PRNT_{50}$ titers were log-transformed and analyzed by linear mixed effects model with adjustments for demographic factors and multiple comparisons by Sidak correction. Demographic factors used for adjustments included age, sex, influenza vaccination prior to 2009 and working department (**Table 1**). The linear-mixed effects model analyses were performed in IBM SPSS Statistics version 26 and was the statistical test used unless otherwise stated. Analyzes of statistical difference between the single and repeated group was done by non-parametric Kruskal-Wallis test in GraphPad Prism 9. Correlation coefficients were calculated by non-parametric

TABLE 1 | Demographics of the study participants.

Demographics	All HCWs	Single group	Repeated group
Number of participants	50	24	26
Male (%)	9 (18)	4 (17)	5 (19)
Female (%)	41 (82)	20 (83)	21 (81)
Median age (range)	39 (22 – 63)	38 (26 – 59)	43 (22 – 63)
Seasonal vaccination before 2009 (%)	32 (65.3)	11 (47.8)	21 (80.8)
Working department(non-clinical, clinical, infectious)	23, 21, 6	13, 9, 2	10, 12, 4

HCW healthcare workers (HCWs). The single group had only pandemic vaccination in 2009. The repeated group were vaccinated with pandemic vaccine in 2009 and trivalent influenza vaccine in two or three seasons after 2009.

Spearman correlation in GraphPad Prism 9. Statistical significance was defined as P<0.05 for all tests.

RESULTS

In this study we investigated NA-specific antibody responses after pandemic vaccination and subsequent annual influenza vaccination. Fifty HCWs were included in the study, which consisted of 9 men and 41 women. These numbers reflect the gender distribution in the Norwegian healthcare system. The median age at the start of the study was 38 years old (range 22 – 63). The majority of the HCWs (65%) had been vaccinated with TIVs before 2009 (**Table 1**).

Robust and Durable NA-Specific Antibody Responses After 2009 Pandemic Vaccination

One objective of this study was to investigate the induction of NA-specific antibody responses after AS03-adjuvanted monovalent pandemic vaccine (H1N1pdm09) in healthy adults. All HCWs in the study were vaccinated with the H1N1pdm09 vaccine in 2009 and blood samples were collected before and 21 days, 3, 6 and 12 months after vaccination. Endpoint titers were determined by ELISA against recombinant N1 NA Cal09 (**Figure 1A**). NA-specific endpoint titers were detected in all HCWs pre-vaccination with a geometric mean titer (GMT) of 322. The endpoint titers were significantly boosted to a GMT of 773, a geometric fold rise (GMFR) of 2.4, at 21 days post-vaccination (P<0.0001). The endpoint titers gradually waned during the following 12 months, although titers were significantly higher than pre-vaccination levels up to the 3-month time point (P=0.004).

The capacity of the antibody response to inhibit NA enzyme activity was measured by ELLA. A reassortant H7N1 virus, with an irrelevant H7 HA from A/Equine/Prague/02/56 and N1 NA from Cal09, was used to avoid interference from HA-specific antibodies. The H1N1pdm09 vaccine met the European Committee for Medicinal Products for Human Use (CHMP) criteria for immunogenicity set for HI titers (**Supplementary Table 1**). These criteria were used to assess induction of NAI titers. Pre-vaccination NAI titers were detected in all HCWs, albeit with a modest NAI GMT of 19. H1N1pdm09 vaccination significantly increased NAI GMT at 21 days post-vaccination to 84 (P<0.0001), a 4.4-fold increase from pre-vaccination levels (**Figure 1B**). The seroconversion rate for NAI titers was 53% (32/49). Similarly to endpoint titers, the NAI titers gradually waned but remained significantly higher than the pre-vaccination level up to 12 months after vaccination (P=0.014).

Approximately half of the HCWs (26/50) chose to receive two or three TIVs during the four-year follow-up study after the 2009 pandemic (repeated group). The remaining 24 HCWs chose not to be further vaccinated (single group) (**Figure 2A**). The repeated group had higher endpoint and NAI titers than the single group, especially during the influenza season (defined as November – April) (**Figures 2B, C**). Annual blood samples were collected prior to the start of each season from the single group, which allowed us to investigate the durability of antibody responses induced by the H1N1pdm09 vaccine. We found that three HCWs in the single group seroconverted during the study (HI titer >4-fold increase), probably due to infection. Samples collected after seroconversion were excluded to ensure that the durability was only measured from pandemic vaccination. Endpoint and NAI titers were maintained at low stable levels above baseline in the single group throughout the study (**Figures 2B, C**). The GMFR was 1.38- and 1.33-fold above pre-vaccination levels for endpoint and NAI titers, respectively, five years after H1N1pdm09 vaccination. This demonstrated that a single dose of AS03-adjuvanted H1N1pdm09 vaccine induced durable antibody responses that persisted for several years after vaccination, suggesting that long-lived plasma cells were generated.

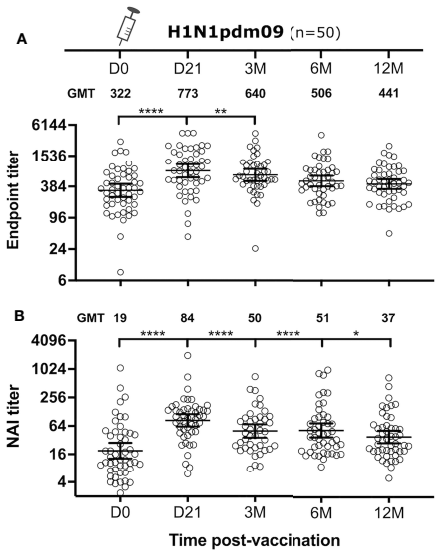

FIGURE 1 | NA-specific antibody responses after H1N1pdm09 vaccination. Health care workers (n = 50) were vaccinated with AS03-adjuvanted H1N1pdm09 vaccine. The NA-specific antibody response was measured before and 21 days, 3, 6 and 12 months after vaccination (D0, D21, 3M, 6M, 12M, respectively). Endpoint titers were measured by ELISA **(A)** and NA inhibition (NAI) titers were measured by ELLA **(B)**. Each subject is shown as one symbol with geometric mean and 95% confidence intervals. A linear mixed effects model was used for statistical analyses between pre- and post-vaccination titers with adjustments for demographic factors. *P ≤ 0.05, **P ≤ 0.01, ***P ≤ 0.0001.

Trivalent Influenza Vaccines Boost NA-Specific Antibody Responses

HCWs in the repeated group received two or three TIVs during the study, resulting in variation in vaccination intervals. The majority of the HCWs received three TIVs (81%), whereas the remaining HCWs received two TIVs (19%) (**Supplementary Table 2**). We observed that HCWs that had delayed their first TIV until the 2011/2012 season (6/26) had higher NAI titer than the HCWs

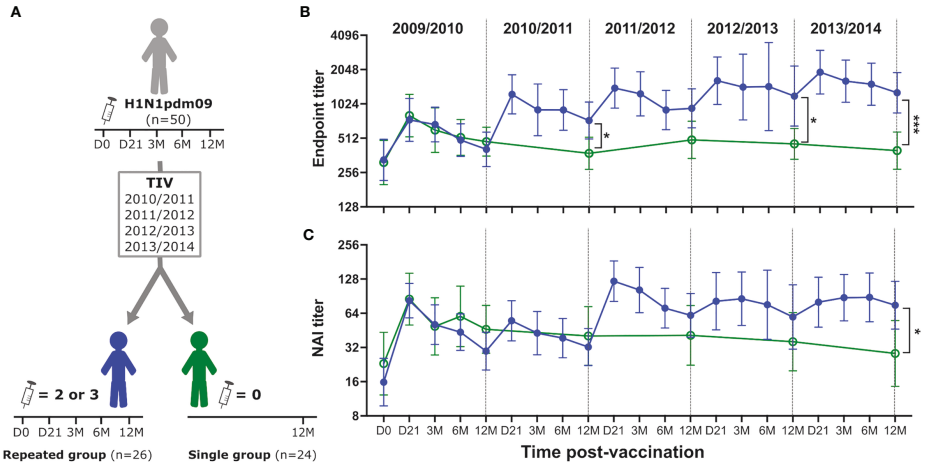

FIGURE 2 | H1N1pdm09 vaccination induced durable NA-specific antibody responses boosted by trivalent influenza vaccines. Study design **(A)**. Health care workers were divided into two groups based on their vaccination status after H1N1pdm09 vaccination in 2009. The repeated group (blue, filled circles) received two or three trivalent influenza vaccines (TIV) during seasons 2010/2011-2013/2014. Blood samples were collected 21 days (D21), and 3, 6, 12 months (3M, 6M, 12M, respectively) after vaccination. The single group (green, open circles) chose not to be further vaccinated but provided yearly blood samples prior to the start of each season (12M). NA-specific antibody responses were measured by ELISA **(B)** and ELLA **(C)** during each influenza season from 2009/2010 to 2013/2014. Data are shown as geometric mean with 95% confidence intervals. Analyzes of statistical difference between the single and repeated group was done by non-parametric Kruskal-Wallis test in GraphPad Prism 9. *P ≤ 0.05, ***P ≤ 0.001.

that received their second TIV that season. Therefore, HCWs in the repeated group were grouped based on number of vaccines, rather than season, in order to study the effect of each vaccine and the impact of repeated vaccination. The quantity of NA-specific antibodies were measured by ELISA and functional antibodies were measured by ELLA and a plaque reduction neutralisation assay in all HCWs in the repeated group. The three assays demonstrated that NA-specific antibody responses were boosted after TIV vaccination (**Figure 3**). These antibody titers gradually decreased but persisted above baseline levels throughout the influenza season. We found that endpoint titers were significantly boosted after the first (P=0.001) and second TIV (P=0.04) (**Figure 3A**), whereas the NAI titers were only significantly boosted on day 21 after the first TIV (P=0.018) (**Figure 3B**). Although the third TIV boosted endpoint and NAI titers, neither were significant. Plaque reduction neutralisation assay was used to further assess the functionality of the NA-specific antibody response *in vitro* using the same reassortant H7N1 virus with N1 NA Cal09. This assay measures inhibition of the viral replication cycle and NA-specific inhibition of plaque formation was confirmed using oseltamivir (**Supplementary Figure 1**). We found a significant increase in antibody titer that resulted in 50% reduction in plaque formation ($PRNT_{50}$ titer) 21 days after H1N1pdm09 (P<0.0001) (**Figure 3C**). Vaccination with TIVs boosted $PRNT_{50}$ titers, although not significant for any of the three TIVs. The $PRNT_{50}$ titers confirmed our findings in the ELLA and demonstrated that the vaccine-induced NA-specific antibodies were capable of inhibiting enzyme activity and viral replication *in vitro*. Collectively, our results show that seasonal TIV vaccination readily boosts NA-specific antibody responses following priming with AS03-adjuvanted H1N1pdm09 vaccination.

Repeated Vaccination Increases Durable Endpoint Titers and Maintains Durability of Functional Antibody Titers

Durable antibody titers were measured 12 months after vaccination. The H1N1 component remained the same in all vaccines used during this study, which allowed us to investigate the impact of repeated vaccination with the same antigen. We compared endpoint and NAI titres in the repeated and single group at the end of the 5-year study to assess the impact of TIVs on the durability of antibody titers. Only HCWs in the repeated group that had been vaccinated with TIV in the final season of the study were used for comparison using samples collected 12 months post-vaccination. 14/18 HCWs in the repeated group had received three TIVs and 4/18 had received two TIVs in that season (**Supplementary Table 2**). We found that the repeated group had 3.2-fold higher endpoint titers (P=0.0002) (**Figure 2A**) and 2.7-fold higher NAI titers (P=0.01) (**Figure 2B**) compared to the single group 5 years after H1N1pdm09 vaccination. This demonstrated that repeated vaccination with TIVs after AS03-adjuvanted H1N1pdm09 vaccination contributed to maintenance and further increase of the durable NA-specific antibody responses.

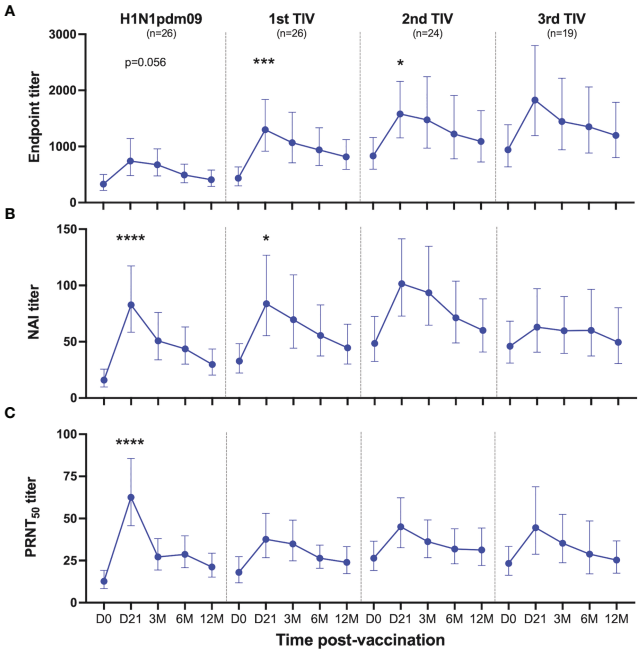

FIGURE 3 | Antibody responses to NA induced by H1N1pdm09 and TIV vaccination. Health care workers in the repeated group received two or three trivalent influenza vaccines (TIV) in the four subsequent seasons after the 2009 pandemic during the five-year study. Blood samples were collected pre-season (D0) and 21 days, 3, 6 and 12 months (D21, 3M, 6M, 12M, respectively) after each vaccination. Antibody responses were measured by ELISA **(A)**, ELLA **(B)** and plaque reduction neutralization assay **(C)** after vaccination with H1N1pdm09 and the first, second or third TIV. All vaccinated HCWs in the repeated group is included in this figure regardless of their vaccination intervals. Data are shown as geometric mean with 95% confidence intervals. A linear mixed effects model with adjustments for demographic factors was used to determine statistical difference between antibody titers measured on day 0 and day 21 for each vaccination. *P ≤ 0.05, ***P ≤ 0.001, ****P ≤ 0.0001.

Immunization with three TIVs gradually increased the magnitude of durable endpoint titers and collectively increased the GMT by 3-fold from titers measured 12 months after the H1N1pdm09 vaccination (**Figure 4B**). Durable antibody levels measured 12 months after the first (P=0.008), second (P=0.001) and third TIV (P<0.0001) were all significantly higher than the level measured after H1N1pdm09 vaccination (**Figure 4B**). This demonstrates that all TIVs contributed to further increase and maintenance of durable endpoint titers. The first TIV increased NAI titers 12 months after vaccination, which reached an antibody ceiling for the two subsequent TIVs (**Figure 4E**). No change was observed in $PRNT_{50}$ titers after vaccination with TIVs (**Figure 4H**). Overall, our results indicate that the TIVs increased durable endpoint titers and maintained the durability of functional antibody titers.

Repeated Vaccination Boosts Antibody Titers but With Reduced Fold-Increase

We analyzed the impact of repeated vaccination on endpoint titers, and functional NAI and $PRNT_{50}$ titers measured at 21 days and 12 months after vaccination in the repeated group. The TIVs boosted endpoint titers measured on day 21 and the endpoint GMT increased gradually with each TIV (**Figure 4A**). The endpoint GMT was measured at 740 after H1N1pdm09 vaccination and was significantly higher after the second TIV when GMT increased to 1579 (P=0.039). Among the HCWs receiving the second TIV, 7/26 had not been vaccinated the year before and one HCW had not been vaccinated for two years (**Supplementary Table 2**). The endpoint GMT further increased to 1827 after the third TIV, which was the highest level measured during the study, although this was not significantly different from the endpoint GMTs measured after H1N1pdm09 or the other TIVs. The number of HCWs that received a third TIV was 19/26, however, two HCWs did not provide day 21 samples. Of these 19 HCWs, only 4 had not been vaccinated the season prior to the third TIV (**Supplementary Table 2**). We observed a different trend for the functional NAI titers on day 21. Although NAI titers were boosted by the TIVs, there were minimal differences in GMT on day 21 after the first, second and third TIV (**Figure 4D**). In fact, NAI GMT measured on day 21 was lowest after the third TIV. $PRNT_{50}$ titers were also boosted after vaccination with TIVs and the highest GMT was observed 21 days after H1N1pdm09 vaccination, whereas TIVs induced lower but

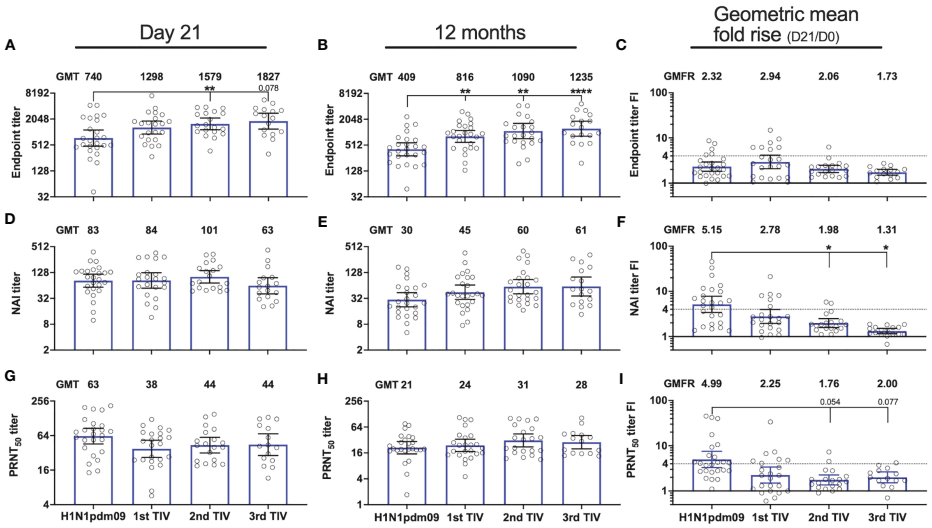

FIGURE 4 | Repeated influenza vaccination boosted durable NA-specific antibody titers but with diminished fold-induction. NA-specific antibody responses were measured 21 days and 12 months after vaccination with AS03-adjuvanted monovalent H1N1pdm09 vaccine and three trivalent influenza vaccines (TIVs) in the four subsequent years after the 2009 pandemic. Antibody titers were measured by ELISA **(A, B)**, ELLA **(D, E)** and plaque reduction neutralization assay **(G, H)** in the repeated group. Geometric mean titers (GMT) are indicated for each vaccine on top of all graphs **(A, B, D, E, G, H)**. Fold-increase (FI) for each subject on day 21 (day 21/day 0) was calculated for the individual vaccines and the geometric mean fold rise (GMFR) for the whole group is indicated on top of each graph **(C, F, I)**. The dotted line represents the threshold set for seroconversion (>4-fold increase). Results are grouped by H1N1pdm09 vaccination and number of trivalent influenza vaccines (TIV) received. The data are presented as geometric mean with 95% confidence intervals. A linear mixed effects model with adjustments for demographic factors was used to determine statistical difference between antibody titers measured after vaccination with H1N1pdm09 and TIVs. *P ≤ 0.05, **P ≤ 0.01, ****P ≤ 0.0001.

similar titers (**Figure 4G**). The level of $PRNT_{50}$ titers measured 21 days after vaccination was not significantly different among the TIVs.

Although TIV vaccination boosted NA-specific antibody responses, the magnitude of the fold- increase on day 21 was not augmented by the number of vaccinations reflecting an antibody ceiling (**Figures 4C, F, I**). The GMFR for functional NAI and $PRNT_{50}$ titers in the repeated group was highest after H1N1pdm09 vaccination and declined with each subsequent TIV (**Figures 4F, I**). The GMFR for NAI titers was significantly lower after the second (P=0.038) and third TIV (P=0.014) compared to H1N1pdm09 vaccination. A trend of decreasing GMFR for the $PRNT_{50}$ titers was observed after the second (P=0.054) and third TIVs (P=0.077) although not significant compared to H1N1pdm09 vaccination. The seroconversion rate for NAI titers also declined with each TIV, where none of the HCWs had >4-fold increase after the third TIV. Seroconversion rates for the first and second TIV were 27 and 11%, respectively. Reduction in GMFR for endpoint titers was also observed with repeated vaccination but the effect was less pronounced than for functional antibody titers (**Figure 4C**).

Pre-existing antibody titers to HA may have a negative effect on boosting of antibody titers after vaccination, however, it is unknown if this applies to NA-specific responses. Spearman correlation analysis was performed to investigate the relationship between baseline titers and fold-increase 21 days after vaccination (**Figure 5**). We found trends of inverse correlation, which was strongest for functional NAI (**Figures 5E–H**) and $PRNT_{50}$ titers (**Figures 5I–L**). Significant inverse correlations were found for NAI titers after H1N1pdm09 and second TIV, and after H1N1pdm09 and the two first TIVs for $PRNT_{50}$ titers. In contrast, a significant correlation was only found for endpoint titers after the first TIV (**Figures 5A–D**). Although the sample size was low, HCWs did not have a higher fold-increase when they had not been vaccinated during the previous year compared to those who had been vaccinated in the previous year (**Figure 5**). Overall, our results indicate that vaccination boosts and maintains NA-specific antibody titers but the magnitude of fold-increase at day 21 is reduced by repeated vaccination with the same vaccine strain over five years. The level of pre-existing antibody titers influenced the magnitude of fold-increase, particularly for functional antibody titers.

DISCUSSION

NA is required to be present in current influenza vaccines, however, there are no regulatory requirements for the amount

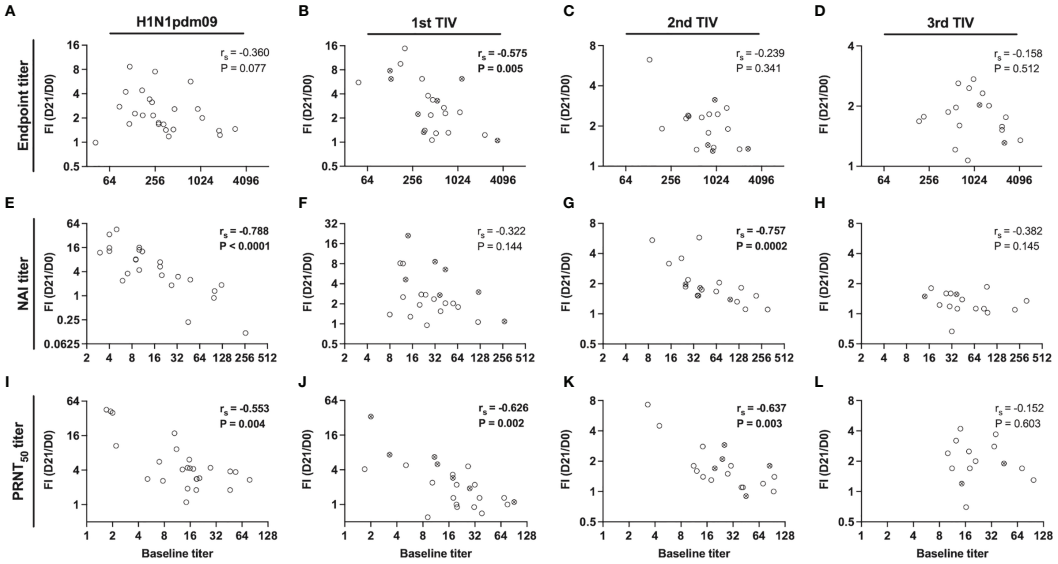

FIGURE 5 | Relationship between pre-existing titers and fold-increase 21 days post-vaccination. Correlation between baseline titers and fold-increase (FI) of titers on day 21 post-vaccination (day 21/day 0) for endpoint **(A–D)**, NAI **(E–H)** and $PRNT_{50}$ titers **(I–L)** in the repeated group. Health care workers (HCWs) were vaccinated with H1N1pdm09 and two or three trivalent influenza vaccines (TIVs) during influenza seasons 2009/2010 – 2013/2014. The antibody responses have been grouped by the vaccine number that were administered. All vaccinated HCWs in the repeated group is included in this figure regardless of their vaccination intervals. Open circles represent HCWs that were vaccinated the previous season and crossed circles represent HCWs that had chosen to not be vaccinated the previous season. The correlation coefficient (r_s) was calculated by non-parametric Spearman correlation.

or the quality of the antigen. Historically, NA content has not been regulated for vaccines due to a lack of standardized assays for measuring the NA concentration and also NA immunogenicity. Recent studies have emphasized the importance of NA-specific antibodies in protection against influenza disease and found that it may be an independent correlate of protection (6, 7). Here, we studied NA-specific antibody responses in HCWs after AS03-adjuvanted monovalent H1N1pdm09 vaccination in 2009 and annual vaccination with TIVs in the four subsequent influenza seasons. Our main finding is repeated influenza vaccination contributes to durable functional H1N1pdm09 NA-specific antibodies, although there is a reduced magnitude of fold-induction with increasing number of TIVs.

Early studies have shown that individuals with high pre-existing HAI titers have reduced boosting after re-vaccination (19, 20). Others have since reported that repeated vaccination and high pre-existing titers may reduce boosting of B cell responses and antibody titers after vaccination (12, 13, 21, 22). These studies have mostly focused on HA-specific antibody responses, however, lower antibody responses to NA after a second vaccination have been reported in individuals vaccinated in two consecutive years (23). Here we show that repeated vaccination has a similar effect on the NA-specific antibody response also after a third and fourth vaccination. We found that, although antibody titers were boosted after repeated vaccination, the magnitude of fold-induction declined, which was most prominent for functional NAI and $PRNT_{50}$ titers. Additionally, the NAI and $PRNT_{50}$ titer fold-increase on day 21 was inversely correlated with pre-existing titers. Others have hypothesized that boosting after repeated vaccination could be limited by pre-existing immunity and several mechanisms has been suggested based on mathematical modeling, which includes epitope masking model (24). This model proposes that pre-existing antibodies will bind and mask epitopes, blocking B cells that bind to the same or nearby epitopes, which results in limited B cell stimulation and expansion. Epitope masking may be a possible explanation for why the functional NA antibodies (measured by fold-increase for NAI and $PRNT_{50}$ titers) peak after H1N1pdm09 vaccination but declines after subsequent TIVs, whereas this effect is less prominent for total NA-specific IgG binding antibodies measured by ELISA. Functional antibodies that are capable of conferring NAI activity bind directly or close to the enzyme active site, however, antigenic sites for human mAbs that do not have functional NAI activity have been described (25). Masking of NAI epitopes would still allow for stimulation of B cells reactive to other parts of the NA, which are readily measured by ELISA. Our observational study

showed that repeated vaccination with the same strain induced durable NA-specific antibodies although it may reduce the magnitude of fold-increase, particularly functional antibodies capable of NAI. The persistence of durable antibody titers suggests that long-lived plasma cells are generated after adjuvanted H1N1pdm09 and subsequent non-adjuvanted TIVs. Further studies are warranted to understand the immunological mechanisms influencing this. This study was unique because the H1N1 vaccine component was the same for five consecutive influenza seasons. Antibody responses after vaccination with TIV during seasons 2006 – 2013 was found to be highest whenever one or more of the vaccine strains varied from year to year (21). More diversification of the H1N1 vaccine strain or addition of adjuvant could possibly have reduced the negative impact of repeated vaccination on antibody responses to NA and should be taken into consideration when choosing the vaccine strains for seasonal vaccines in the future.

A second objective of our study was to investigate the induction of NA-specific antibodies after AS03-adjuvanted monovalent H1N1pdm09 vaccination in healthy adults. This vaccine only contained 3.75 μg HA per dose due to dose-sparing during the 2009 pandemic, whereas TIVs are required to contain 15 μg HA. Quantification of the H1N1pdm09 vaccine composition by mass spectrometry revealed that one dose contained 21% HA and 6.9% NA, demonstrating that the amount of NA was even lower than that of HA per dose. Based on this estimation, the amount of NA would have been 1.23 μg per dose (26). Despite this, we found robust induction of NA-specific antibodies and a 53% seroconversion rate for NAI titers defined seroconversion as >4-fold increase. Other studies have found seroconversion rates ranging from 23 – 64%, however, the definition of seroconversion in these studies varied from 2 – 4-fold increase on day 21 from baseline (7, 10, 11). The seroconversion rate in our study is among the highest reported after influenza vaccination. This shows that robust and durable NA-specific antibody responses can be induced, even with low amounts of antigen when given with an appropriate adjuvant. Our results further support that standardization of the amount and stability of the NA antigen should be implemented for optimization of current influenza vaccines.

NA may undergo antigenic drift and shift independently of HA and NA immunity could provide protection in the event of mismatching of vaccine and circulating strains, and possibly against newly emerging strains. Broadly reactive NA antibodies have been described, demonstrating the breadth of immunity that could potentially be achieved through vaccination (8, 27). Standardizing the amount and supplementing current vaccines with NA have been proposed as a strategy for improving NA immunogenicity (28). A high dosage influenza vaccine containing eight times more NA activity than standard TIVs was found to induce higher levels of NAI antibodies compared to the standard TIV dosage in humans (29). Furthermore, computationally designed NA antigens tested in mice have shown that NA antigens can be designed for optimal cross reactivity (30). These strategies could possibly overcome the influence of pre-existing immunity and aid in the design of diverse antigens for optimal NA immunogenicity.

The current study has several limitations. HCWs may have been infected with influenza virus during the five-year study. This was more easily identified in the single group by increases of HI titers during a season, three HCWs were excluded from further analysis after seroconversion had occurred. However, this was more complicated for HCWs in the repeated group because it is not possible to distinguish increase in HI titer induced by vaccination *versus* infection. Furthermore, HCWs in the repeated group had different intervals of TIV vaccination and the sample size for the various regimens was low. However, we did not find that HCWs that had not been vaccinated for one or two years had higher antibody titer fold-increase compared to those who received TIVs in consecutive years. Only serological responses were measured in this study and therefore it is not known if and how the B cells are affected by repeated vaccination. Others have found inverse correlations between HA-specific pre-existing titers and the number of vaccine-induced antibody secreting cells (12, 21). Investigating this relationship for NA-specific humoral responses is important in future work as it could provide a better understanding of the interplay between pre-existing immunity and boosting, and its role in repeated influenza vaccination.

In conclusion, we found that AS03-adjvuanted pandemic vaccination boosted the NA-specific antibodies that persisted above pre-vaccination levels for 5 years. Repeated vaccination boosted NA-specific antibody titers, although with reduced the magnitude of fold-increase, particularly for functional antibodies. It is important to emphasize that vaccination is the best method of preventing influenza infection and annual vaccination remains beneficial. Our results support continued development and standardization of the NA antigen to supplement current influenza vaccines and reduce the burden of morbidity and mortality.

DATA AVAILABILITY STATEMENT

The raw data supporting the conclusions of this article will be made available by the authors, without undue reservation.

ETHICS STATEMENT

The studies involving human participants were reviewed and approved by Regionale komiteer for medisinsk og helsefaglig forskningsetikk Vest. The patients/participants provided their written informed consent to participate in this study.

AUTHOR CONTRIBUTIONS

LH, FZ, and HA performed the experiments. LH and M-CT performed statistical analyses. LH and RJC wrote the manuscript.

RJC and M-CT conceptualized and designed the study. All authors contributed to the article and approved the submitted version.

FUNDING

LH was supported by Norwegian Research Council grant 271160. This study received intramural funding from the Influenza Centre at the University of Bergen and Haukeland University Hospital. The Influenza Centre is funded by the University of Bergen, Ministry of Health and Care Services, Helse Vest (F-11628), the Trond Mohn Foundation (TMS2020TMT05), the European Union (EU IMI115672 FLUCOP, H2020 874866 INCENTIVE, H2020 101037867 VACCELERATE, EU IMI101007799 Inno4Vac) and Nanomedicines Flunanoair (ERA-NETet EuroNanoMed2, JTC2016), and the Research Council of Norway GLOBVAC program (284930).

ACKNOWLEDGMENTS

We thank all HCWs, clinical staff especially Marianne Sævik and staff at the Influenza Centre for participation in the study. We thank NIBSC for providing the RG virus used in the ELLA assay. We thank Prof. Florian Krammer for providing the baculoviruses used in purifying N1NA proteins.

SUPPLEMENTARY MATERIAL

The Supplementary Material for this article can be found online at: https://www.frontiersin.org/articles/10.3389/fimmu.2021.748264/full#supplementary-material

Supplementary Figure 1 | NA inhibitor oseltamivir was used to verify that the plaque reduction neutralization assay was capable of measuring reduction of plaque forming units per well (PFU/well) as a result of NA inhibition in a dose-dependent manner.

REFERENCES

1. Iuliano AD, Roguski KM, Chang HH, Muscatello DJ, Palekar R, Tempia S, et al. Estimates of Global Seasonal Influenza-Associated Respiratory Mortality: A Modelling Study. *Lancet* (2018) 391(10127):1285–300. doi: 10.1016/S0140-6736(17)33293-2
2. World Health Organization. *Influenza (Seasonal)* (2018). Available at: https://www.who.int/en/news-room/fact-sheets/detail/influenza-(seasonal).
3. Palese P, Tobita K, Ueda M, Compans RW. Characterization of Temperature Sensitive Influenza Virus Mutants Defective in Neuraminidase. *Virology* (1974) 61(2):397–410. doi: 10.1016/0042-6822(74)90276-1
4. Kilbourne ED, Couch RB, Kasel JA, Keitel WA, Cate TR, Quarles JH, et al. Purified Influenza A Virus N2 Neuraminidase Vaccine is Immunogenic and non-Toxic in Humans. *Vaccine* (1995) 13(18):1799–803. doi: 10.1016/0264-410X(95)00127-M
5. Murphy BR, Kasel JA, Chanock RM. Association of Serum Anti-Neuraminidase Antibody With Resistance to Influenza in Man. *N Engl J Med* (1972) 286(25):1329–32. doi: 10.1056/NEJM197206222862502
6. Memoli MJ, Shaw PA, Han A, Czajkowski L, Reed S, Athota R, et al. Evaluation of Antihemagglutinin and Antineuraminidase Antibodies as Correlates of Protection in an Influenza A/H1N1 Virus Healthy Human Challenge Model. *mBio* (2016) 7(2):e00417–16. doi: 10.1128/mBio.00417-16
7. Monto AS, Petrie JG, Cross RT, Johnson E, Liu M, Zhong W, et al. Antibody to Influenza Virus Neuraminidase: An Independent Correlate of Protection. *J Infect Dis* (2015) 212(8):1191–9. doi: 10.1093/infdis/jiv195
8. Chen YQ, Wohlbold TJ, Zheng NY, Huang M, Huang Y, Neu KE, et al. Influenza Infection in Humans Induces Broadly Cross-Reactive and Protective Neuraminidase-Reactive Antibodies. *Cell* (2018) 173(2):417–29.e10. doi: 10.1016/j.cell.2018.03.030
9. Wohlbold TJ, Nachbagauer R, Xu H, Tan GS, Hirsh A, Brokstad KA, et al. Vaccination With Adjuvanted Recombinant Neuraminidase Induces Broad Heterologous, But Not Heterosubtypic, Cross-Protection Against Influenza Virus Infection in Mice. *mBio* (2015) 6(2):e02556. doi: 10.1128/mBio.02556-14
10. Couch RB, Atmar RL, Keitel WA, Quarles JM, Wells J, Arden N, et al. Randomized Comparative Study of the Serum Antihemagglutinin and Antineuraminidase Antibody Responses to Six Licensed Trivalent Influenza Vaccines. *Vaccine* (2012) 31(1):190–5. doi: 10.1016/j.vaccine.2012.10.065
11. Laguio-Vila MR, Thompson MG, Reynolds S, Spencer SM, Gaglani M, Naleway A, et al. Comparison of Serum Hemagglutinin and Neuraminidase Inhibition Antibodies After 2010-2011 Trivalent Inactivated Influenza Vaccination in Healthcare Personnel. *Open Forum Infect Dis* (2015) 2(1):ofu115. doi: 10.1093/ofid/ofu115
12. Sanyal M, Holmes TH, Maecker HT, Albrecht RA, Dekker CL, He XS, et al. Diminished B-Cell Response After Repeat Influenza Vaccination. *J Infect Dis* (2019) 219(10):1586–95. doi: 10.1093/infdis/jiy685
13. Ellebedy AH, Nachbagauer R, Jackson KJL, Dai YN, Han J, Alsoussi WB, et al. Adjuvanted H5N1 Influenza Vaccine Enhances Both Cross-Reactive Memory B Cell and Strain-Specific Naive B Cell Responses in Humans. *Proc Natl Acad Sci USA* (2020) 117(30):17957–64. doi: 10.1073/pnas.1906613117
14. Madhun AS, Akselsen PE, Sjursen H, Pedersen G, Svindland S, Nostbakken JK, et al. An Adjuvanted Pandemic Influenza H1N1 Vaccine Provides Early and Long Term Protection in Health Care Workers. *Vaccine* (2010) 29(2):266–73. doi: 10.1016/j.vaccine.2010.10.038
15. Margine I, Palese P, Krammer F. Expression of Functional Recombinant Hemagglutinin and Neuraminidase Proteins From the Novel H7N9 Influenza Virus Using the Baculovirus Expression System. *J Vis Exp* (2013) 81):e51112. doi: 10.3791/51112
16. Couzens L, Gao J, Westgeest K, Sandbulte M, Lugovtsev V, Fouchier R, et al. An Optimized Enzyme-Linked Lectin Assay to Measure Influenza A Virus Neuraminidase Inhibition Antibody Titers in Human Sera. *J Virol Methods* (2014) 210:7–14. doi: 10.1016/j.jviromet.2014.09.003
17. Matrosovich M, Matrosovich T, Carr J, Roberts NA, Klenk HD. Overexpression of the Alpha-2,6-Sialyltransferase in MDCK Cells Increases Influenza Virus Sensitivity to Neuraminidase Inhibitors. *J Virol* (2003) 77(15):8418–25. doi: 10.1128/JVI.77.15.8418-8425.2003
18. Matrosovich M, Matrosovich T, Garten W, Klenk HD. New Low-Viscosity Overlay Medium for Viral Plaque Assays. *Virol J* (2006) 3:63. doi: 10.1186/1743-422X-3-63
19. Hobson D, Baker FA, Curry RL. Effect of Influenza Vaccines in Stimulating Antibody in Volunteers With Prior Immunity. *Lancet* (1973) 2(7821):155–6. doi: 10.1016/S0140-6736(73)93106-1
20. Pyhala R, Kumpulainen V, Alanko S, Forsten T. HI Antibody Kinetics in Adult Volunteers Immunized Repeatedly With Inactivated Trivalent Influenza Vaccine in 1990-1992. *Vaccine* (1994) 12(10):947–52. doi: 10.1016/0264-410X(94)90039-6
21. Andrews SF, Kaur K, Pauli NT, Huang M, Huang Y, Wilson PC. High Preexisting Serological Antibody Levels Correlate With Diversification of the Influenza Vaccine Response. *J Virol* (2015) 89(6):3308–17. doi: 10.1128/JVI.02871-14
22. Ellebedy AH, Krammer F, Li GM, Miller MS, Chiu C, Wrammert J, et al. Induction of Broadly Cross-Reactive Antibody Responses to the Influenza HA Stem Region Following H5N1 Vaccination in Humans. *Proc Natl Acad Sci USA* (2014) 111(36):13133–8. doi: 10.1073/pnas.1414070111
23. Petrie JG, Ohmit SE, Johnson E, Truscon R, Monto AS. Persistence of Antibodies to Influenza Hemagglutinin and Neuraminidase Following One or Two Years of Influenza Vaccination. *J Infect Dis* (2015) 212(12):1914–22. doi: 10.1093/infdis/jiv313
24. Linderman SL, Ellebedy AH, Davis C, Eberhardt CS, Antia R, Ahmed R, et al. Influenza Immunization in the Context of Preexisting Immunity. *Cold Spring Harb Perspect Med* (2020). doi: 10.1101/cshperspect.a040964
25. Yasuhara A, Yamayoshi S, Kiso M, Sakai-Tagawa Y, Koga M, Adachi E, et al. Antigenic Drift Originating From Changes to the Lateral Surface of the Neuraminidase Head of Influenza A Virus. *Nat Microbiol* (2019) 4(6):1024–34. doi: 10.1038/s41564-019-0401-1
26. Jacob L, Leib R, Ollila HM, Bonvalet M, Adams CM, Mignot E. Comparison of Pandemrix and Arepanrix, Two Ph1n1 AS03-Adjuvanted Vaccines

Differentially Associated With Narcolepsy Development. *Brain Behav Immun* (2015) 47:44–57. doi: 10.1016/j.bbi.2014.11.004

27. Stadlbauer D, Zhu X, McMahon M, Turner JS, Wohlbold TJ, Schmitz AJ, et al. Broadly Protective Human Antibodies That Target the Active Site of Influenza Virus Neuraminidase. *Science* (2019) 366(6464):499–504. doi: 10.1126/science.aay0678
28. Giurgea LT, Morens DM, Taubenberger JK, Memoli MJ. Influenza Neuraminidase: A Neglected Protein and Its Potential for a Better Influenza Vaccine. *Vaccines (Basel)* (2020) 8(3):409. doi: 10.3390/vaccines8030409
29. Cate TR, Rayford Y, Nino D, Winokur P, Brady R, Belshe R, et al. A High Dosage Influenza Vaccine Induced Significantly More Neuraminidase Antibody Than Standard Vaccine Among Elderly Subjects. *Vaccine* (2010) 28(9):2076–9. doi: 10.1016/j.vaccine.2009.12.041
30. Skarlupka AL, Bebin-Blackwell AG, Sumner SF, Ross TM. Universal Influenza Virus Neuraminidase Vaccine Elicits Protective Immune Responses Against Human Seasonal and Pre-Pandemic Strains. *J Virol* (2021) 95(7):e0075921. doi: 10.1128/JVI.00759-21

Conflict of Interest: The authors declare that the research was conducted in the absence of any commercial or financial relationships that could be construed as a potential conflict of interest.

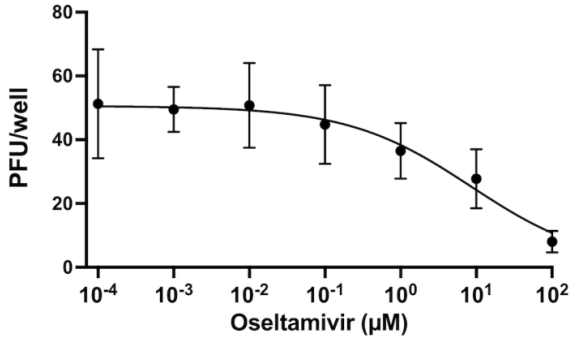

Supplementary Figure 1 | NA inhibitor oseltamivir was used to verify that the plaque reduction neutralization assay was capable of measuring reduction of plaque forming units per well (PFU/well) as a result of NA inhibition in a dose-dependent manner.

Supplemental table 1. CHMP immunological criteria for influenza vaccines

CHMP criteria for HI titer		**All HCWs (day 21)**
Geometric mean fold rise	>2.5	49.4
Seroconversion rate (>4-fold increase)	>40%	92%
Seroprotection rate (HI titer >40)	>70%	100%

European Medicines Agency Committee for Medicinal product for human use (CHMP)

Supplemental table 2. Overview of vaccination intervals and number of vaccinations in the repeated group

Vaccine intervals 2009-2010-2011-2012-2013	**HCWs** n (%)
1-0-0-1-1	1 (4)
1-0-1-0-1	2 (8)
1-1-0-0-1	1 (4)
1-1-1-0-0	1 (4)
1-0-1-1-1	5 (19)
1-1-0-1-1	5 (19)
1-1-1-0-1	4 (15)
1-1-1-1-0	7 (27)

HCW healthcare workers (HCWs).

Papers I-III

III

Durable immune responses after BNT162b2 vaccination in home-dwelling old adults

Lena Hansen[a*], Karl Albert Brokstad[a,c], Amit Bansal[a], Fan Zhou[a], Geir Bredholt[b], Therese Bredholt Onyango[a], Helene Heitmann Sandnes[b], Rebecca Elyanow[d], Anders Madsen[a], Mai-Chi Trieu[a], Marianne Sævik[e], Hanne Søyland[e], Jan Stefan Olofsson[a], Juha Vahokoski[a], Nina Urke Ertesvåg[a], Elisabeth Berg Fjelltveit[a], Shahin Shafiani[d], Camilla Tøndel[b,f,g], Heidi Chapman[d], Ian Kaplan[d], Kristin GI Mohn[a,e], on behalf of the Bergen COVID-19 Research Group, Nina Langeland[b,e,h†], Rebecca Jane Cox[a,i*†].

[a]Influenza Centre, Department of Clinical Science, University of Bergen; Bergen, Norway.
[b]Department of Clinical Science, University of Bergen; Bergen, Norway.
[c]Department of Safety, Chemistry and Biomedical Laboratory Sciences, Western Norway University of Applied Sciences; Bergen, Norway.
[d]Adaptive Biotechnologies; Seattle, WA, USA.
[e]Department of Medicine, Haukeland University Hospital; Bergen, Norway.
[f]Department of Pediatrics, Haukeland University Hospital; Bergen, Norway.
[g]Department of Research and Innovation, Haukeland University Hospital; Bergen, Norway.
[h]National Advisory Unit for Tropical Infectious Diseases, Haukeland University Hospital; Bergen, Norway.
[i]Department of Microbiology, Haukeland University Hospital; Bergen, Norway.
[†]Authors contributed equally

[*]Corresponding authors:
E-mail: Rebecca.Cox@uib.no; Lena.Hansen@uib.no
Postal address: Jonas Lies Vei 87, N-5021 Bergen, Norway

Highlights

- Humoral and cellular responses after SARS-CoV-2 vaccination or infection in elderly
- Elderly vaccinees had narrower spike-specific T-cell receptor repertoires
- T-cell responses short-lived after vaccination but long-lived after infection
- Memory B-cells maintained 9-months post-vaccination and 12-months post-infection
- Neutralizing antibodies lasted 6 months in old and 12 months in younger vaccinees

Abstract

Objectives

Elderly are an understudied, high-risk group vulnerable to severe COVID-19. We comprehensively analyzed the durability of humoral and cellular immune responses after BNT162b2 vaccination and SARS-CoV-2 infection in elderly and younger adults.

Methods

Home-dwelling old (n=100, median 86 years) and younger adults (n=449, median 38 years) were vaccinated with two doses of BNT162b2 vaccine at 3-week intervals and followed for 9-months. Vaccine-induced responses were compared to home-isolated COVID-19 patients (n=183, median 47 years). Our analysis included neutralizing antibodies, spike-specific IgG, memory B-cells, IFN-γ and IL-2 secreting T-cells and sequencing of the T-cell receptor (TCR) repertoire.

Results

Spike-specific breadth and depth of the $CD4^+$ and $CD8^+$ TCR repertoires were significantly lower in the elderly after one and two vaccinations. Both vaccinations boosted IFN-γ and IL-2 secreting spike-specific T-cells responses, with 96% of the elderly and 100% of the younger adults responding after the second dose, although responses were not maintained at 9-months. In contrast, T-cell responses persisted up to 12-months in infected patients. Spike-specific memory B-cells were induced after the first dose in 87% of the younger adults compared to 38% of the elderly, which increased to 83% after the second dose. Memory B-cells were maintained at 9-months post-vaccination in both vaccination groups. Neutralizing antibody titers were estimated to last for 1-year in younger adults but only 6-months in the older vaccinees. Interestingly, infected older patients (n=15, median 75 years) had more durable neutralizing titers estimated to last 14-months, 8-months longer than the older vaccinees.

Conclusions

Vaccine-induced spike-specific IgG and neutralizing antibodies were consistently lower in the older than younger vaccinees. Overall, our data provide valuable insights into the kinetics of the humoral and cellular immune response in the elderly after SARS-CoV-2 vaccination or infection, highlighting the need for two doses, which can guide future vaccine design.
Clinical trials.gov;NCT04706390

Keywords

Elderly, BNT162b2, memory B-cell, T-cell, SARS-CoV-2, neutralising antibody

Introduction

The rapid development and licensing of mRNA vaccines has resulted in a significant reduction in morbidity and mortality due to coronavirus disease 2019 (COVID-19) [1, 2]. Based on preclinical studies of severe acute respiratory syndrome coronavirus (SARS-CoV) and Middle Eastern Respiratory Syndrome Coronavirus (MERS-CoV) [3], the spike protein was quickly identified as an antigenic target for SARS-CoV-2 vaccines. The elderly are at the highest risk of severe disease and death after COVID-19 [4, 5], thus optimal protection for this group is a major goal of vaccine design and public health efforts. Despite this, the elderly were not included in the original COVID-19 vaccine licensure trials [6]. BNT162b2 vaccine induced a strong humoral response against SARS-CoV-2 in people over 80, while cellular responses were only detectable in 63% [7]. Furthermore, humoral and cellular immune responses in older persons are lower compared to younger adults up to 6-months post-vaccination [8].

A reliable correlate of protection recognized by regulators has yet to be defined, however, there is compelling evidence in support of both humoral and cellular immunity in preventing severe disease [9, 10]. Although protection against severe disease for the first few months after vaccination is well documented, the duration of vaccine-induced protection has been found to wane 6-months after vaccination [11]. It is currently unclear how the durability of humoral and cellular responses differs between younger adults and elderly persons after vaccination, and how this compares to immunity after infection.

We conducted a longitudinal study comparing the magnitude and durability of the immune responses elicited after vaccination and infection in different age groups. Here, we measured the immune response for up to 9-months after BNT162b2 vaccination in SARS-CoV-2 naive old and younger adults. We performed a comprehensive analysis of both humoral and cellular immune responses covering SARS-CoV-2 spike-binding and neutralizing antibodies, memory B-cells, functional T-cell responses and sequencing of the T-cell receptor (TCR) repertoire. Our data provide valuable information on the kinetics and durability of SARS-CoV-2 immune responses for younger adults and an understudied, high-risk, elderly group. We also compared the durability of vaccine-induced immune responses with those after mild-to-moderate infection in unvaccinated individuals, demonstrating that age differentially shapes immune responses after vaccination and infection.

Methods

Participants

We conducted a prospective cohort study of adults receiving pandemic COVID-19 vaccine (BNT162b2 Pfizer-BioNTech) between January and November 2021 from Eidsvåg general practice and Haukeland University Hospital in Bergen, Norway. All subjects provided written informed consent before inclusion in the study, which was approved by the regional ethics committee (Regional Committee for Medical Research Ethics, Northern Norway (REK Nord). The study is registered in the National Institute for Health database Clinical trials.gov (NCT04706390). The inclusion criteria were willingness to attend scheduled blood sampling visits and no previous SARS-CoV-2 infection. The exclusion criteria were history of anaphylaxis or hypersensitivity to vaccines. The infected cohort was recruited during March and April 2020 from home-isolated SARS-CoV-2 infected individuals and were followed clinically and immunologically at 2-, -6 and 12-months post-infection. The inclusion criteria were positive PCR test or antibody positivity at convalescence. All patients had mild-to-moderate infection and were not hospitalized, details are described elsewhere [12].

Vaccine

Each dose (0.45 ml) of BNT162b2 mRNA vaccine embedded in lipid nanoparticles contained 30 μg of a purified single-stranded, 5'-capped mRNA, encoding the spike protein from the founder Wuhan-Hu1 strain.

Vaccine study design

All participants were vaccinated intramuscularly into the deltoid muscle with two doses of BNT162b2 mRNA vaccine at 3-week intervals. Subjects provided blood samples prior to and 3- and 6-weeks, 5- and 9-months after vaccination. Blood samples were collected using plastic serum tubes (BD Biosciences) and ethylene diamine tetra acetic acid (EDTA) tubes (BD Biosciences). A subgroup of the vaccination and infection cohorts provided a cell preparation tube (CPT) (BD Biosciences) for PBMC separation pre- and post-vaccination or post-infection, respectively, to examine MBC and T-cell responses. The infected cohort provided serum at 8-weeks, 6- and 12-months post-infection.

Clinical information

Electronic case report forms (eCRF) were developed using the Research Electronic Data Capture database (REDCap®) (Vanderbilt University, Nashville, Tennessee). The eCRF

contained demographics, comorbidities, medication, exposure and infection history (RT-PCR results and presence of symptoms) and vaccination data.

Serological assays

ELISA

ELISA was used for detecting spike-specific IgG [12, 13]. Baseline sera were screened by RBD ELISA to test for seropositivity, positive samples were run in spike IgG ELISA. Endpoint titers were calculated as the reciprocal of the serum dilution giving an optical density value of 3 standard deviations above the mean of historical pre-pandemic sera (n=128).

Microneutralization assay

The microneutralization assay was performed with ancestral D614G hCoV-19/Norway/Bergen-01/2020 (GISAID accession ID EPI_ISL_541970) in a certified Biosafety Level 3 Laboratory, as previously described [13]. Neutralizing titers were calculated as the reciprocal of the serum dilution giving 50% inhibition of virus infectivity. For calculation purposes negative titers (<20) were assigned a value of 10.

Memory B-cell ELISPOT

PBMCs were resuspended in RPMI-1640 (Lonza) with 10% fetal bovine serum (Hyclone), 100 U/ml penicillin, 0.1 mg/ml streptomycin (Sigma Aldrich) (negative control) or in medium containing 1 µg/ml R848 (MabTech) and 1 µg/ml rhIL-2 (MabTech) for expansion of B-cells. Two million cells were added per well in 24-well plates (Nunc) and incubated for 6 days at 37°C, 5% CO_2. ELISPOT plates (Millipore) were coated with 15 µg/ml anti-human IgG (MabTech), 10 µg/ml SARS-CoV-2 spike protein, or PBS only (negative control) at 4°C overnight. Lymphocytes were incubated in ELISPOT plates for 16 hours (37°C, 5% CO_2). IgG^+ MBCs were detected with 1 µg/ml biotinylated anti-IgG monoclonal antibody (MabTech) for 2 hours at room temperature followed by Streptavidin-HRP (1:1000) (MabTech). Spots were developed with 3,3',5,5'-tetramethylbenzidine (TMB) ELISPOT substrate (MabTech). The plates were counted using an ELISPOT reader (Advanced Imaging Devices, Germany). Spike-specific spots were calculated as the mean of duplicate wells after subtraction of negative controls and presented as spot forming units per million PMBCs (SFU/10^6 PBMCs).

SARS-CoV-2 T-cell responses

Spike-specific interferon-γ (IFN-γ), interleukin 2 (IL-2), and double-positive IFN-γ^+, IL-2^+ cytokine-producing T-cells were quantified using an IFN-γ/IL-2 FluoroSpot kit (MabTech), as previously described [14].

T-cell receptor (TCR) variable beta chain sequencing

EDTA samples were collected 0, 3- and 6-weeks post-vaccination from all vaccinees for immunosequencing of the human TCRβ chains complementarity determining region 3 (CDR3) using the immunoSEQ Assay (Adaptive Biotechnologies, Seattle, WA). Extracted genomic DNA was amplified in a bias-controlled multiplex PCR, followed by high-throughput sequencing. Sequences were collapsed and filtered in order to identify and quantitate the absolute abundance of each unique TCRβ CDR3 for further analysis as previously described [15].

Identifying SARS-CoV-2-associated TCRβ sequences

One-tailed Fisher's exact tests were performed on all unique TCRβ sequences comparing their presence in SARS-CoV-2 PCR-positive samples (n=1954) with negative controls (n=3903) generating a list of SARS-CoV-2-associated sequences which are exclusive to, or greatly enriched, in PCR-positive samples. Filtering was performed to remove potential false positives associated with cytomegalovirus (CMV) seropositivity or human leukocyte antigen (HLA) alleles in SARS-CoV-2 negative healthy populations[16]. SARS-CoV-2-associated sequences contains 8631 rearrangements.

We assigned subsets of our enhanced TCR sequences to spike and non-spike antigens based on data from multiplexed antigen stimulation assays. 917 TCRs were assigned to the SARS-CoV-2 spike protein and 1564 to non-spike viral proteins. We inferred whether an enhanced sequence was a $CD4^+$ or $CD8^+$ T-cell by statistically associating each sequence to a Class II or Class I HLA. HLA associations are derived from a set of 657 SARS-CoV-2 positive individuals who have genotyped HLAs. We built a binary logistic regression classifier with L1 regularization to determine which HLA best predicts the observed distribution of a given enhanced sequence across all HLA-typed cases. The L1 regularization strength was tuned to yield a single non-zero coefficient, giving a single inferred HLA association for each enhanced sequence. The inferred HLA associations were validated against the subset of enhanced sequences which overlap with our multiplex antigen stimulation assays [15, 17].

Spike-specific TCR clonal breadth and depth were calculated as previously described, using the set of SARS-CoV-2-associated TCRβ sequences [18]. Breadth is calculated as the number of unique SARS-CoV-2-associated rearrangements out of the total number of unique productive rearrangements, while depth accounts for the frequency of those rearrangements in the repertoire.

Statistical analysis

Data were plotted using Graphpad Prism (version 9, La Jolla, USA). Statistical analyses were performed in R (Version 4.1.2) using the following libraries: nlme, emmeans, and ggplot. We used linear mixed-effect models to compare humoral and cellular responses after vaccination in younger and older adults over the 9-months and compared to infected individuals with adjustments for demographic and clinical data, and for subject variation with repeated measures. A single global test for all possible 2-way interaction terms was performed for each model to avoid multiple testing. The interaction term was included in the model only if $P \leq 0.01$ to lower the likelihood of a false positive result. The estimated effects of covariates are presented with 95% confidence intervals. Statistical differences between pairs of group means was done by post-hoc tests using Bonferroni adjustment for multiple comparisons. $P<0.05$ was considered statistically significant.

Results

Demographics of study population

We prospectively enrolled elderly and younger adults after BNT162b2 vaccination (2 doses at 3-week intervals), consisting of 449 younger adults (median 38 years old (yo), range 23-69yo, 69% female) and 100 elderly (median 86yo, range 70-99yo, 63% female) (**Fig. 1, Table 1**). The elderly had more comorbidities (84%), mainly chronic heart disease, than younger adults (12%). Fifteen percent of the elderly were taking immunosuppressive medication compared to 1% of the younger adults. Blood samples were collected at baseline, at 3-weeks, 6-weeks, 5- and 9-months after the first vaccination (**Fig. 2A**) and all vaccinees were pre-vaccination seronegative by RBD ELISA.

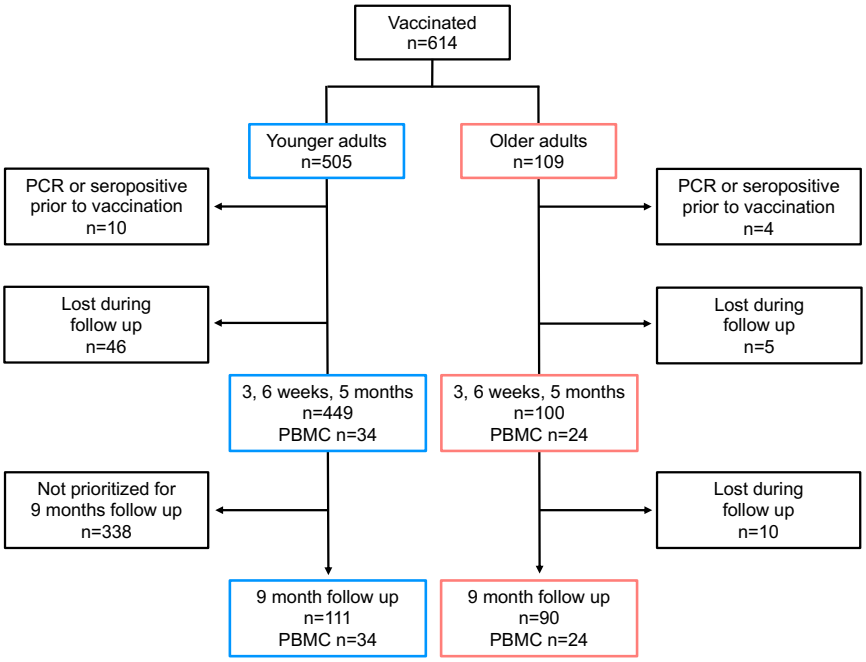

FIG 1. Study population flowchart
Number of vaccinees eligible for inclusion at baseline and sampling of serum and peripheral blood mononuclear cell (PBMC) for the participants during the study.

Table 1. Demographics of the study population

	Younger adults, n (%)			**Older adults, n (%)**		**Infected, n (%)**	
Subgroup	**All[1]**	**B- and T-cells[2]**	**Subgroup 9 months**	**All[2]**	**B- and T-cells[2]**	**All[3]**	**B- and T-cells[4]**
Total number of subjects	449	34	111	100	24	183	68
Female/male	309/140 (69/31)	22/13 (63/37)	75/36 (66/34)	63/37 (63/37)	15/9 (62/38)	95/88 (52/48)	33/35 (5149)
Median age [range]	38 [23-69]	39 [27-63]	41 [23-66]	86 [70-99]	86 [73-93]	47 [23-80]	45 [16-80]
Comorbidity[5]	54 (12)	2 (6)	13 (12)	84 (84)	21 (88)	74 (40)	27 (40)
Immunosuppression[6]	6 (1)	1 (3)	3 (3)	15 (15)	7 (29)	5 (3)	2 (3)

[1]Sampled on day 0, 3- and 6-weeks, 5-months
[2]Sampled on day 0, 3- and 6-weeks, 5-months, 9-months
[3]Sampled at 2-, 6- and 12-months after diagnosis
[4]Sampled at 6-months (B-cells n=10, T-cells n=38) and 12 months (B- and T-cells n=63)
[5]Comorbidities include chronic heart disease, chronic lung disease, chronic liver disease, chronic kidney disease, diabetes, cancer, rheumatic disease, neurological disease, autoimmune disease.
[6]Inherent immunosuppressive disease, HIV, organ transplant, chemotherapy, other immunosuppressive medication.

BNT162b2 vaccination induces durable, but less robust humoral immunity in older adults

We have conducted a comprehensive analysis of the kinetics and durability of the humoral and cellular responses after BNT162b2 vaccination. Binding IgG titers were measured against recombinant spike protein by ELISA. The first vaccination elicited spike-specific IgG in both groups, although the elderly had significantly lower geometric mean titers (GMT) than the younger adults (GMT 1503 vs 9578, P<0.0001) (**Fig. 2B**). The second vaccination boosted spike-specific IgG titers in all vaccinees with the highest titers observed in younger adults, however, the elderly had a higher fold increase after the second dose (mean fold increase 30 vs 7). In addition to age, a mixed-effects model showed that IgG titers were also significantly lower for men than women and for vaccinees with comorbidities (**Table S1**). The elderly had significantly lower spike-specific IgG titers compared to the younger adults at 5- and 9-months (GMT 5 months 4048 vs. 14713, 9-months 1483 vs. 2724, P<0.0001) (**Fig. 2B**). We used linear regression models to calculate the half-life of the spike-specific IgG response from peak levels measured after the second dose. We found that the geometric mean of the estimated IgG half-life was 3.1 months for the elderly compared to 3.6 months for the younger adults.

We studied the neutralizing antibody response after vaccination in the elderly and a representative subgroup of younger adults (**Fig. 2C**). Neutralizing titers were lower in the elderly than the younger adults after the first dose (GMT 16 vs 29), where only 32% of the elderly had detectable (≥20) neutralizing antibodies compared to 71% of younger adults. The second dose boosted neutralizing titers for both groups, with 92% of the elderly having neutralizing titer ≥20 (GMT 115) compared to 100% of the younger adults (GMT 469). Although neutralizing antibodies waned in both groups, titers were detectable in 100% of younger adults (GMT 142) and 82% of elderly (GMT 45) after 5-months. At 9-months post-vaccination, 95% of younger adults still had detectable neutralizing antibodies (GMT 57), whereas the percentage of elderly had decreased to 58% (GMT 24). We estimated the half-life and time for the neutralizing titers to fall below the level of detection (<20). The geometric mean of the estimated half-life of neutralizing titers was comparable for the younger adults (4.0 months) and the elderly (4.3 months). However, the estimated duration of detectable neutralizing titers was 12.5 months for the younger adults and only 6.2 months in the elderly (**Fig. S1**). Similarly to spike-specific IgG, the linear mixed-effects model analysis showed that the neutralizing antibodies were also lower for the elderly and for men (**Table S1**).

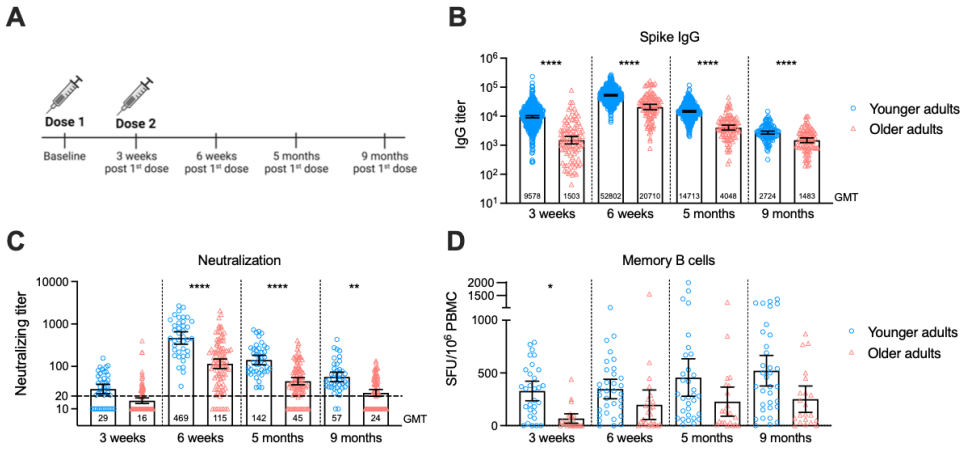

FIG 2. Durability of spike-specific humoral immune responses after BNT162b2 vaccination
(**A**) Study design showing time points for vaccination and blood sampling in young adults (blue circles) aged 23-69 years (n=449) and elderly persons (red triangles) aged 70-99 years (n=100). Each symbol represents one individual.
(**B**) Anti-spike serum IgG endpoint titers measured by ELISA. Data are presented as geometric mean titer (GMT) with 95% confidence intervals (CIs).
(**C**) Neutralizing antibody responses measured by microneutralization assay against the ancestral D614G strain in all elderly and a subgroup of adults including those that provided peripheral blood mononuclear cells (PBMCs) (n=41). The neutralizing titer was defined as the reciprocal serum dilution resulting in 50% neutralization. The data are presented as GMT with 95% CIs.
(**D**) Spike-specific memory B-cell responses were measured by ELISpot using PBMCs collected from a subgroup of vaccinated younger adults (n=35) and elderly (n=24). The frequency of spike-specific memory B-cells were defined as spot forming units (SFU) per 10^6 PBMC. The data are presented as mean with 95% CIs.
Mixed-effects model with normalized outcome variables with fixed effects of sex, age group, presence of comorbidity, use of immunosuppressive medication and age-by-time interaction (except neutralization and memory B-cells), and individual repeated measures as a random factor. Significance of differences between pairs of group means was assessed by post-hoc tests. P values were only reported if they were significant at the 5% level after Bonferroni correction.
****P<0.0001, **P<0.01, *P<0.05

We collected PBMC from a subgroup of 34 younger adults and 24 elderly to investigate the spike-specific memory B-cell (MBC) response by ELISpot after the first and second dose, and long-term after 5- and 9-months (**Table 1, Fig. 2D**). The first dose induced significantly higher levels of MBCs in the younger adults compared to the elderly (P<0.05). After the first dose, 87% of younger adults had detectable spike-specific MBCs (mean SFU 329, range 0-790), whereas MBCs were only detected in 38% of the elderly (mean SFU 68, range 0-440). The second vaccination boosted the number of MBCs in the elderly (mean SFU 198, range 0-1560),

although four elderly subjects were non-responders (17%), two of whom were taking immunosuppressive medication. In contrast, we found that the second dose induced limited boosting of MBCs in the younger adults (mean SFU 348, range 0-1030), where two younger adults (6%) had no increase in MBCs. The MBCs were generally maintained after 5- and 9-months post-vaccination or increased moderately in younger adults. The frequency of MBCs in the elderly increased to mean SFU 228 (range 0-1240) after 5-months and mean SFU 251 (range 0-870) after 9-months, although this increase was not significant. Similarly, the frequency of MBCs in younger adults increased moderately to mean SFU 456 (range 10-2000) after 5-months and mean SFU 521 (range 0-1360) after 9-months.

BNT162b2 vaccination expands the spike-specific T-cell response

The immunoSEQ assay is a high throughput ultra-deep sequence-based method to quantify spike-specific T-cell responses after natural infection or vaccination [18]. This method allowed us to assess the breadth and depth of the spike-specific TCR repertoire for all vaccinees at baseline and after the first and second vaccination. Clonal breadth was defined as the relative number of distinct spike-specific T-cell clonotypes as a fraction of the overall repertoire, and clonal depth as the extent of expansion of spike-specific T-cells.

The spike-specific TCR breadth and depth increased in both groups after the first and second vaccination, demonstrating expansion of spike-specific T-cells (**Fig. 3**). The younger adults had significantly higher TCR breadth (**Fig. 3A**) and depth (**Fig. 3B**) compared to the elderly after the first and the second vaccination, indicating that the elderly had fewer expanded T-cells and a narrower spike-specific TCR repertoire (**Table S2**). The younger adults had the highest fold increase in spike-specific TCR breadth after the first vaccination (mean fold increase 11 vs. 4), while the fold increase was comparable between the groups after the second dose (mean fold increase 1 vs. 2). Overall, both the breadth and depth of the spike-specific TCR repertoire was highest for the human leukocyte antigen (HLA) class II-associated T-cells, indicating that $CD4^+$ T-cells made up the largest proportion of the vaccine-induced T-cell response.

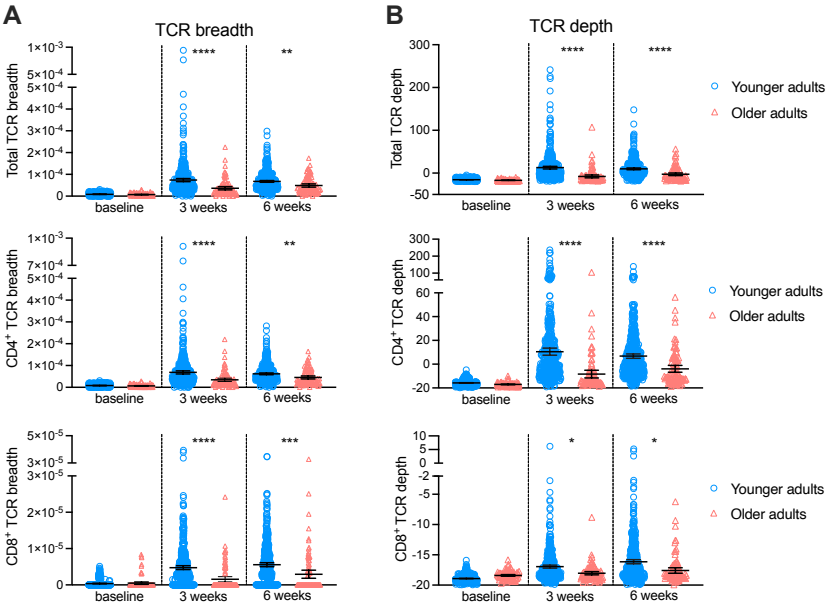

FIG 3. Spike-specific T-cell receptor sequencing after BNT162b2 vaccination
(**A**) The clonal breadth of the spike-specific T-cell receptor (TCR) repertoire measured by immunoSEQ in vaccinated adults (blue circles) aged 23-69 years (n=449) and elderly persons (red triangles) aged 70-99 years (n=100). Blood samples were tested at baseline, and 3 weeks after first and second vaccination (6 weeks post-first vaccination). Each symbol represents one individual. The proportion of unique spike-specific TCR sequences (breadth) for all T-cells (top), $CD4^+$ T-cells (middle) and $CD8^+$ T-cells (bottom). Data are presented as mean with 95% confidence intervals.
(**B**) The frequency of unique spike-specific TCR sequences (depth) for the total TCR repertoire (top), $CD4^+$ T-cells (middle) and $CD8^+$ T-cells (bottom).
Mixed-effects model with normalized outcome variables with fixed effects of sex, age group, presence of comorbidity, use of immunosuppressive medication and age-by-time interaction (except $CD8^+$ TCR depth), and individual repeated measures as a random factor. Significance of differences between pairs of group means was assessed by post-hoc tests. P values were only reported if they were significant at the 5% level after Bonferroni correction.
****P<0.0001, ***P<0.001, **P<0.01, *P<0.05

To complement the TCR data, we analyzed the functionality of the spike-specific T-cell response using PBMCs in the FluoroSpot assay in a subgroup of younger adults (n=34) and elderly (n=24) (**Fig. 4, Table 1**). Single cytokine-producing (IFN-γ or IL-2) T-cells (**Fig. 4A-B**) and double cytokine-producing IFN-γ^+, IL-2^+ T-cells (**Fig. 4C**) were measured using overlapping peptide pools from the spike protein. Spike-specific TCR breadth and depth correlated with the number of functional spike-specific T-cells measured by FluoroSpot (**Fig. S2**). The first vaccination increased IFN-γ and IL-2 single-producing and double-producing T-

cells from baseline levels in both groups, with all but one younger adult and two elderly responding. The magnitude of the response was higher in the younger adults than the elderly after the first dose, although not significant. The second vaccination boosted T-cell responses in both groups, with 96% (23/24) responders among the elderly and 100% (34/34) responders among the younger adults. No significant difference in the T-cell responses were observed between the younger adults and the elderly, although a trend towards higher frequencies was consistently observed in the younger adults. The spike-specific T-cells gradually declined from peak levels after the second dose in both groups. Low frequencies of T-cells were detected at 9-months in both vaccine groups, with no significant differences between the groups. The proportion of single cytokine-producing T-cells secreting IFN-γ or IL-2 was similar after 3-weeks in both groups but became skewed more towards IFN-γ over time. This transition was faster in the younger adults than the elderly (**Fig. 4D**). The proportion of IFN-γ and IL-2 double-producing T-cells was always lower than single cytokine producing cells for both groups at all timepoints.

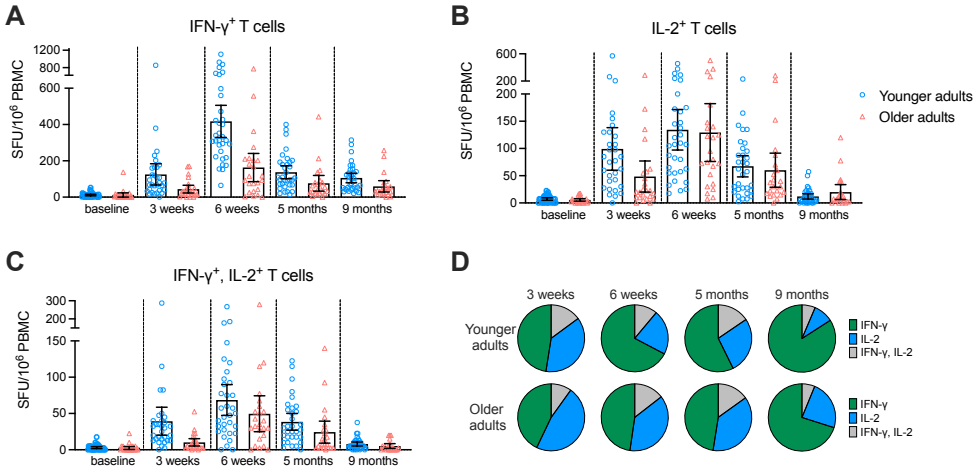

FIG 4. Functional spike-specific T-cell responses after BNT162b2 vaccination
(**A-C**) The frequency of interferon-γ (IFN-γ) (**A**), interleukin-2 (IL-2) (**B**) and double cytokine-producing spike-specific T-cell responses (**C**) measured by fluorospot in vaccinated adults (n=35, blue circles) and elderly (n=24, red triangles). Each symbol represents one individual. T-cell frequencies are reported as spot-forming units (SFU) per 10^6 peripheral blood mononuclear cells at baseline, and 3 weeks after first and second vaccination (6 weeks post-first vaccination) and 5- and 9-months post-first vaccination. Data are presented as mean with 95% confidence intervals.
(**D**) The proportion of T-cells producing single cytokines IFN-γ (green) or IL-2 (blue), or double-producing IFN-γ and IL-2 (gray) in adults (top row) and elderly (bottom row). The proportions are presented as percentage of single or double-producing T-cells of the total number of T-cells measured in the younger (n=35) and older adults (n=24).

Age-dependent variation in spike-specific immune responses induced by SARS-CoV-2 infection and vaccination

We then compared the magnitude and durability of spike-specific immune responses induced by vaccination and SARS-CoV-2 infection. Home-isolated, naturally infected participants were prospectively recruited in March and April 2020 during the first pandemic wave [12]. The infected group experienced mild-to-moderate COVID-19 and consisted of 183 subjects (median age 47 yo, range 23-80 yo, 52% female and 48% male), where 40% had comorbidities and 15% were taking immunosuppressive medication (**Table 1**). Immune responses were measured 8-weeks, 6- and 12-months after SARS-COV-2-confirmed diagnosis and were compared with responses measured at 6-weeks, 5- and 9-months after first vaccination, respectively.

The second dose boosted spike-specific IgG to higher peak levels at 6-weeks in both vaccine groups than the infected group 8-weeks post-infection. Vaccinees had significantly higher IgG titers at 5-months compared to the infected patients after 6-months, although only the younger adults remained significantly higher than the infected group after 9-months (**Fig. 5A**). Furthermore, the younger adults had significantly higher peak neutralizing titers at 6-weeks while the infected group had significantly higher neutralizing titers after 12-months compared to the vaccinated elderly at 9-months.

The durability of the spike-specific memory B and T-cell responses were compared after vaccination and infection in a subgroup of individuals (**Table 1**). There was a non-significant trend of higher frequencies of MBCs in the infected group compared to the vaccinees, with lower responses consistently observed in the vaccinated elderly (**Fig. 5A**). Durable single cytokine-producing IL-2^+ and double cytokine-producing IFN-γ^+, IL-2^+ T-cells were significantly higher 12-months post-infection compared to 9-months post-vaccination in elderly and younger adults (**Fig. 5B**). Whereas, single cytokine-producing IFN-γ^+ T-cells were significantly higher in the infected group at 6-12 months compared to only the elderly vaccinees after 5-9 months. The radar chart shows that the infected group maintained humoral and cellular responses between 6- and 12-months, whereas this was not observed in either of the vaccine groups between 5- and 9-months post-vaccination with the exception of MBCs (**Fig. 5C**).

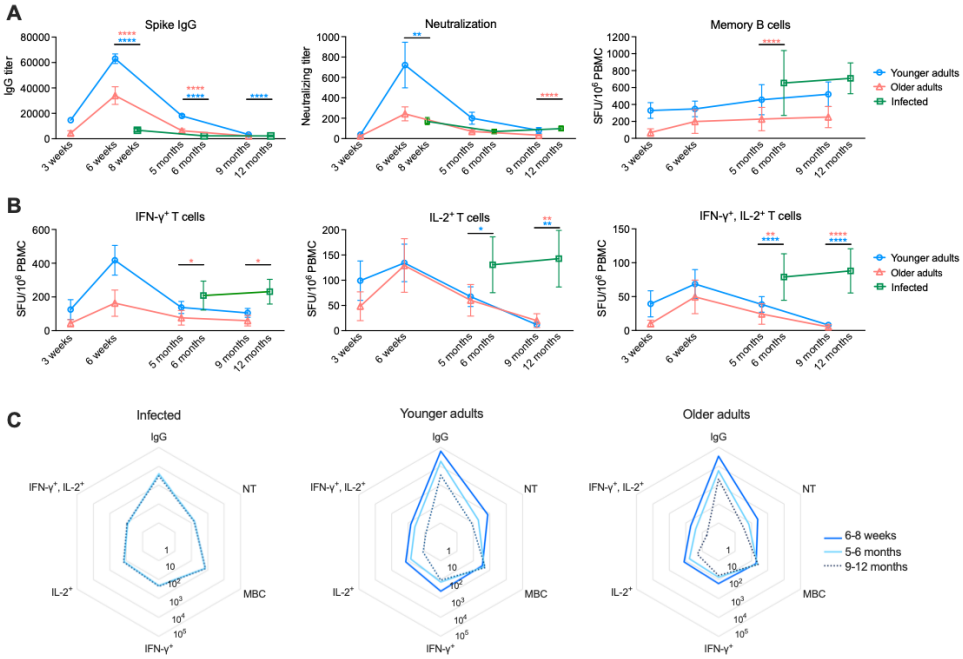

FIG 5. Spike-specific immune responses after vaccination and SARS-CoV-2 infection

(**A**) Spike-specific IgG titers, neutralizing titers and spike-specific memory B-cell responses were measured for vaccinees 3 and 6 week, and 5- and 9-months post-vaccination and infected subjects at 8 weeks, 6- and 12-months post-infection. Spike-specific IgG and neutralizing titers are presented as geometric means with 95% confidence intervals (CIs). Spike-specific memory B-cell responses were measured by ELISpot using peripheral blood mononuclear cells (PBMCs). The frequency of spike-specific memory B-cells were defined as spot forming units (SFU) per 10^6 PBMC. The data are presented as the mean with 95% CIs. Statistical significance was assessed between the infected group (green) and vaccinated older (red) or younger adults (blue) using a mixed effects model for normalized outcome measures, adjusted for repeated-measure subject variance and demographic factors, and post-hoc tests with Bonferroni correction. Red stars represent the significance level between the older adults and the infected group and blue stars represent significance level between the younger adults and the infected group. IgG titer: younger adults n=449, older adults n=100, infected n=198. Neutralizing titer: younger adults n=43, older adults n=100. Memory B-cells: younger adults n=34, older adults n=24, infected 6 months n=10, infected 12 months n=63.

(**B**) Spike-specific T-cell responses measured as the frequency of interferon-γ (IFN-γ), interleukin-2 (IL-2) and double cytokine-producing spike-specific T-cells measured by FluoroSpot assay in vaccinees at 3- and 6-week, and 5- and 9-months post-vaccination (younger adults n=35, older adults n=24) and infected subjects at 6 and 12 months post-infection (6 months n=38, 12 months n=63). Data are reported as mean SFU/10^6 PBMC with 95% CIs.

(**C**) Radar chart summarizing durable spike-specific immune responses in SARS-CoV-2 infected (left) and vaccinated younger adults (middle) and older adults (right). The data are presented as means on a log-axis. NT (neutralizing titer), memory B-cell (MBC).

We further compared the age-specific magnitude and durability of spike-specific antibody responses following vaccination and infection. There were notable differences in the magnitude and durability of IgG and neutralizing titers following vaccination and infection for all age groups. We found that younger vaccinated subjects (23-55 yo) had significantly higher IgG and neutralizing titers than infected individuals of the same age during peak levels (6 vs. 8 weeks post-infection) (**Fig. 6A, D, Table S3**). The difference in IgG and neutralizing titers between younger infected and vaccinated individuals decreased at 5-months (**Fig. 6B, E**), with no significant differences between infected and vaccinated individuals aged 40-69 yo observed by 9-months (**Fig. 6C, F)**. In contrast, the infected older individuals (70-99 yo) had significantly higher peak neutralizing titers, although similar peak IgG titers, than the vaccinees of the same age group. These infected 70-99 yo individuals also had higher and more durable IgG and neutralizing titers at 12-months post-infection compared to vaccinated subjects at 9-months (**Fig. 6C, F**).

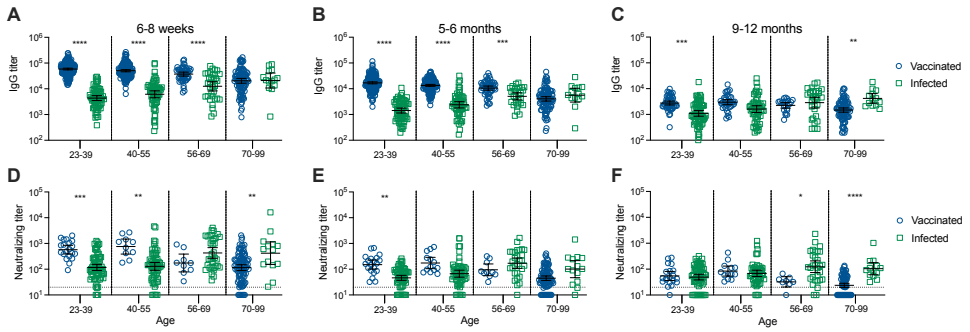

FIG 6. Age-specific antibody responses after vaccination and natural SARS-CoV-2 infection (**A-F**) Spike-specific IgG (**A-C**) and neutralizing titers (**D-F**) in vaccinated individuals (n=549) (dark blue circles) and infected individuals (n=183) (green squares) were divided into 15-year age groups. Blood samples were collected 6-weeks after the first vaccination (3-weeks after the second vaccination), 5- and 9-months post-vaccination. Home-isolated SARS-CoV-2 infected individuals (n=183) provided blood samples 8-weeks, 6- and 12-months post-acute infection. Data are presented as geometric mean titer (GMT) with 95% confidence interval (CI) and each symbol represents one individual. The threshold for detectable neutralizing antibodies (<20) is indicated with a dotted line. Multiple linear regression analysis was used to test if vaccination or infection group predicted log normalized IgG or neutralizing titers, adjusted for repeated-measure subject variance and covariates sex, age, comorbidity, use of immunosuppressive medication and age-by-group interaction. P values were only reported if they were significant at the 5% level after Bonferroni correction.
****P<0.0001, ***P<0.001, **P<0.01, *P<0.05

We compared the geometric mean of estimated time for neutralizing titers to fall below the level of detection (neutralizing titer <20) for infected and vaccinated subjects. Our calculation estimated that infected subjects aged 70-99 yo (n=15) would have detectable neutralizing antibodies for up to 14-months compared to only 6-months for vaccinated elderly (n=93), demonstrating increased durability after infection for the oldest individuals. This disparity was largest for subjects aged 56-69 yo where the vaccinees (n=13) were estimated to have detectable neutralizing antibodies for 15-months compared to 28-months in the infected subjects (n=36). The durability of neutralizing antibody titers was more comparable for the two youngest age groups 23-39 yo (vaccinees 12 months, n=20 vs. infected 12 months, n=72) and 40-55 yo (vaccinees 15 months, n=13 vs. infected 17 months, n=65).

In summary, infected individuals had more durable spike-specific humoral and cellular immune responses at all ages, but particularly antibody responses in older infected individuals.

Discussion

The rapid development and implementation of COVID-19 vaccines have changed the trajectory of the COVID-19 pandemic. Vaccination is the best method for protection against severe disease and long-term sequalae. There is limited data on the longevity of immune responses exceeding 6-months post-vaccination, especially among elderly persons who are at high risk of severe COVID-19, which we aimed to address in this study. Here, we have comprehensively investigated the kinetics and durability of humoral and cellular immune responses in younger and old adults following two doses of BNT162b2 vaccination for up to 9-months and compared this to naturally infected home-isolated individuals.

Overall, we found that home-dwelling old adults had markedly lower spike IgG and neutralizing antibody responses compared to younger adult vaccinees, particularly 3-weeks after the first and second vaccinations. At 9-months, both younger and older adults had low neutralizing antibody titers, with only 58% of the elderly having detectable neutralizing antibodies compared to 95% in the younger adults. COVID-19 mRNA vaccines have been found to induce a persistent germinal center reaction in young adults leading to durable antibody responses [19]. Immunosenescence is commonly observed in older persons and has been associated with lower humoral and cellular immunity following SARS-CoV-2 vaccination [8, 20, 21]. A diminished germinal center response has been identified as a key contributing factor of poor humoral immunity in elderly [20], which could explain the lower magnitude and

hence durability of the antibody response. Although antibody levels wane over time, MBCs are detectable after mRNA vaccination and have been reported to increase between 3 to 6-months, and also recognize Delta and Omicron VOC [21-23]. Here we have extended these findings to show that MBCs continue to increase up to 5-months post-vaccination in the elderly and up to 9-months in younger adult vaccinees. MBCs are an important part of durable protection and two doses of BNT162b2 vaccine induce persistent MBCs that rapidly respond to infection and produce neutralizing antibodies to limit the infection, also local IgA in the saliva [24]. Furthermore, a third booster vaccination results in expansion of MBCs that produce more potent and broadly reactive antibodies [25]. We found that MBCs also persisted in the elderly for up to 9-months, likely contributing to protection and immunogenicity of future booster vaccinations for this high-risk group.

Older individuals are at significantly higher risk of severe disease and death from COVID-19 [4, 5], thus optimal immunogenicity of vaccines is of great importance for this group. Longer spacing between priming and booster doses could be beneficial for vaccine distribution during a pandemic, where vaccine supply is limited. The original licensure trials used a 3-week interval between the first and second dose [2], however, longer intervals have been associated with improved vaccine immunogenicity [26, 27]. Our study showed that the kinetics of homologous humoral immunity differed between older and younger adults. We found that younger adults had robust antibody responses after the first dose and had minimal boosting of MBCs after the second dose, indicating that a prolonged interval is acceptable for this group. In contrast, the first dose was markedly less immunogenic in the elderly who had superior boosting of spike-specific IgG titers and MBCs after the second dose compared to the younger adults. Our data demonstrates the necessity of a short 3-week interval between first and second vaccine doses for the elderly to provide optimal protection. Another important aspect to inform public health responses and vaccine deployment is the durability of the vaccine induced immunity in different age groups. We calculated the estimated half-life for spike-specific IgG and neutralizing titers and found that the rate of waning was comparable between the younger and older adults. However, the older vaccinees had significantly lower magnitude of IgG and neutralizing titers compared to the younger adults at all time points after vaccination, which may impact the durability of protection. Detectable neutralizing titers were estimated to last twice as long in the younger adults than the elderly after vaccination. Interestingly, natural infection induced more durable neutralizing titers estimated to last 8-months longer than vaccination among the elderly. Real world effectiveness studies show reduced protection from

infection and symptomatic disease 6-months after vaccination, with older adults having the greatest reduction [28]. These findings suggest that SARS-CoV-2 naive individuals over 70 years would benefit from a third booster dose by 5-months after the first vaccination. Overall, our data provide valuable insights into the kinetics of the antibody response in the elderly and may have implications for vaccine regimens and distribution in the future.

Emerging data have demonstrated the importance of T-cells in reducing infection and disease severity [29]. IL-2 is a cytokine primarily produced by activated $CD4^+$ T-cells and it is essential for T-cell survival and differentiation, whilst IFN-γ is important for modulating the adaptive immune response and for clearance of viral pathogens. The frequencies of the spike-specific single and double IFN-γ and IL-2 producing T-cells were higher in the younger adults than the elderly at early time points after vaccination, although not significant, which is in agreement with previous findings [8]. Single $IL\text{-}2^+$ and double $IFN\text{-}\gamma^+$, $IL\text{-}2^+$ T-cell responses were maintained at a significantly higher level one year after infection than in vaccinees, irrespective of age. Future studies to investigate hybrid immunity after infection and vaccination are needed for the elderly.

The immunoSEQ assay is a sequence-based method to quantify spike-specific T-cell responses after natural infection or vaccination [18]. Our study demonstrates how recent developments in understanding of the unique rearrangements (breadth) and frequency of unique TCRs (depth) allows for high-throughput evaluation of spike-specific T-cell responses in large cohorts after vaccination. Lower TCR diversity against SARS-CoV-2 epitopes has been associated with severe COVID-19 [30, 31], demonstrating the value of broader TCR repertoires. We found that BNT162b2 vaccination increased the breadth and depth of the spike-specific $CD4^+$ and $CD8^+$ TCR repertoire in both younger and older adults, with the second vaccination being particularly important in the elderly. Others have shown that mRNA vaccination induce durable polyfunctional $CD4^+$ and $CD8^+$ T-cell responses with a stem cell memory phenotype [32]. Our results show that one dose of mRNA BNT162b2 vaccine elicited broader spike-specific T-cell responses, compared to previous reports of one dose of Ad26.COV2.S vaccine [33]. Importantly, vaccine-induced spike-specific T-cell responses are not severely impacted by SARS-CoV-2 VOC [33] and Omicron is predicted to have 20-30% reduction in $CD4^+$ and $CD8^+$ spike-specific T-cell responses [34, 35]. Therefore, T-cells may still provide some degree of protection severe disease.

Strengths of our study include the comprehensive immunological comparison over time of vaccinated and infected cohorts, and inclusion of the oldest vaccinees. Although the elderly subjects in our study were home-dwelling with a number of comorbidities, they may have been healthier than similar age groups in other geographical areas, as Norway has a high life expectancy. Although the infected individuals experienced mild-to-moderate COVID-19 and did not require hospitalization, we cannot determine if age and disease severity independently influence immune responses. This study focused on spike-specific immune responses, but infected individuals also have antibody and cross-reactive T-cell responses to the more conserved nucleocapsid and membrane proteins [36]. Furthermore, a caveat of this study is the number of subjects providing PBMC, which limits our assessment of MBC and T-cell responses.

Our data provide valuable information on the kinetics and durability of SARS-CoV-2 immune responses for younger adults and an understudied, high-risk, elderly group. Of importance is our finding of more durable binding and neutralizing antibody levels 12-months after natural infection compared to 9-months after vaccination, even in older individuals 70-99 years old. Likewise, spike-specific MBC and T-cell responses were maintained one year after infection, particularly evident for T-cell responses, which waned after vaccination but were maintained after infection. Although older adults had consistently lower spike-specific immune responses after vaccination compared to younger adults, the elderly had more robust and durable antibody responses after infection. Our results indicate that infection induces more robust and durable immune responses in the elderly, which is not achieved by two doses of BNT162b2 vaccine. It is important to emphasize that the persistence of symptoms and complications after COVID-19 are well-documented and vaccine-induced immunity is therefore the best and safest way to acquire immunity to SARS-CoV-2 [37, 38]. However, our study suggests that SARS-CoV-2 immune responses induced by vaccination and infection are inherently different in young and old adults. Further studies to investigate how age affects the immune responses induced by infection and vaccination are needed, and have the potential to inform the rationale design of vaccines for older adults.

Acknowledgements

We are grateful to all the vaccinees and home-isolated patients who altruistically gave their time and blood samples to the study. We would also like to thank the Clinical trials unit, Occupational Health department and Infectious diseases unit at Haukeland University Hospital

for help with the study. We thank Professor Florian Krammer, Department of Microbiology, Icahn School of Medicine, Mount Sinai, New York, for supplying the RBD and spike constructs, the clinical study staff and the Research Unit for Health Surveys (RUHS), University of Bergen for collecting the infected patient's data.

Funding

The Influenza Centre is supported by the Trond Mohn Stiftelse [TMS2020TMT05], the Ministry of Health and Care Services, Norway; Helse Vest [F-11628, F-12167, F-12621], the Norwegian Research Council Globvac [284930]; the European Union [EU IMI115672, FLUCOP, IMI2 101007799 Inno4Vac, H2020 874866 INCENTIVE, H2020 101037867 Vaccelerate]; the Faculty of Medicine, University of Bergen, Norway; and Nanomedicines Flunanoair [ERA-NETet EuroNanoMed2 i JTC2016] and Pasteur legatet & Thjøtta's legat, University of Oslo, Norway [101563]. Research unit for health surveys/Forskningsenhet for helseundersøkelse received support from Trond Mohn stiftelsen (TMS).

Author contributions

RJC, NL, KAB and KGIM conceptualized the study. LH, KAB, AB, FZ, GB, TBO, AM, JSO, MCT performed experiments. RE, SS, HC, IK performed the TCR sequencing and data analysis. HHS, NUE, EBF, MS, HS, JSO, CT, KIGM performed the clinical studies. LH visualized and managed the data. AB performed the statistical analyses. LH, RJC, NL wrote the original draft and all authors reviewed and edited draft.

Declaration of competing interests

RE, SS, HC and IK are employed by Adaptive Biotechnologies. The other authors declare that they have no competing interests.

Data and materials availability

All data are available in the main text or the supplementary materials.

Bergen COVID-19 Research group:

Kanika Kuwelker, Olav Ervik, Sonja Ljostveit, Bjørn Blomberg, Siri Øyen, Lisbeth Mørk, Per Espen Akselsen, Trude Duelien Skorge, Liv Heiberg Okkenhaug, Sarah Lartey, Håkon Amdam, Hauke Bartsch, Dagrun Waag Linchausen.

References

[1] Baden LR, El Sahly HM, Essink B, Kotloff K, Frey S, Novak R, et al. Efficacy and Safety of the mRNA-1273 SARS-CoV-2 Vaccine. N Engl J Med. 2021;384:403-16.
[2] Polack FP, Thomas SJ, Kitchin N, Absalon J, Gurtman A, Lockhart S, et al. Safety and Efficacy of the BNT162b2 mRNA Covid-19 Vaccine. N Engl J Med. 2020;383:2603-15.
[3] Pallesen J, Wang N, Corbett KS, Wrapp D, Kirchdoerfer RN, Turner HL, et al. Immunogenicity and structures of a rationally designed prefusion MERS-CoV spike antigen. Proc Natl Acad Sci U S A. 2017;114:E7348-E57.
[4] Clift AK, Coupland CAC, Keogh RH, Diaz-Ordaz K, Williamson E, Harrison EM, et al. Living risk prediction algorithm (QCOVID) for risk of hospital admission and mortality from coronavirus 19 in adults: national derivation and validation cohort study. BMJ. 2020;371:m3731.
[5] Williamson EJ, Walker AJ, Bhaskaran K, Bacon S, Bates C, Morton CE, et al. Factors associated with COVID-19-related death using OpenSAFELY. Nature. 2020;584:430-6.
[6] Helfand BKI, Webb M, Gartaganis SL, Fuller L, Kwon C-S, Inouye SK. The Exclusion of Older Persons From Vaccine and Treatment Trials for Coronavirus Disease 2019—Missing the Target. JAMA Internal Medicine. 2020;180:1546-9.
[7] Parry H, Tut G, Bruton R, Faustini S, Stephens C, Saunders P, et al. mRNA vaccination in people over 80 years of age induces strong humoral immune responses against SARS-CoV-2 with cross neutralization of P.1 Brazilian variant. Elife. 2021;10.
[8] Tober-Lau P, Schwarz T, Vanshylla K, Hillus D, Gruell H, Group ECS, et al. Long-term immunogenicity of BNT162b2 vaccination in older people and younger health-care workers. Lancet Respir Med. 2021;9:e104-e5.
[9] Khoury DS, Cromer D, Reynaldi A, Schlub TE, Wheatley AK, Juno JA, et al. Neutralizing antibody levels are highly predictive of immune protection from symptomatic SARS-CoV-2 infection. Nat Med. 2021;27:1205-11.
[10] McMahan K, Yu J, Mercado NB, Loos C, Tostanoski LH, Chandrashekar A, et al. Correlates of protection against SARS-CoV-2 in rhesus macaques. Nature. 2021;590:630-4.
[11] Zhong D, Xiao S, Debes AK, Egbert ER, Caturegli P, Colantuoni E, et al. Durability of Antibody Levels After Vaccination With mRNA SARS-CoV-2 Vaccine in Individuals With or Without Prior Infection. JAMA. 2021.
[12] Kuwelker K, Zhou F, Blomberg B, Lartey S, Brokstad KA, Trieu MC, et al. Attack rates amongst household members of outpatients with confirmed COVID-19 in Bergen, Norway: A case-ascertained study. Lancet Reg Health Eur. 2021;3:100014.
[13] Trieu M-C, Bansal A, Madsen A, Zhou F, Sævik M, Vahokoski J, et al. SARS-CoV-2–Specific Neutralizing Antibody Responses in Norwegian Health Care Workers After the First Wave of COVID-19 Pandemic: A Prospective Cohort Study. The Journal of Infectious Diseases. 2020;223:589-99.
[14] Mohn KG, Bredholt G, Zhou F, Madsen A, Onyango TB, Fjelltveit EB, et al. Durable T-cellular and humoral responses in SARS-CoV-2 hospitalized and community patients. PLoS One. 2022;17:e0261979.
[15] Robins HS, Campregher PV, Srivastava SK, Wacher A, Turtle CJ, Kahsai O, et al. Comprehensive assessment of T-cell receptor beta-chain diversity in alphabeta T cells. Blood. 2009;114:4099-107.

[16] Elyanow R, Snyder TM, Dalai SC, Gittelman RM, Boonyaratanakornkit J, Wald A, et al. T-cell receptor sequencing identifies prior SARS-CoV-2 infection and correlates with neutralizing antibody titers and disease severity. medRxiv. 2021.
[17] Snyder TM, Gittelman RM, Klinger M, May DH, Osborne EJ, Taniguchi R, et al. Magnitude and Dynamics of the T-Cell Response to SARS-CoV-2 Infection at Both Individual and Population Levels. medRxiv. 2020:2020.07.31.20165647.
[18] Snyder TM, Gittelman RM, Klinger M, May DH, Osborne EJ, Taniguchi R, et al. Magnitude and Dynamics of the T-Cell Response to SARS-CoV-2 Infection at Both Individual and Population Levels. medRxiv. 2020.
[19] Turner JS, O'Halloran JA, Kalaidina E, Kim W, Schmitz AJ, Zhou JQ, et al. SARS-CoV-2 mRNA vaccines induce persistent human germinal centre responses. Nature. 2021;596:109-13.
[20] Lee JL, Linterman MA. Mechanisms underpinning poor antibody responses to vaccines in ageing. Immunol Lett. 2021;241:1-14.
[21] Sokal A, Barba-Spaeth G, Fernandez I, Broketa M, Azzaoui I, de La Selle A, et al. mRNA vaccination of naive and COVID-19-recovered individuals elicits potent memory B cells that recognize SARS-CoV-2 variants. Immunity. 2021;54:2893-907 e5.
[22] Kotaki R, Adachi Y, Moriyama S, Onodera T, Fukushi S, Nagakura T, et al. SARS-CoV-2 Omicron-neutralizing memory B-cells are elicited by two doses of BNT162b2 mRNA vaccine. Sci Immunol. 2022:eabn8590.
[23] Goel RR, Apostolidis SA, Painter MM, Mathew D, Pattekar A, Kuthuru O, et al. Distinct antibody and memory B cell responses in SARS-CoV-2 naive and recovered individuals following mRNA vaccination. Sci Immunol. 2021;6.
[24] Terreri S, Piano Mortari E, Vinci MR, Russo C, Alteri C, Albano C, et al. Persistent B cell memory after SARS-CoV-2 vaccination is functional during breakthrough infections. Cell Host Microbe. 2022.
[25] Muecksch F, Wang Z, Cho A, Gaebler C, Tanfous TB, DaSilva J, et al. Increased Potency and Breadth of SARS-CoV-2 Neutralizing Antibodies After a Third mRNA Vaccine Dose. bioRxiv. 2022.
[26] Grunau B, Goldfarb DM, Asamoah-Boaheng M, Golding L, Kirkham TL, Demers PA, et al. Immunogenicity of Extended mRNA SARS-CoV-2 Vaccine Dosing Intervals. JAMA. 2021.
[27] Tauzin A, Gong SY, Beaudoin-Bussieres G, Vezina D, Gasser R, Nault L, et al. Strong humoral immune responses against SARS-CoV-2 Spike after BNT162b2 mRNA vaccination with a 16-week interval between doses. Cell Host Microbe. 2021.
[28] Feikin DR, Higdon MM, Abu-Raddad LJ, Andrews N, Araos R, Goldberg Y, et al. Duration of effectiveness of vaccines against SARS-CoV-2 infection and COVID-19 disease: results of a systematic review and meta-regression. Lancet. 2022;399:924-44.
[29] Kundu R, Narean JS, Wang L, Fenn J, Pillay T, Fernandez ND, et al. Cross-reactive memory T cells associate with protection against SARS-CoV-2 infection in COVID-19 contacts. Nat Commun. 2022;13:80.
[30] Nelde A, Bilich T, Heitmann JS, Maringer Y, Salih HR, Roerden M, et al. SARS-CoV-2-derived peptides define heterologous and COVID-19-induced T cell recognition. Nat Immunol. 2021;22:74-85.

[31] Peng Y, Mentzer AJ, Liu G, Yao X, Yin Z, Dong D, et al. Broad and strong memory CD4(+) and CD8(+) T cells induced by SARS-CoV-2 in UK convalescent individuals following COVID-19. Nat Immunol. 2020;21:1336-45.
[32] Guerrera G, Picozza M, D'Orso S, Placido R, Pirronello M, Verdiani A, et al. BNT162b2 vaccination induces durable SARS-CoV-2 specific T cells with a stem cell memory phenotype. Sci Immunol. 2021:eabl5344.
[33] Alter G, Yu J, Liu J, Chandrashekar A, Borducchi EN, Tostanoski LH, et al. Immunogenicity of Ad26.COV2.S vaccine against SARS-CoV-2 variants in humans. Nature. 2021;596:268-72.
[34] Keeton R, Tincho MB, Ngomti A, Baguma R, Benede N, Suzuki A, et al. SARS-CoV-2 spike T cell responses induced upon vaccination or infection remain robust against Omicron. medRxiv. 2021:2021.12.26.21268380.
[35] May DH, Rubin BER, Dalai SC, Patel K, Shafiani S, Elyanow R, et al. Immunosequencing and epitope mapping reveal substantial preservation of the T cell immune response to Omicron generated by SARS-CoV-2 vaccines. medRxiv. 2021:2021.12.20.21267877.
[36] Le Bert N, Tan AT, Kunasegaran K, Tham CYL, Hafezi M, Chia A, et al. SARS-CoV-2-specific T cell immunity in cases of COVID-19 and SARS, and uninfected controls. Nature. 2020;584:457-62.
[37] Blomberg B, Mohn KG, Brokstad KA, Zhou F, Linchausen DW, Hansen BA, et al. Long COVID in a prospective cohort of home-isolated patients. Nat Med. 2021;27:1607-13.
[38] Davis HE, Assaf GS, McCorkell L, Wei H, Low RJ, Re'em Y, et al. Characterizing long COVID in an international cohort: 7 months of symptoms and their impact. EClinicalMedicine. 2021;38:101019.

Supplemental files

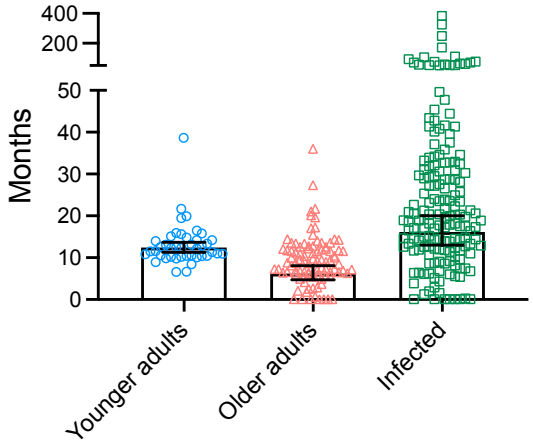

Supplementary figure 1. Estimated duration of SARS-CoV-2 neutralizing antibodies
A linear regression model was fitted for each individual to estimate the time for neutralizing titers to fall below the level of detection (neutralizing titer <20) for vaccinated younger (n=41) and older adults (n=100), and naturally infected individuals (n=183). Data are presented as geometric mean with 95% confidence interval (CI) and each symbol represents one individual.

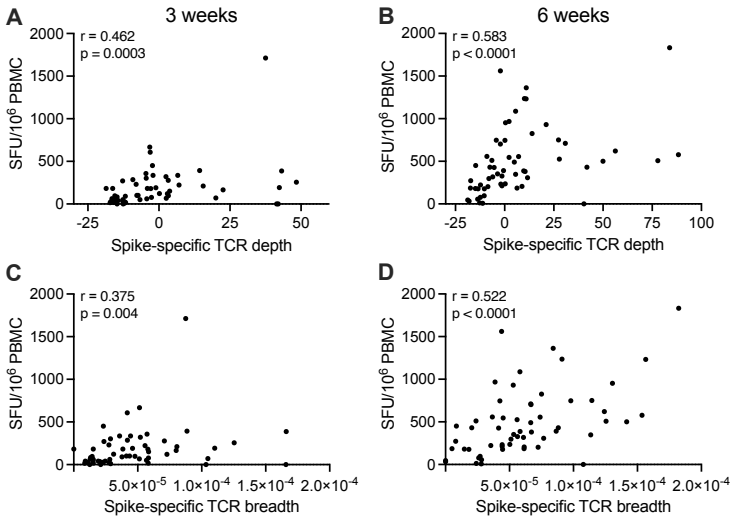

Supplementary figure 2. Correlation between functional T cell responses and TCR sequencing
Spike-specific T cell responses measured by fluorospot assay three weeks after vaccination (left) and 6 weeks after vaccination (right) (n=58). Correlation coefficient was calculated by non-parametric spearman correlation.

Supplementary table 1: Factors associated with humoral immune responses after vaccination

Effect	Anti-spike IgG titer n=549		Neutralizing titer n=141		Memory B cells n=58	
	Est. (95% CI)	**P**	**Est. (95% CI)**	**P**	**Est. (95% CI)**	**P**
Intercept	10.8 (10.7, 10.9)	**<0.0001**	5.8 (5.5, 6.1)	**<0.0001**	5.8 (5.0, 6.6)	**<0.0001**
Group: Elderly	-0.8 (-1.0, -0.6)	**<0.0001**	-0.9 (-1.4, -0.5)	**<0.0001**	-1.4 (-2.9, 0.1)	0.072
Time: 3 weeks	-1.7 (-1.8, -1.6)	**<0.0001**	-2.2 (-2.4, -2.1)	**<0.0001**	-0.8 (-1.4, -0.2)	**0.012**
5 months	-1.3 (-1.4, -1.2)	**<0.0001**	-1.0 (-1.2, -0.9)	**<0.0001**	0.3 (-0.3, 1.0)	0.299
9 months	-2.9 (-3.0, -2.8)	**<0.0001**	-1.8 (-1.9, -1.6)	**<0.0001**	0.5 (-0.1, 1.1)	0.098
Immunosuppression	-0.2 (-0.5, 0.1)	0.208	-0.1 (-0.6, 0.3)	0.521	- [a]	-
Comorbidities	-0.2 (-0.4, -0.004)	**0.045**	-0.2 (-0.6, 0.2)	0.324	-0.4 (-1.9, 1.1)	0.616
Sex: Female	0.2 (0.04, 0.3)	**0.011**	0.3 (0.02, 0.6)	**0.038**	0.4 (-0.5, 1.2)	0.402
Interaction between age group and time point						
Elderly: 3 weeks	-1.0 (-1.1, -0.8)	**<0.0001**	- [b]	-	- [b]	-
Elderly: 5 months	-0.4 (-0.6, -0.2)	**<0.0001**	-	-	-	-
Elderly: 9 months	0.2 (-0.01, 0.4)	0.060	-	-	-	-

Mixed-effects models to evaluate the effect of age group (younger adults as reference) and time after vaccination (6 weeks as reference) on IgG titers, neutralizing titers or memory B cells, adjusted for immunosuppression, comorbidities, sex (male as reference), age-by-time interaction, and repeated-measure subject variance in R (Version 4.1.2). Antibody responses were natural log-transformed, and memory B cell responses were inverse hyperbolic sine transformed. Estimates of a fitted model are reported with 95% confidence intervals (CIs) and p values. Missing data was omitted. For factors with significance level $P<0.05$, the p values are shown in bold.

[a] Variable excluded for the mixed-effects model.

[b] Age-by-time interactions were not included as $P>0.01$. No other interaction term was found.

Supplementary table 2: Factors associated with spike-specific T cell responses after vaccination

Effect	TCR breadth n=549		TCR depth n=549		IFN-γ^+ T cells n=58		IL-2^+ T cells n=58		IFN-γ^+, IL-2^+ T cells n=58	
	Est. (95% CI)	P	Est. (95% CI)	P	Est. (95% CI)	P	Est. (95% CI)	P	Est. (95% CI)	P
Intercept	6×10^{-5} (5×10^{-5}, 6×10^{-5})	**<0.0001**	0.5 (0.01, 0.9)	**0.045**	6.1 (5.6, 6.6)	**<0.0001**	5.2 (4.7, 5.7)	**<0.0001**	4.3 (3.8, 4.8)	**<0.0001**
Group: Elderly	-2×10^{-5} (-4×10^{-5}, -9×10^{-5})	**0.001**	-2.2 (-3.0, -1.3)	**<0.0001**	-0.7 (-1.6, 0.2)	0.113	-0.01 (-0.9, 0.9)	0.979	-0.5 (-1.3, 0.3)	0.247
Time: 3 weeks	2×10^{-6} (-2×10^{-6}, 6×10^{-6})	0.344	-0.1 (-0.3, 0.03)	0.128	-1.5 (-1.8, -1.2)	**<0.0001**	-0.9 (-1.3, -0.5)	**<0.0001**	-0.9 (-1.4, -0.5)	**0.0001**
5 months	-	-	-	-	-1.0 (-1.3, -0.6)	**<0.0001**	-0.9 (-1.3, -0.5)	**<0.0001**	-0.6 (-1.1, -0.2)	**0.005**
9 months	-	-	-	-	-1.2 (-1.5, -0.9)	**<0.0001**	-2.7 (-3.1, -2.3)	**<0.0001**	-2.2 (-2.7, -1.8)	**<0.0001**
Immunosuppression	1×10^{-5} (-7×10^{-6}, 4×10^{-5})	0.182	-0.4 (-1.7, 0.9)	0.524	-[a]	-	-[a]	-	-[a]	-
Comorbidities	4×10^{-6} (-8×10^{-6}, 2×10^{-5})	0.516	0.1 (-0.6, 0.8)	0.770	-0.5 (-1.5, 0.4)	0.246	-0.4 (-1.3, 0.5)	0.350	-0.5 (-1.3, 0.4)	0.272
Sex: Female	1×10^{-5} (6×10^{-6}, 2×10^{-5})	**0.001**	0.9 (0.4, 1.4)	**0.0005**	0.5 (-0.05, 1.0)	0.074	0.4 (-0.2, 0.9)	0.182	0.4 (-0.1, 0.8)	0.137
Interaction between age group and time point										
Elderly 3 weeks	-2×10^{-5} (-3×10^{-5}, -8×10^{-6})	**0.0002**	-1.0 (-1.4, -0.7)	**<0.0001**	-[b]	-	-[b]	-	-[b]	-

Mixed-effects models to evaluate the effect of age group (younger adults as reference) and time after vaccination (6 weeks as reference) on TCR breadth, TCR depth or T cells as outcome measures, adjusted for immunosuppression, comorbidities, sex (male as reference), age-by-time interaction, and repeated-measure subject variance in R (Version 4.1.2). Outcome measures were inverse hyperbolic sine transformed. Estimates of a fitted model are reported with 95% confidence intervals (CIs) and P values. Missing data was omitted. For factors with significance level $P<0.05$, the p values are shown in bold.

[a] Variable excluded for the mixed-effects model

[b] Age-by-time interactions were not included as $P>0.01$. No other interaction term was found.

Supplementary table 3: Factors associated with antibody responses after vaccination and SARS-CoV-2 infection

	Anti-spike IgG titer						Neutralizing titer					
Effect	6-8 weeks (n=712)		5-6 months (n=677)		9-12 months (n=363)		6-8 weeks (n=315)		5-6 months (n=30)		9-12 months (n=285)	
	Est. (95% CI)	P	Est. (95% CI)	P	Est. (95% CI)	P	Est. (95% CI)	P	Est. (95% CI)	P	Est. (95% CI)	P
Intercept	8.4 (8.2, 8.6)	**<0.0001**	7.4 (7.2, 7.6)	<0.0001	7.1 (6.78 7.4)	**<0.0001**	5.5 (5.1, 6.0)	**<0.0001**	4.7 (4.4, 5.0)	**<0.0001**	4.7 (4.3, 45.0)	**<0.0001**
Group: Vaccinated	2.5 (2.3, 2.8)	**<0.0001**	2.3 (2.1, 2.5)	<0.0001	0.7 (0.4, 1.1)	**0.0001**	1.5 (0.8, 2.2)	**<0.0001**	0.95 (0.4, 1.5)	**0.001**	-0.04 (-0.6, 0.5)	0.880
Age: 40–55yo	0.3 (0.0, 0.6)	0.019	0.5 (0.2, 0.8)	0.0002	0.4 (0.1, 0.7)	**0.022**	-0.01 (-0.5, 0.4)	0.976	0.3 (-0.02, 0.7)	**0.061**	0.3 (-0.02, 0.7)	0.062
56–69yo	1.0 (0.7, 1.4)	**<0.0001**	1.2 (0.9, 1.5)	<0.0001	0.9 (0.5, 1.3)	**<0.0001**	136 (0.7, 1.8)	**<0.0001**	1.2 (0.8, 1.7)	**<0.0001**	0.9 (0.4, 1.3)	**0.0001**
70–99yo	1.7 (1.2, 2.2)	**<0.0001**	1.4 (1.0, 1.9)	<0.0001	1.2 (0.6, 1.8)	**<0.0001**	1.3 (0.5, 2.2)	**0.002**	0.8 (0.1, 1.4)	**0.028**	0.7 (0.03, 1.3)	**0.041**
Immunosuppression	-0.04 (-0.4, 0.3)	0.802	-0.18 (-0.5, 0.1)	0.275	-0.05 (-0.5, 0.4)	0.805	-0.25 (-0.83, 0.34)	0.413	-0.01 (-0.5, 0.3)	0.957	-0.04 (-0.5, 0.4)	0.857
Comorbidities	-0.1 (-0.3, 0.05)	0.177	-0.3 (-0.4, -0.1)	0.001	-0.3 (-0.5, -0.05)	**0.016**	-0.2 (-0.6, 0.2)	0.265	-0.4 (-0.7, -0.2)	**0.002**	-0.3 (-0.6, 0.01)	0.055
Sex: Female	0.2 (0.02, 0.3)	**0.020**	0.2 (0.03, 0.3)	0.014	0.3 (0.1, 0.5)	**0.005**	0.1 (-0.2, 0.4)	0.463	0.23 (-0.01, 0.5)	0.056	0.2 (0.01, 0.5)	**0.041**
Interactions of age with vaccinated or infected group												
Vaccinated 40-55yo	-0.5 (-0.8, -0.2)	**0.005**	-0.7 (-1.0, -0.4)	<0.0001	-0.3 (-0.8, 0.2)	0.284	0.20 (-0.93, 1.34)	0.722	-0.3 (-1.1, 0.5)	0.462	0.05 (-0.8, 0.9)	0.905
Vaccinated 56-69yo	-1.4 (-1.9, -1.0)	**<0.0001**	-1.6 (-2.0, -1.2)	<0.0001	-1.0 (-1.7, -0.4)	**0.001**	-2.19 (-3.52, -0.87)	**0.001**	-1.4 (-2.4, -0.4)	**0.006**	-1.2 (-2.3, -0.1)	**0.026**
Vaccinated 70-99yo	-2.7 (-3.2, -2.1)	**<0.0001**	-2.68 (-3.2, -2.2)	<0.0001	-1.6 (-2.3, -0.9)	**<0.0001**	-2.77 (-3.90, -1.65)	**<0.0001**	-1.64 (-2.5, -0.8)	**0.0002**	-1.3 (-2.2, -0.5)	**0.003**

Multivariate regression models to evaluate the effect of vaccination group (infected as reference) and age (23-39yo as reference) on natural log-transformed IgG titers or neutralizing titers, adjusted for immunosuppression, comorbidities, sex (male as reference), and age-by-group interaction in R (Version 4.1.2). No other interaction term was found. Estimates of a fitted model are reported with 95% confidence intervals (CIs) and p values. Missing data was omitted. For factors with significance level $P<0.05$, the p values are shown in bold.

Errata for
Strategies for improving influenza vaccines: insights from the influenza A H1N1 and SARS-CoV-2 pandemics

Lena Hansen

Thesis for the degree philosophiae doctor (PhD)

at the University of Bergen

Lena Hansen

_01/09/2022_____ _____

(date and sign. of candidate) (date and sign. of faculty)

Errata

Summary Missing words: "the most abundant surface protein" – corrected to "the second most abundant surface protein"

Sammendrag Missing word: "Acute Respiratory Syndrome Coronavirus-2" – corrected to "Severe Acute Respiratory Syndrome Coronavirus-2"

Page 23 Misspelling: "inactivate" – corrected to "inactivated"

Page 27 Missing word: "Each seasonal vaccine dose" – corrected to "One dose of seasonal inactivated vaccine"

Page 33 Misspelling: "were" – corrected to "was"

Page 48 Missing words: "the cells were infected with A/Singapore/GP1908/15 (H1N1) virus diluted in 1X MEM" – corrected to "the cells were infected with $1x10^4$ pfu of A/Singapore/GP1908/15 (H1N1) virus diluted in 1X MEM (200 µl/well) with TPCK-treated trypsin (1 µg/ml)"

Pages 15, 43, 50 Misspelling: "fabs" – corrected to "Fabs"

Graphic design: Communication Division, UiB / Print: Skipnes Kommunikasjon AS

uib.no

ISBN: 9788230861349 (print)
9788230858622 (PDF)